PLASTIC WAVE PROPAGATION WITH
COMBINED STRESSES

Thesis for the Degree of Ph. D.
MICHIGAN STATE UNIVERSITY
RAM PARKASH GOEL
1969

THESIS

This is to certify that the

thesis entitled
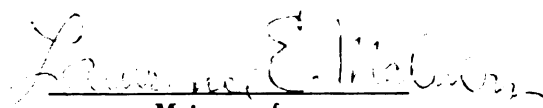
Plastic Wave Propagation with Combined Stesses

presented by

Ram Parkash Goel

has been accepted towards fulfillment
of the requirements for

___Ph. D.___ degree in __Mechanics__

Dept. of Metallurgy, Mechanics & Materials Science

_____
Major professor

Date__August 15, 1969__

O-169

MAGIC 2

JAN 1 1 1998

ABSTRACT

PLASTIC WAVE PROPAGATION WITH
COMBINED STRESSES

By Ram Parkash Goel

This investigation analyzes combined-stress wave
propagation for loading beyond the elastic limit in two
geometries: a thin-walled semi-infinite tube subjected
to simultaneous axial and torsional impact, and a half
space under compressive and shear impact loadings. The
major part of the results presented are for the thin-
walled tube case, where the effect of different harden-
ing assumptions has been investigated. For the half
space, isotropic hardening was assumed throughout the
study. One type of simple-wave solution not previ-
ously investigated is presented and also one example of
a numerical solution for a nonsimple wave.

For the thin-walled tube analysis the consti-
tutive equations were obtained by combining the two most
widely used hardening postulates, namely isotropic hard-
ening and kinematic hardening. A hardening parameter m

1

(varying from m = 0 for purely kinematic hardening to m = 1 for purely isotropic hardening) was used to define the fraction of total hardening attributable to isotropic hardening. The boundary value problems of a thin-walled tube were solved for different values of the hardening parameter m and with different initial stress states and different tension-torsion impact loadings on the boundary $x = 0$ of the tube, such that simple wave solutions occurred. For some choices of initial and boundary conditions, both qualitative and quantitative differences were observed in the particle stress histories between the predictions of isotropic hardening and the predictions of kinematic or combined kinematic and isotropic hardening. In some cases a discontinuity in shear stress occurs, propagating at the elastic shear wave speed c_2, followed by a slow plastic simple wave, according to the kinematic hardening or the combined kinematic and isotropic hardening assumptions, when no such discontinuity is predicted by isotropic hardening. It is considerably more difficult to obtain simple wave solutions for the kinematic hardening or the combined kinematic and isotropic hardening case than it is for the isotropic hardening case, because a family of simple-wave

stress trajectories must be constructed to obtain one par-
ticular stress trajectory for a prescribed initial and
boundary state of the tube.

For the isotropic-hardening half space loaded with
step function impacts in compression and two shears τ_2 and
τ_3, each simple-wave solution implies a radial loading pro-
jection in the τ_2, τ_3-plane. But the radial loading τ_3/τ_2
ratio for the fast wave may be different from the ratio
for the slow wave. The transition is accompanied by jumps
both in τ_2 and τ_3 traveling at the elastic shear-wave
speed c_2.

A surprising result was obtained for the one example
of numerical solution for a nonsimple wave in a half space.
The plotted level lines of stress and velocity turned out
to be straight even though it was not a simple wave. More-
over the compressive and shear waves appeared to be un-
coupled. No general conclusions can be drawn from these
limited results, but the possibility exists that closed-
form solutions could be obtained in future studies of non-
simple waves, for some boundary conditions.

PLASTIC WAVE PROPAGATION WITH

COMBINED STRESSES

By

Ram Parkash Goel

A THESIS

Submitted to

Michigan State University

in partial fulfillment of the requirements

for the degree of

DOCTOR OF PHILOSOPHY

in

Mechanics

Department of Metallurgy, Mechanics and Materials Science

August 1969

To my parents . . .

ACKNOWLEDGMENTS

TABLE OF CONTENTS

TABLE OF CONTENTS (cont.)

TABLE OF CONTENTS (cont.)

LIST OF SYMBOLS

$\underset{\sim}{A}$ coefficient matrix, multiplying $\underset{\sim}{w}_t$

a   slope of the shear stress and shear velocity level lines

$\underset{\sim}{B}$ coefficient matrix, multiplying $\underset{\sim}{w}_x$

b   slope of the normal stress and velocity level lines; proportionaltiy scalar function in obtaining the translation of the yield surface

c   characteristic wave speed

c_1 elastic dilatational wave speed

c_2 elastic shear wave speed

c_f fast wave speed

c_o elastic bar-wave speed

c_p $= \sqrt{E_t/\rho}$

c_s slow wave speed

D_{ij} components of the rate-of-deformation tensor

$\underset{\sim}{D}$ submatrix of partitioned matrix $\underset{\sim}{A}$

$\underset{\sim}{D}^e$ elastic part of $\underset{\sim}{D}$

$(\underset{\sim}{D}^e)^*$ adjoint of $\underset{\sim}{D}^e$

dS_o surface element in the undeformed configuration

dS surface element in the deformed configuration

ds_1 motion of the local yield surface element due to isotropic hardening

ds_2 motion of the local yield surface element due to kinematic hardening

ds total motion of the local yield surface element

E Young's modulus

E_t tangent modulus

$\hat{\underset{\sim}{e}}_{ij}$ unit vector in stress space

F function of effective plastic strain $\int \overline{d\epsilon}^p$

f yield function

G shear modulus

g slope of effective stress--effective plastic strain curve

$H = \dfrac{3}{4gk^2}$

$\underset{\sim}{I}_j$ unit matrix of order j

I_2 second invariant of plastic strain increments

J_2' second invariant of deviatoric stresses

k size parameter of the yield surface (yield stress in shear for isotropic hardening)

k_o initial yield stress in shear

$L = MN - S^2$

$\underset{\sim}{\ell}$ eigenvector

$\underset{\sim}{\ell}^T$ transpose of $\underset{\sim}{\ell}$

$\underset{\sim}{M}$ submatrix of $\underset{\sim}{B}$

$M = \dfrac{1}{G} + 4H\eta^2$

$M = \dfrac{1}{G} + 4H\eta^2$

m   hardening parameter

$N = \dfrac{1}{E} + H\,(\xi')^2$

$\hat{\underset{\sim}{n}}$ unit normal to yield surface

P   grid point at time $(t + \Delta t)$

Q   grid point at time t

R   radius of yield surface in σ_{11} direction

$\underset{\sim}{r}$ radius vector of the yield surface in stress space

$\underset{\sim}{S}$ submatrix of $\underset{\sim}{A}$

$\underset{\sim}{S}^e$ elastic part of $\underset{\sim}{S}$

$S = 2H\xi'\eta$

$s = \dfrac{2}{3}(\sigma_1 - \sigma_2)$

$\underset{\sim}{T}^O$ first Piola-Kirchoff stress tensor (nonsymmetric)

T^O_{Ji} elements of $\underset{\sim}{T}^O$

t   time

U   displacement in the longitudinal direction

u   longitudinal particle velocity

V   displacement in the tangential direction

v_i particle velocity in the i direction

v   particle velocity in the tangential direction

$\underset{\sim}{w}, \underset{\sim}{w}_x, \underset{\sim}{w}_t$ solution vector and its partial derivatives

X_K material Cartesian coordinates (Lagrangian coordinates) in Appendix 2

x_k spatial Cartesian coordinates (Eulerian coordinates) in Appendix 2

x particle coordinate in the undeformed state, in the text

Y uniaxial yield stress

Y_R uniaxial yield stress with reversed loading

Y_o initial yield stress

$\underset{\sim}{\alpha}$ position vector of the center of the yield surface in the stress space

α_{ij} components of the position vector $\underset{\sim}{\alpha}$ in Chap. 3; coefficient of jth element in the ith equation in Section 4.4

$\beta = \dfrac{2(1+\nu)}{1-2\nu}$

γ engineering shear strain in Chapter 3; ratio of shear stresses (τ_3/τ_2) in Chapters 4 and 5

γ^p plastic angle change (plastic shear strain)

γ^e elastic angle change (elastic shear strain)

γ^b ratio of boundary shear stresses

γ^1 ratio of prestress shear stresses

δ_{ij} Kronecker delta, unity when i=j, otherwise 0

$\underset{\sim}{\epsilon}$ total strain vector

ϵ longitudinal unit extension

ϵ^e elastic longitudinal unit extension

ϵ^p plastic longitudinal unit extension

$\overline{d\epsilon}^p$ effective plastic strain increment

ζ distance in the characteristic direction in the x,t-plane, in Appendix 1

η $= \tau - \tau^*$

η^f η coordinate of a point on the fast-wave stress path just before the jump

$\dot{\lambda}$ scalar function used in the plastic potential theory

ν Poisson's ratio

$\underset{\sim}{\xi}$ $= \underset{\sim}{\sigma} - \underset{\sim}{\alpha}$

ξ $= \sigma - \sigma^*$

ξ' $= \dfrac{2}{3} \sigma - \sigma^*$ (deviatoric part of ξ)

ρ mass density

$\underset{\sim}{\sigma}$ stress vector in nine-dimensional stress space

σ_{ij} components of $\underset{\sim}{\sigma}$; also Cartesian tensor Cauchy stress components

σ^f σ-coordinate of a point on the fast-wave stress path just before jump

$\underset{\sim}{\sigma}'$ deviatoric stress vector in nine space

σ_Y yield stress in tension (or compression)

σ^o normal stress coordinate where the slow-wave stress path starts

σ^* σ-coordinate of the yield surface center

TABLE OF CONTENTS (Cont.)

$d\bar{\sigma}$ effective stress increment

τ shear stress component; resultant shear stress of τ_2 and τ_3

τ_2 shear stress in y-direction

τ_2^b value of τ_2 on the boundary

τ_3 shear stress in z-direction

τ_3^b value of τ_3 on the boundary

τ^* τ-coordinate of the yield surface center

τ^1 initial prestress in shear

τ^b boundary shear stress

τ^o shear stress coordinate where the slow-wave stress path starts

ϕ distance in the direction normal to characteristic lines in the x,t-plane in Appendix 1; an element of an eigenvector in Chaps. 3 and 4

ψ $d\sigma/d\tau$; an element of an eigenvector

CHAPTER 1

INTRODUCTION

1.1. PURPOSE

The general purpose of this study is to investigate the dynamic response of metal structural elements subjected to dynamic loads leading to combined-stress deformation beyond the elastic limit, with different material behavior assumptions. To accomplish this purpose, specific boundary value problems will be analyzed, dealing with a tension-torsion impact on a thin-walled tube and with plane waves from combined compressive and shear impact loading of a half space. These two cases are considered because they can be checked experimentally. (The transient response of the half space is the same as that of one of two impacting plates in a "plate-slap" experiment, until release waves arrive from the edges or reflections occur from the face opposite to the impacted face.)

Understanding the dynamic response of structural elements subjected to impact loads beyond the elastic

limit has practical value. Moreover the analysis under different material assumptions may, when experimental evidence becomes available, contribute to a better understanding of the material response and to the construction of better continuum theories of plasticity.

The plastic behavior of metals is not adequately accounted for by any of the present theories, especially the hardening behavior during combined-stress deformation. Several different idealizations have been proposed, but only two of them, namely isotropic hardening and kinematic hardening (see Chapter 2), have received much attention in the literature. Actual material behavior is probably intermediate between the isotropic hardening and kinematic hardening idealizations, although some experimental evidence indicates that sometimes a corner develops on the yield surface in stress space at the active point, a result not predicted by either isotropic hardening or kinematic hardening. The thin-walled tube analyses in this study assume a combination of isotropic hardening and kinematic hardening. The half space analyses assume isotropic hardening.

The hardening assumptions and the constitutive equations of plasticity are presented in Chapter 2 after

the background history on plasticity and on plastic wave

propagation is reviewed in Section 1.2, and the scope of

the present study outlined in Section 1.3.

1.2   BACKGROUND HISTORY

1.2.1   Theory of Plasticity

When a part of a metallic body is deformed beyond

its elastic limit, the part is said to become plastic.

Constitutive equations, i.e., the mathematical descrip-

tions of physical relations, in the plastic state, are

still not well established, although the plasticity of

metals has been studied extensively since Tresca,* in

1864, published a preliminary account of experiments on

punching and extrusion, which led him to formulate the

yield condition now given his name. Tresca proposed that

a metal yields plastically (i.e., exceeds the elastic

limit) when the maximum shear stress attains a critical

---

*For references to the early papers on plasticity men-
tioned in this section, see Hill (1950). Dates given
in parentheses refer to books and papers referenced in
the bibliography at the end of this thesis.

value. In 1871, Lévy proposed a three-dimensional rela-
tion between stress and plastic strain. Von Mises in
1913 also independently proposed equations similar to
those given by Lévy. Prandtl in 1924 for the plane prob-
lem, and Reuss in 1930 and R. Schmidt in 1932 for three-
dimensional problems generalized the Lévy-Mises theory--
bringing elastic strains and work-hardening within the
framework of the Lévy-Mises theory.

The yield condition usually called the Mises
yield condition was proposed by Von Mises in 1913 and in-
dependently by Huber in 1904. The Mises yield condition,
which stipulates that yield occurs when the second invar-
iant of the deviatoric stress reaches a critical value,
is the most widely used yield condition. It gives good
agreement with experimental observations for the initial
yield of most polycrystalline metals, when the crystallite
orientation is reasonably random and the grain size is
small compared to the dimensions of the yielding region.
When plastic deformation leads to residual stresses and
preferred orientation of the crystallites, neither the
Mises yield condition nor any other isotropic yield con-
dition is really accurate for a subsequent loading. This
is because the hardening is not isotropic.

In a series of papers beginning in 1950, Drucker showed that in a stable work-hardening plastic material, the yield function (a function of the stresses) is also a plastic potential function, such that the plastic natural strain rates (plastic rate-of-deformation components) are in the same proportion as the partial derivatives of the yield function with respect to the stresses; see Drucker (1951). Thus, if the yield condition is $f(\sigma_{pq}) = $ constant, where f is a function of the nine stress components σ_{pq}, then

$$\dot{\epsilon}^p_{ij} = \dot{\lambda}\frac{\partial f}{\partial \sigma_{ij}} \qquad (1.1-1)$$

where the $\dot{\epsilon}^p_{ij}$ are the plastic natural strain rates, and $\dot{\lambda}$ is a scalar function to be determined by the hardening behavior. If the equation f = constant is visualized as a hypersurface in a nine-dimensional space where the nine σ_{ij} are Cartesian coordinates, then Equation (1.1-1) implies that the vector whose nine components are $\dot{\epsilon}^p_{ij}$ is parallel to the normal to the yield surface at the active point (the outer normal for the usual definitions of f and $\dot{\lambda}$).

When the yield function f is the second invariant of the deviatoric stress components, then $\frac{\partial f}{\partial \sigma_{ij}} = \sigma'_{ij}$, and the "plastic potential theory" of Equation (1.1-1) implies

$$\dot{\epsilon}^p_{ij} = \dot{\lambda} \, \sigma'_{ij} \, , \tag{1.1-2}$$

where

$$\sigma'_{ij} = \sigma_{ij} - \frac{1}{3} \, \delta_{ij} \sigma_{kk}$$

is the deviatoric stress. Equation (1.1-2) is precisely the Lévy-Mises stress-strain relation mentioned above. Thus plastic potential theory shows that the Mises yield condition implies the Lévy-Mises equations.

The Lévy-Mises equations and the Mises yield condition, suitably modified for the kinematic hardening cases, will be used throughout the present study.

The Lévy-Mises equations are the most widely used incremental plasticity theory, so called because it gives the increment of plastic strain $d\epsilon^p_{ij} = d\lambda \, \sigma'_{ij}$ instead of the total strain.

Hencky in 1924 proposed a small-strain plastic theory, alternatively known as "total-strain or deformation theory," which gives the total strains. It has the

advantage of simplicity, and it agrees with the predictions of the Lévy-Mises theory when the loading path is a straight line radially outward from the origin in stress space. For a more detailed review of the early historical background of the theory of plasticity, see: Hill (1950).

World War II, the advent of high speed computers and development in experimental techniques have stimulated work in the theory of plasticity, and extensive studies of non-elastic metal behavior under dynamic loads have been going on in the United States and in the Soviet Union for the last three decades.

1.2.2   Plastic Wave Propagation

The entire field of dynamic plasticity is of comparatively recent origin. L. H. Donnell (1930) analyzed the problem of a uniaxial stress pulse propagating in the longitudinal direction of a nonlinear elastic thin bar. He regarded the transient loading pulse as a superposition of stress increments, each traveling at its appropriate speed $c_p = (E_t/\rho)^{\frac{1}{2}}$, where E_t is the tangent modulus and

ρ is the mass density of the material of the bar. The idea was an extension of the linear elastic bar speed $c_o = (E/\rho)^{\frac{1}{2}}$. Donnell showed that such a wave suffers a change in form as it moves along the bar. For the loading part of the pulse the nonlinear elastic wave does not differ from a plastic wave in a rate-independent plastic material.

More than a decade later Von Kármán in the United States, Taylor in Great Britain, and Rakhmatulin in the Soviet Union, working independently of each other, derived the partial differential equations for plane longitudinal plastic waves in thin bars. In treating the problem, Von Kármán and Duwez (1946) and Rakhmatulin (1945) used Lagrangian coordinates and derived a single second order nonlinear wave equation for the axial displacement. Taylor (1942) developed the basic theory of one-dimensional finite-amplitude plastic wave propagation using Eulerian coordinates and observed that the governing equations were formally identical with those for the propagation of one-dimensional finite-amplitude waves in an ideal compressible fluid (the pressure being a function only of the density). He noted that, when suitable transformations

of the coordinates are made, his theory was similar to
that of Von Kármán (the essential equivalence was estab-
lished by Bohnenblust and others*).

A series of longitudinal impact tests were per-
formed By Duwez, Clark and others* to check the validity
of the Von Kármán theory. The results were in fairly
good agreement with the theory, but there were some dis-
crepancies. In particular, in some of the early tests
it appeared that the force-time variation at the fixed
end of the bar showed higher stress than the theory pre-
dicted, which indicated that stress increments were propa-
gated at a higher wave speed than predicted. It was sug-
gested that these discrepancies might be due to strain-
rate effect.

To explain the discrepancies exhibited by Von
Kármán theory, many authors have proposed various consti-
tutive equations for materials that exhibit a rate effect.
For a work-hardening material Malvern (1949) solved the
bar problem on the basis of a constitutive relation of
the form

---

*The reference to these papers can be found in a survey
 article by H. G. Hopkins (1966).

$$E\dot{\epsilon} = \dot{\sigma} + g(\sigma, \epsilon)$$

where g is an arbitrary function expressing the strain

rate dependence. He obtained numerical results only for

g of the form $g[\sigma-f(\epsilon)]$, where $\sigma = f(\epsilon)$ is the static

stress-strain relation. Sokolovskii (1948) had already

considered a special case of this constitutive relation

for non-workhardening material.

More recent experimental studies have shown that

the rate-independent theory gives a good account of fin-

ite amplitude waves in bars of copper, steel, and annealed

aluminum alloys, if a single dynamic stress-strain curve

is used, not explicitly containing rate effects. See,

for example, Bell (1965). Some impact experiments in

one-dimensional strain ("plate-slap") [Barker, Lundergan,

and Herrmann (1964), Butcher and Karnes (1966)] have indi-

cated that no single dynamic curve can correlate their

results, while a Malvern-type rate-effect law can. There

is also some evidence that the rate-dependent theory gives

a better account of the propagation of the leading edge of

an incremental plastic wave traveling into a prestressed

plastic region. See the discussion by Williams and Mal-

vern (1969). In the present study the effect of rate de-

pendence on the constitutive equations will not be included.

For additional details of the history of plastic wave propagation, see: Hopkins (1966), Cristescu (1967), and Craggs (1961).

Most of the papers cited so far have been connected with waves of uniaxial stress. Craggs does present a derivation of the wave speeds for combined-stress plane waves in an unbounded medium (based on a paper published by Craggs in 1957), and Cristescu includes some treatment of combined-stress waves in his book.

1.2.3   Combined-Stress Plastic Waves

The study of stress wave propagation in metals is not always simple even when there is perfect elastic behavior. When the metal behavior is nonelastic, it becomes quite complex even when there is only one stress component acting. The complexity is compounded for combined-stress plastic waves. Craggs (1957) derived the wave speeds for combined-stress plane waves in an unbounded medium (for small strain and rotation). He found that quite generally there are two wave speeds, a fast wave speed c_f and a slow wave speed c_s, such that

$$c_s \leq c_2 \leq c_f \leq c_1,$$

where c_1 is the elastic dilatational wave speed and c_2 is the elastic shear wave speed. See also Craggs (1961).

Rakhmatulin (1958) studied analytically the problem of combined-stress loading in the edge impact of two plates with the velocities of impact directed in the planes of the plates and oblique to the impacting faces, assuming zero normal strain in the direction parallel to the impacting faces and the plane of the plates, and using total-deformation theory. Rakhmatulin assumed that in the case of combined-stress in a plastic body, resulting from an impact, there propagates at first a plastic uniaxial stress state II followed by a constant state III, then a combined-stress state propagating as a wave of strong discontinuity $x = bt$ followed by a constant state IV. See Fig. 1.1. Cristescu (1959) considered another possible solution of the same equations established by Rakhmatulin, and postulated that combined dynamic stress is transmitted in a body only by combined stress waves, either continuous waves or waves of strong discontinuity. For an instantaneous loading, he asserted, one will have four regions:
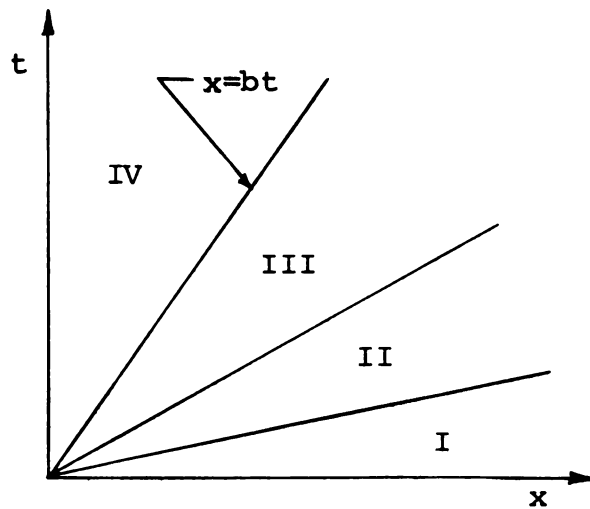
Fig. 1.1

the region I is not deformed, the region II is an elastic

region, and the regions III and IV are plastic regions,

which may be separated from each other or from region II

by a combined-stress plastic wave of strong discontinuity.

See Fig. 1.1.

Bleich and Nelson (1965) presented a closed form

solution for the case of a uniformly distributed step

load of pressure and shear on a half space for an elastic,

perfectly plastic material.

Clifton (1966) presented the solution of a thin-

walled cylindrical tube with end impacts in torsional

shear and axial compression for an elastic-plastic iso-

tropic hardening material. He concurred with Cristescu's

conclusion that there could be a plastic simple wave of

combined stress, but he disagreed with Cristescu in that, according to Clifton, (1) a wave of strong discontinuity occurs only in elastic regions, and (2) a leading uniaxial plastic wave exists for a step load of normal stress and shear. A part of the present study considers the same problem formulated by Clifton for the thin-walled tube, but the material behavior assumed is a combination of isotropic hardening and kinematic hardening.

Ting and Nan (1968) generalized the half space problem treated by Bleich and Nelson to a general elastic-plastic isotropic hardening material. Ting (Dec. 1968) gave a formulation of the partial differential equations for a general plane wave in a half space. In another paper (May 1968) Ting also solved a boundary value problem for a half space with two shear loadings and no compressive loading. A part of the present study uses a formulation similar to Ting's formulation for the general plane wave in a half space, but treats boundary loadings not treated by Ting or Ting and Nan. Nan (1968) obtained numerical solutions for a half space subjected to two impact loads in shear or one compression and one shear.

1.3   SCOPE OF THE STUDY

The study presently reported was undertaken to

(1)   understand the effect of a combination of iso-
      tropic and kinematic material hardening assump-
      tions,

(2)   carry out some simple wave solutions for a general
      plane wave in a half-space,

(3)   carry out nonsimple wave solutions of a plane
      wave in a half-space.

For (1), examples of a semi-infinite thin-walled cylin-
drical tube subjected to normal and shear step loads at
the boundary have been solved, while for (2), a half
space of isotropic hardening material with uniformly
distributed pressure and two independent shear loads on
the boundary was considered. For the nonsimple wave
solutions only one shear load and a compressive load
were considered to be acting on the boundary of the half
space, in such a combination that simple waves do not
result.

The stress-strain curve for simple tension was assumed to be concave toward the strain axis, and independent of the rate of strain. The curve was also assumed smooth at yield. It was assumed that the material satisfies Mises yield condition (suitably modified for the kinematic hardening cases), that the elastic and plastic strain rates are additive, and that the plastic strain rate is related to the yield function by plastic potential theory. In other words, the constitutive theory is the same as the quasi-static elastic-plastic theory. The analysis differs only in that the inertia terms are included.

Chapter 2 gives the formulation of the constitutive equations for an elastic, plastic strain-hardening material governed by the Mises yield condition under the assumptions of isotropic hardening, kinematic hardening, and combined isotropic and kinematic hardening. In Chapter 3, simple wave solutions for a thin-walled tube under tension-torsion impact are obtained for the different hardening assumptions. The characteristic conditions that would be used for a numerical nonsimple wave solution are also given in Chapter 3, although no such numerical solutions for the tube case are included in this study.

In Chapter 4, simple wave solutions for loading of a half space of isotropic hardening material by combined compression and two independent shear loadings are given. A formulation for nonsimple wave numerical solutions in a half space is also given in Chapter 4; the numerical scheme used is an adaptation of the one developed by Vitiello and Clifton (1967) for the thin-walled tube.

In Chapter 5 the specific problems solved are further described and the results and conclusions presented. These results show both quantitative and qualitative differences between the simple-wave solutions for isotropic hardening obtained previously by Clifton (1966) and the solutions for kinematic hardening or combined kinematic and isotropic hardening. For example, with some boundary conditions the solutions assuming kinematic or combined kinematic and isotropic hardening show a discontinuity in shear stress propagating at the elastic shear wave speed c_2, while isotropic hardening predicts no discontinuity for those particular boundary conditions.

The half-space simple-wave solution for step-function loading by compression and two shears reduces

to the result for loading by compression and a single shear, previously obtained by Ting and Nan (1968), when there is no initial prestress beyond yield, since the simple-wave equations require the ratio of the two shear stresses to be constant. But when the half space is pre-stressed statically beyond yield by shear in one direction there may occur a fast simple wave with a constant ratio of the two shear stress components followed by a slow simple wave with a different constant ratio of the two shear stress components. The transition from the fast wave to the slow wave involves a discontinuity in both shear stress components propagating at the elastic shear wave speed c_2. This discontinuity wave either follows immediately after the fast simple wave, or in some cases it may be separated from the fast wave by a constant state region in the x,t-plane.

One specific example of a numerical solution is given for nonsimple waves in a half space loaded by compression and shear boundary tractions that increase linearly with time after the initial impact in such a way that simple waves are not produced.

CHAPTER 2

WORK HARDENING ASSUMPTIONS

2.1   INTRODUCTION

The question of just how the yield function

changes during plastic deformation under combined stresses

is a very important one. Several hardening hypotheses

have been proposed for incorporation into phenomenolog-

ical theories of plasticity, all failing to account for

all the phenomena observed. Only two of the hypotheses

have received much attention.

The oldest and most widely used assumption is

that of isotropic hardening, which assumes that the yield

surface in stress space maintains its shape, center, and

orientation, while its size increase is defined by a

single parameter depending on the plastic deformation

or on the plastic work done. Hill (1950) attributes

the earliest formulations of isotropic hardening for com-

bined stresses (with elastic strains neglected) to Taylor

and Quinney in 1931, Schmidt in 1932, and Odquist in 1933.

The isotropic-hardening assumption has been fairly

successful in correlating different kinds of radial paths
in stress space (paths, such that the stress components
maintain their ratios as they increase). See, for example,
Lubahn and Felgar (1961). But the isotropic-hardening
assumption has not been so successful when the loading is
not radial and especially when unloading and reversed
loading occur.

For such reversed loadings, most metals exhibit
a Bauschinger effect, such that the yield stress for the
reversed loading is smaller in magnitude than it would be
for continued loading in the original direction and may
even be smaller than the yield stress would have been for
an initial loading in the reverse direction. See, for
example, Lubahn and Felgar (1961). The Baushinger effect
is illustrated schematically for a uniaxial stress load-
ing in Fig. 2.1 where Y_R is the yield stress after re-
versal while Y is the yield stress for continued loading
in the original direction, and Y_O is the initial yield
stress. Isotropic hardening would require $Y_R = -Y$ and
therefore implies no Bauschinger effect.

The simplest hypothesis incorporating a Bauschin-
ger effect is <u>Prager's kinematic-hardening</u> assumption,
where the yield surface does not change its size, shape,
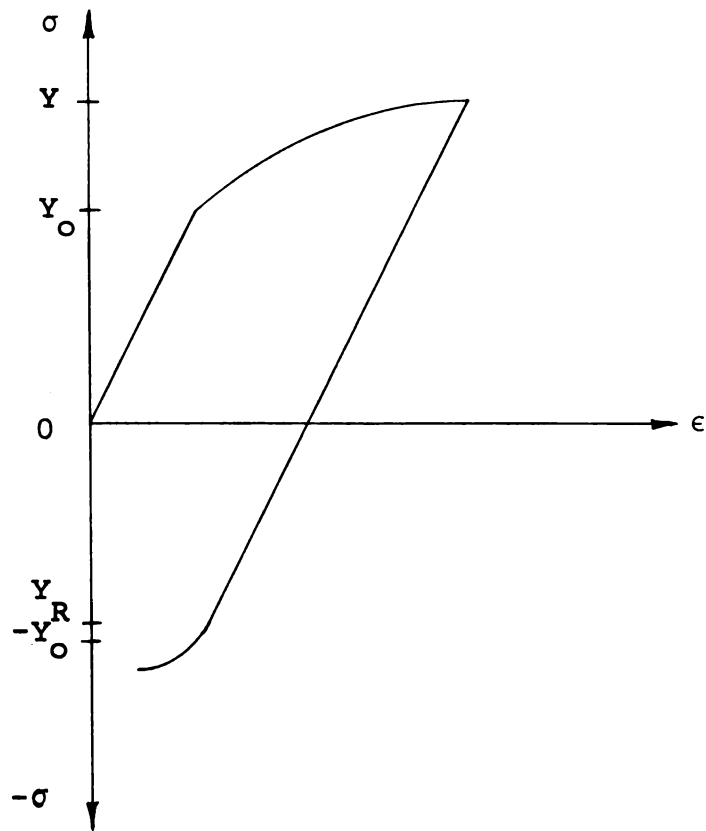
Fig. 2.1.--Bauschinger effect for uniaxial stress
      (schematic)

or orientation but merely translates in stress space in

such a way that its center always moves in a direction

parallel to the normal to the yield surface at the active

point.

Hodge (1957) and Ke-chzhi (1958) have introduced

combinations of kinematic hardening with isotropic harden-

ing. The present study will examine the effect on com-

bined-stress waves in a thin-walled tube of varying the

mixture of the two hardening assumptions. The basis for
the combination will be discussed in connection with the
normal component of the motion of the local surface ele-
ment of the yield surface in stress space.

Fig. 2.2.--Yield surface in stress space (schematic).

Figure 2.2 is a schematic illustration of the
yield surface in stress space; it should be understood
to represent a hypersurface in a nine-dimensional

Euclidean space in which the nine stress components σ_{ij} are Cartesian coordinates. The vector $\underset{\sim}{\sigma}$ in this space represents the state of stress, while the vector $\underset{\sim}{\alpha}$ is the position vector of the center of the yield surface and $\underset{\sim}{\xi} = \underset{\sim}{\sigma} - \underset{\sim}{\alpha}$.

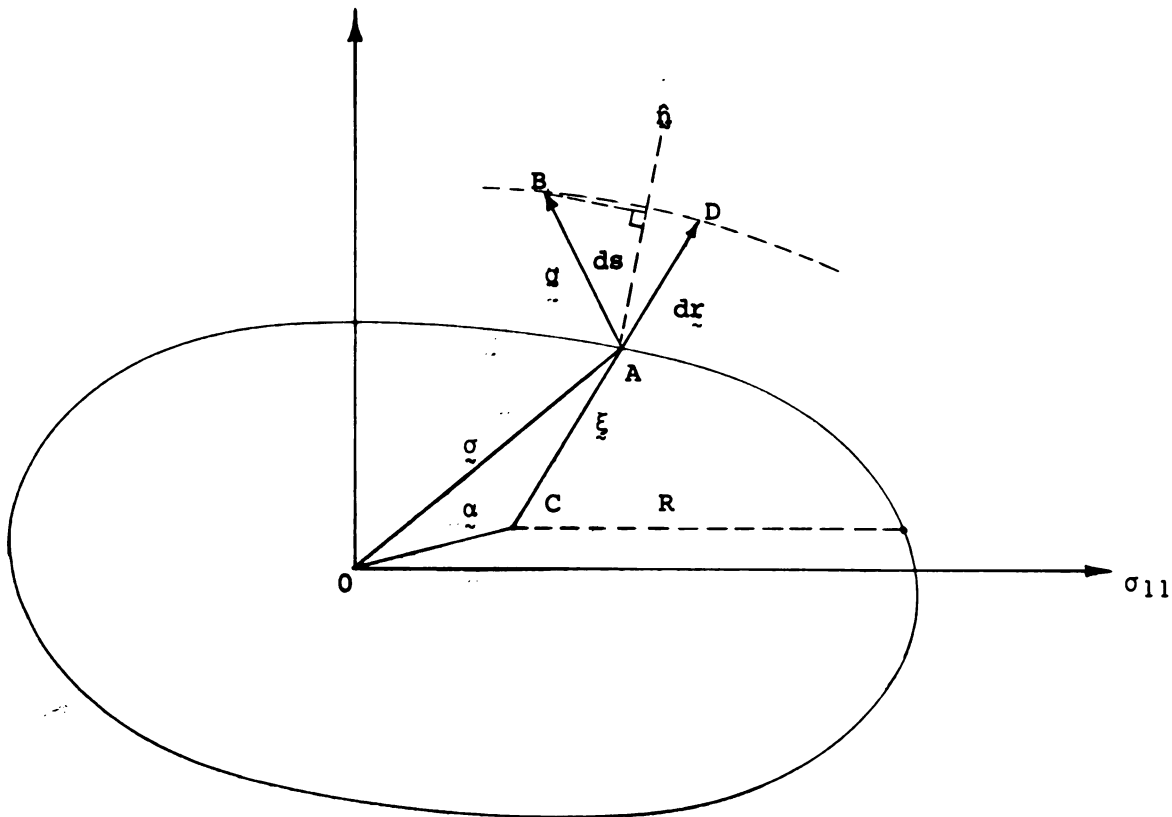For purely isotropic hardening we have $\underset{\sim}{\alpha} = o$ and $\underset{\sim}{\sigma} = \underset{\sim}{\xi}$, and the origin O coincides with the center C. Then, for any infinitesimal incremental loading $d\underset{\sim}{\sigma}$, the yield surface simply expands, and the normal component $ds = d\underset{\sim}{r} \cdot \hat{n}$ of the motion of the surface element is equal to $d\underset{\sim}{\sigma} \cdot \hat{n}$. Here $d\underset{\sim}{r}$ denotes the vector from A to D; it would coincide with $d\underset{\sim}{\sigma}$ if the new loading were radially outward from the previous center to the subsequent yield surface.

For purely kinematic hardening, we have again $ds = d\underset{\sim}{\sigma} \cdot \hat{n}$, but this time the motion of the surface element is entirely in the normal direction, and it is caused by a translation of the whole surface rather than by an enlargement.

For combined kinematic and isotropic hardening, the normal motion ds will be taken to be the sum of a part produced by enlargement and a part produced by

translation. This combined hardening will be discussed in Section 2.4. First we shall consider isotropic hardening and kinematic hardening separately in Sections 2.2 and 2.3.

2.2   ISOTROPIC HARDENING

This simple assumption is the only one that has received extensive application. According to the isotropic hardening assumption the yield surface merely enlarges, with its size governed by a single parameter, as was pointed out in Section 2.1. What remains to discuss is how the size parameter depends upon the deformation and how this is related to the normal component ds of the motion of the local surface element. The magnitude of this single parameter is usually assumed to depend on the plastic deformation by one of the following two schemes, which are equivalent when used with the Mises yield condition. According to the first scheme, a uni-versal plastic stress-strain curve is assumed to relate two scalar quantities, the effective stress $\bar{\sigma}$ (measuring the size of the yield surface) and the integral of the

effective plastic strain increment $\overline{d\epsilon}^p$, while the second

scheme assumes that $\overline{\sigma}$ is a single-valued function of the

total plastic work $W_p = \int \sigma_{ij}\, d\epsilon^p_{ij}$. When the Mises yield

condition is used, $\overline{\sigma}$ and $\overline{d\epsilon}^p$ are defined as follows.

See, for example, Hill (1950).

$$\overline{\sigma} = (3J_2')^{\frac{1}{2}} = (\frac{3}{2}\, \sigma'_{ij}\, \sigma'_{ij})^{\frac{1}{2}} \qquad (2.2-1)$$

$$\overline{d\epsilon}^p = (\frac{4}{3}\, I_2)^{\frac{1}{2}} = (\frac{2}{3}\, d\epsilon^p_{ij}\, d\epsilon^p_{ij})^{\frac{1}{2}} \qquad (2.2-2)$$

Here the σ_{ij} are the components of the stress tensor for

$i,j = 1,2,3$ while the primes denote the deviatoric stress

components. Repeated letter subscripts imply summation.

J_2' and I_2 are the second invariants of the deviatoric

stress tensor and the plastic strain increment tensor

respectively. The numerical factors in Equations (2.2-1)

and (2.2-2) are so chosen that, for a uniaxial stress

state, $\overline{\sigma}$ and $\overline{d\epsilon}^p$ reduce to σ_{11} and $d\epsilon^p_{11}$ respectively.

Hence the assumption of a universal stress strain curve

$$\overline{\sigma} = F[\int \overline{d\epsilon}^p] \qquad (2.2-3)$$

permits the determination of the function F, in principle,

by a single stress-strain curve in simple tension. The

assumption that one universal stress-strain curve governs

all possible combined-stress loadings of a given material

is a very strong one, but it has been fairly successful

in correlating radial paths in stress space.

How does the assumption of Equation (2.2-3) re-

late to the motion of the yield surface element in the

stress space? Fig. 2.2 is reproduced in Fig. 2.3 for

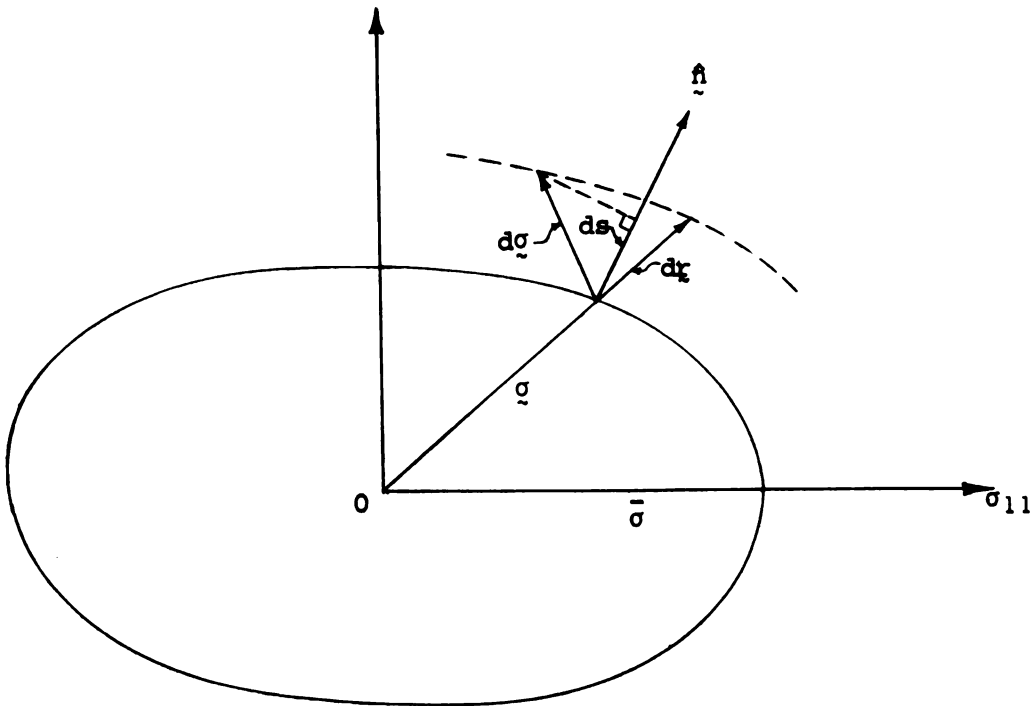the isotropic hardening case where $\underset{\sim}{\alpha} \doteq 0$ and $\underset{\sim}{\xi} \equiv \underset{\sim}{\sigma}$.

Fig. 2.3.--Isotropic hardening case (schematic)

For isotropic hardening all radii increase in proportion.

Thus

$$d\underset{\sim}{r} = (d\overline{\sigma}/\overline{\sigma})\underset{\sim}{\sigma}, \qquad (2.2\text{-}4)$$

and

$$ds = d\underset{\sim}{r} \cdot \hat{n} = (d\overline{\sigma}/\overline{\sigma})\underset{\sim}{\sigma} \cdot \frac{d\underset{\sim}{\epsilon}^P}{|d\underset{\sim}{\epsilon}^P|} \qquad (2.2\text{-}5)$$

since $d\underset{\sim}{\epsilon}^P$ is parallel to the normal at the active point of the yield surface, by plastic potential theory, if the $d\epsilon_{ij}^P$ coordinate directions are superposed on the σ_{ij} directions of the stress space. Let g denote the slope of the universal stress-strain curve of Equation (2.2-3). Then, since $|d\underset{\sim}{\epsilon}^P| = \sqrt{\frac{3}{2}}\,\overline{d\epsilon}^P$, and $\frac{d\overline{\sigma}}{\overline{d\epsilon}^P} = g$, Equation (2.2-5) yields

$$ds = \sqrt{\frac{2}{3}}\,\frac{g}{\overline{\sigma}}\,\underset{\sim}{\sigma}\cdot d\underset{\sim}{\epsilon}^P . \qquad (2.2\text{-}6)$$

For the Mises yield condition, the plastic work increment is

$$\overline{\sigma}\,\overline{d\epsilon}^P = \underset{\sim}{\sigma}\cdot d\underset{\sim}{\epsilon}^P , \qquad (2.2\text{-}7)$$

whence

$$ds = \sqrt{\frac{2}{3}}\,g\,\overline{d\epsilon}^P = \frac{2}{3}g\,|d\underset{\sim}{\epsilon}^P| . \qquad (2.2\text{-}8)$$

The last result is a form convenient to work with later on.

Attempts to construct a more complicated iso-
tropic hardening theory than the one based on the Mises
yield condition have met with little success because of
the inherent inaccuracy of isotropic hardening, which
always neglects the Bauschinger effect. The simplest
assumption incorporating a Bauschinger effect is Prager's
kinematic hardening.

2.3   PRAGER'S KINEMATIC HARDENING

Prager (1956) proposed an alternative assumption,
which he called kinematic hardening. In kinematic hard-
ening the yield surface in stress space does not change
its size, shape or orientation, but merely translates in
the direction of its normal at the active point. Thus
an initial yield surface $f(\sigma_{ij}) = 0$ is changed into

$$f(\sigma_{ij} - \alpha_{ij}) = f(\xi_{ij}) = 0 , \qquad (2.3\text{-}1)$$

where ξ_{ij} and α_{ij} are the nine components of $\underline{\xi}$ and $\underline{\alpha}$,
respectively, defined in Section 2.1.

Prager assumed that the plastic strain history
determines the α_{ij} history as follows. The time deriva-
tives $\dot{\alpha}_{ij}$ and $\dot{\epsilon}^p_{ij}$ are assumed to be related by

$$\dot{\alpha}_{ij} = b \ \dot{\epsilon}^{p}_{ij} \ , \qquad\qquad (2.3\text{-}2)$$

where b is a scalar function, whose dependence on the deformation history is to be specified. Hodge (1957) pointed out that the concept of kinematic hardening must be applied in the nine-dimensional stress space even when the loading is such that some of the stress components are zero. Apparently all applications up to the present have assumed linear kinematic hardening in which the parameter b does not change during the deformation. In order to make the hardening prediction reduce in uniaxial tension to a stress-strain curve with a nonlinear plastic range, it will be assumed in the present study that b is the same function of the accumulated effective strain $\int\overline{d\epsilon}^{p}$ in a combined-stress deformation as it is in uniaxial tension. There is of course no fundamental justification for making this assumption (or for assuming kinematic hardening). But it leads to a stress-strain history which coincides with the predictions of isotropic hardening when the loading is radial, and isotropic hardening has been fairly successful in radial loadings.

In a uniaxial tension loading σ_{11} the nonzero components of the unit normal $\hat{n}$ to the yield surface are proportional to the nonzero deviatoric stresses.

$$\sigma'_{11} = \frac{2}{3} \sigma_{11}$$

$$\sigma'_{22} = \sigma'_{33} = -\frac{1}{3} \sigma_{11} \qquad (2.3\text{-}3)$$

Hence, for uniaxial σ_{11},

$$\hat{n} = \frac{2}{\sqrt{6}} \hat{e}_{11} - \frac{1}{\sqrt{6}} \hat{e}_{22} - \frac{1}{\sqrt{6}} \hat{e}_{33} \qquad (2.3\text{-}4)$$

where each $\hat{e}_{ij}$ is a dimensionless unit vector in the direction of the σ_{ij} axis in the stress space. Since $d\underset{\sim}{\sigma} = d\sigma_{11} \hat{e}_{11}$, we have

$$ds = d\underset{\sim}{\sigma} \cdot \hat{n} = \frac{2}{\sqrt{6}} d\sigma_{11} . \qquad (2.3\text{-}5)$$

Also, in general, purely kinematic hardening implies

$$ds = |d\underset{\sim}{\alpha}| = b \, |d\underset{\sim}{\epsilon}^p| . \qquad (2.3\text{-}6)$$

Hence, for uniaxial tension σ_{11}, kinematic hardening gives

$$ds = \sqrt{\frac{3}{2}} \, b \, d\epsilon_{11}^p . \qquad (2.3\text{-}7)$$

From equating the two expressions for ds given in Equations (2.3-5) and (2.3-7) it follows that, in uniaxial tension,

$$b = \frac{2}{3} \, (d\sigma_{11}/d\epsilon_{11}^p) = \frac{2}{3} \, g , \qquad (2.3\text{-}8)$$

where g is the slope of the curve of stress versus plastic strain. In a combined-stress deformation with kinematic

hardening, it will be assumed that b is two-thirds of the slope of the uniaxial curve at the point on the curve where ϵ_{11}^p is equal to the value that $\int \overline{d\epsilon}^p$ has in the combined-stress case.

Since the Mises yield condition will be used, the normal to the yield surface will have no component in the direction of the hydrostatic line $\sigma_{11} = \sigma_{22} = \sigma_{33}$. Hence the normal component of the surface-element motion will be parallel to the deviatoric hyperplane

$$\sigma_{11} + \sigma_{22} + \sigma_{33} = 0 \ . \tag{2.3-9}$$

Thus

$$d\underset{\sim}{\sigma} \cdot \hat{\underset{\sim}{n}} = d\underset{\sim}{\sigma}' \cdot \hat{\underset{\sim}{n}} = ds \ , \tag{2.3-10}$$

and

$$d\underset{\sim}{r} \cdot \hat{\underset{\sim}{n}} = d\underset{\sim}{r}' \cdot \hat{\underset{\sim}{n}} = |d\underset{\sim}{r}'| = ds, \tag{2.3-11}$$

where $d\underset{\sim}{\sigma}'$ is the deviatoric stress increment with components $d\sigma_{ij}'$ and $d\underset{\sim}{r}'$ is the deviator of $d\underset{\sim}{r}$. (For the Mises yield condition, the normal is parallel to $\underset{\sim}{\xi}'$ and hence to $d\underset{\sim}{r}'$.)

For any radial loading under combined stresses, both $\hat{\underset{\sim}{n}}$ and $d\underset{\sim}{\sigma}'$ will be parallel to $\underset{\sim}{\sigma}'$ and the center moves on the line from the origin to the deviatoric stress point

at the initial yield, so that $\underset{\sim}{\xi}'$ is also parallel to $\underset{\sim}{\sigma}'$.
Then for radial loading

$$ds = d\underset{\sim}{\sigma} \cdot \hat{\underset{\sim}{n}} = d\underset{\sim}{\sigma}' \cdot \hat{\underset{\sim}{n}} = |d\underset{\sim}{\sigma}'| \ . \qquad (2.3\text{-}12)$$

Also

$$ds = b|d\underset{\sim}{\epsilon}^p| = \frac{2}{3} g \ |d\underset{\sim}{\epsilon}^p| \ , \qquad (2.3\text{-}13)$$

whence for radial loading

$$|d\underset{\sim}{\sigma}'| = \frac{2}{3} g \ |d\underset{\sim}{\epsilon}^p| \qquad (2.3\text{-}14)$$

or

$$\sqrt{\frac{2}{3}} \, d\overline{\sigma} = (\frac{2}{3} g) \sqrt{\frac{3}{2}} \, \overline{d\epsilon}^p \qquad (2.3\text{-}15)$$

Thus for combined-stress radial loading this kind of kinematic hardening gives

$$d\overline{\sigma} = g \ \overline{d\epsilon}^p \qquad (2.3\text{-}16)$$

where g is the same function of $\int \overline{d\epsilon}^p$ as it is in uniaxial
tension, in agreement with the predictions of isotropic
hardening based on the same uniaxial curve.

There is some evidence (see, for example, Naghdi
(1960)) that the kinematic hardening assumption in some
cases predicts phenomena better than does isotropic

hardening, although such a simple assumption cannot give
an accurate account of the extremely complex actual ma-
terial behavior. It is expected that a combination of
the above two assumptions might offer an improvement
over the separate ones.

2.4 COMBINED ISOTROPIC AND KINEMATIC HARDENING

Hodge (1957) has used combined isotropic and
kinematic hardening in a general approach to the problem
of piecewise linear plasticity. He assumed Tresca's
yield condition for the initial yield. A similar formu-
lation was given by Ke-chzhi (1958). In the present in-
vestigation, a combination of isotropic and kinematic
hardening is also used, but with the Mises yield condi-
tion and without any restriction to linear hardening.
It is assumed that the total hardening is a combination
of expansion and translation of the yield surface in the
stress space.

In Fig. 2.2 the solid curve gives schematically
the instantaneous position of the yield surface, while
the dashed curve represents a portion of the new yield

surface after an infinitesimal stress increment $d\underset{\sim}{\sigma}$. The

normal component ds $\underset{\sim}{\hat{n}}$ of the motion of the local surface

element at A will be considered to be the sum of a motion

produced by expansion of the surface from its current

center C (as in isotropic hardening from the center 0)

and a translation of the surface in the direction of the

normal $\underset{\sim}{\hat{n}}$ at A. The portion ds_1 of ds caused by the ex-

pansion can be calculated as in Section 2.2, if $\overline{\sigma}$ is re-

placed everywhere by R. Here

$$R = (\frac{3}{2} \xi_{ij}' \xi_{ij}')^{\frac{1}{2}}$$

is the radius of the current yield surface in a direction

parallel to the σ_{11} axis, just as $\overline{\sigma} = (\frac{3}{2} \sigma_{ij}' \sigma_{ij}')^{\frac{1}{2}}$ was

when the center remained at the origin 0. From Equation

(2.2-8), the result is

$$ds_1 = \frac{2}{3} \frac{dR}{d\overline{\epsilon}^p} \mid d\underset{\sim}{\epsilon}^p \mid ,\qquad (2.4-1)$$

where $dR/d\overline{\epsilon}^p$ would be equal to g, the slope of the uni-

axial σ_{11} versus ϵ_{11}^p curve at the point where ϵ_{11}^p equals

the current value of $\int d\overline{\epsilon}^p$, if the incremental hardening

were all associated with expansion of the yield surface

from the current center C. The translation of the yield

surface causes additional motion. Let this translation be denoted by ds_2; it can be written as

$$ds_2 = b \mid d\underset{\sim}{\epsilon}^P \mid \qquad (2.4-2)$$

as explained in Section 2.3. If there were no incremental expansion, we would have $b = \frac{2}{3} g$, and $dR/d\bar{\epsilon}^P = 0$.

When expansion and translation occur simultaneously, we let m denote the fraction of g accounted for by the expansion term and 1-m the fraction accounted for by the translation. Then

$$dR/d\bar{\epsilon}^P = mg \qquad (2.4-3)$$

$$b = \frac{2}{3}(1-m) g \qquad (2.4-4)$$

$$ds_1 = \frac{2}{3} mg \mid d\underset{\sim}{\epsilon}^P \mid \qquad (2.4-5)$$

$$ds_2 = \frac{2}{3}(1-m) g \mid d\underset{\sim}{\epsilon}^P \mid \ , \qquad (2.4-6)$$

and the total ds is

$$ds = \left[\frac{2}{3} \ dR/d\bar{\epsilon}^P + b \right] \mid d\underset{\sim}{\epsilon}^P \mid$$

$$\qquad\qquad (2.4-7)$$

$$= \frac{2}{3} g \mid d\underset{\sim}{\epsilon}^P \mid = \sqrt{\frac{2}{3}} \ g \ \overline{d\epsilon}^P \ .$$

The fraction m can also evidently be interpreted as the fraction of the total ds accounted for by the expansion, i.e. $ds_1 = m \, ds$, as the foregoing equations demonstrate. Thus

$$d\underset{\sim}{\sigma} \cdot \hat{n} = ds = \frac{1}{m} ds_1 = \frac{2}{3} g \left| d\underset{\sim}{\epsilon}^p \right| = \sqrt{\frac{2}{3}} g \, \overline{d\epsilon}^p \, ,$$

$$(2.4-8)$$

whence

$$d\underset{\sim}{\sigma} \cdot (\nabla f / |\nabla f|) = \sqrt{\frac{2}{3}} g \, \overline{d\epsilon}^p \, , \qquad (2.4-9)$$

where ∇f denotes the gradient of the yield function f.

For the Mises yield function,

$$f = \frac{1}{2} \xi'_{ij} \xi'_{ij} - k^2 = 0 \, , \qquad (2.4-10)$$

we have

$$\partial f / \partial \sigma_{ij} = \partial f / \partial \xi_{ij} = \xi'_{ij}$$

and

$$\qquad (2.4-11)$$

$$|\nabla f| = (\xi'_{ij} \xi'_{ij})^{\frac{1}{2}} = \sqrt{2} \, k \, .$$

Hence

$$d\underset{\sim}{\sigma} \cdot \nabla f = \xi'_{pq} \, d\sigma_{pq} \, , \qquad (2.4-12)$$

and Equation (2.4-9) furnishes the expression

$$\overline{d\epsilon}^p = \frac{\sqrt{3}}{2gk} \, \xi'_{pq} \, d\sigma_{pq} \tag{2.4-13}$$

which will be useful in transforming the plastic strain increment constitutive equation.

The fraction m is still to be assigned. It could be supposed to vary during the deformation, but in this investigation it will be assumed constant during the deformation, and the effect of assuming different constant values for m between zero and unity will be examined.

The plastic potential flow rule determines the plastic strain increments as follows

$$d\epsilon^p_{ij} = d\lambda \, \xi'_{ij} \, , \tag{2.4-14}$$

where $d\lambda$ is a scalar multiplier to be determined. Squaring and adding the nine component equations gives

$$d\epsilon^p_{ij} \, d\epsilon^p_{ij} = (d\lambda)^2 \, \xi'_{ij} \, \xi'_{ij} \tag{2.4-15}$$

or

$$\frac{3}{2} \, (\overline{d\epsilon}^p)^2 = (d\lambda)^2 \, (\frac{2}{3} \, R^2) \, , \tag{2.4-16}$$

whence

$$d\lambda = \frac{3}{2} \; (\overline{d\epsilon}^P/R) \qquad\qquad (2.4\text{-}17)$$

and Equation (2.4-14) becomes

$$d\epsilon^P_{ij} = \frac{3}{2} \; \frac{\overline{d\epsilon}^P}{R} \; \xi'_{ij} \; . \qquad\qquad (2.4\text{-}18)$$

This equation can be transformed by use of Equation (2.4-13) and $R = \sqrt{3}\; k$ to the form

$$d\epsilon^P_{ij} = [3/4gk^2] \; [\xi'_{pq} \; d\sigma_{pq}] \; \xi'_{ij}$$

$$(2.4\text{-}19)$$

$$= H \; [\xi'_{pq} \; d\sigma_{pq}] \; \xi'_{ij} \; ,$$

where

$$H = 3/4gk^2 \; . \qquad\qquad (2.4\text{-}20)$$

The last Equation (2.4-19) is the form that will be used in Chapter 3. It should be recalled that g is the slope of the uniaxial curve of σ_{11} versus ϵ^P_{11} at the point where ϵ^P_{11} equals the current value of $\int \overline{d\epsilon}^P$ in the combined-stress deformation, and that $k^2 = \frac{1}{2} \; \xi'_{ij} \; \xi'_{ij}$ is not a constant except in the case of purely kinematic hardening.

It should also be noted that in the usual formulation of combined-stress plasticity theory the strain increments $d\epsilon_{ij}$ are the natural strain increments, such that

$$\frac{d\epsilon_{ij}}{dt} = D_{ij} = \frac{1}{2} (\frac{\partial v_i}{\partial x_j} + \frac{\partial v_j}{\partial x_i}) ,$$

where the D_{ij} are the components of the rate of deformation tensor, and the x_k are spatial or Eulerian coordinates. The natural-strain increments are approximately equal to the increments of Lagrangian small strain in a finite body when the displacement gradient components are everywhere small compared to unity. In the combined-stress wave propagation problems to be considered, the displacement gradients will be sufficiently small that the ϵ_{ij} may be interpreted as Lagrangian small strains.

The stress components of the combined-stress plasticity theory are also the usual Cauchy stress components σ_{ij}, defined relative to the deformed configuration. In Appendix 2 it is shown that, for the small strains considered, $\sigma_{11} = T_{11}^o$, and $\sigma_{12} = T_{12}^o$, where T_{11}^o and T_{12}^o are the only components of the nonsymmetric first Piola-Kirchoff

stress tensor that appear (for plane waves in the x-direction) in the equations of motion written in material coordinates (Lagrangian formulation). For the half space case, the equality is not limited to small strains.

This completes the formulation of the plastic part of the constitutive equations. In Chapters 3 and 4 these equations will be combined with the usual elastic Hooke's law and applied to combined tension and torsion waves in a thin-walled tube and compression and shear waves in a half space.

CHAPTER 3

THIN-WALLED TUBE

3.1   INTRODUCTION

In the following Section 3.2, the equations governing the motion of a loading wave of combined normal and shear stresses (with nonelastic deformations) in a thin-walled cylindrical tube are given and solved. These equations are a generalization of the equations originally derived by Von Kármán for a thin unstretched wire subjected to an impact load in tension. The generalized equations for the tube case were solved by Clifton (1966) under the assumption of isotropic hardening. Characteristics and characteristic conditions for the problem, and the particularly simple forms to be integrated for simple wave solutions are given in Section 3.3.

3.2   EQUATIONS GOVERNING THE MOTION

The system of governing equations for the propagation of combined longitudinal normal stress and

torsional shear stress in a thin-walled cylindrical tube given below is obtained by assuming that plane sections remain plane and that the stress is uniform across each section. Lateral inertia effects are assumed to be negligible. Thus all the stresses and particle velocities are functions of x, the initial coordinate along the axis of the tube, and the time t. Material (Lagrangian) coordinates will be used. In Appendix 2, it is shown that, for small strains and for the geometry considered, the assumption that stress and particle velocity are independent of the coordinates other than x implies that the Cauchy stress component σ_{11} is equal to the first Piola-Kirchoff tensor component T_{11}^{o} for the same particle. Their common value will be denoted by σ. Similarly $\sigma_{12} = T_{12}^{o}$, which will be denoted by τ. The other components of the two tensors are not all equal, but only these two appear in the equations of motion.

To facilitate writing, the following symbols are adopted,

x = initial coordinate of the section, measured along the axis of the tube

t = time period elapsed after the boundary x = 0 is loaded

σ = axial stress

τ = shear stress

σ^* = σ — coordinate of the yield surface center

τ^* = τ — coordinate of the yield surface center

ξ = $\sigma - \sigma^*$

$\xi' = \frac{2}{3} \sigma - \sigma^*$

η = $\tau - \tau^*$

u = longitudinal particle velocity

v = tangential particle velocity

ϵ = axial unit extension

γ = engineering shear strain (angle change)

ρ = mass density of the material of the tube in the reference state

E = Young's modulus

G = shear modulus

Subscripts x and t denote the partial derivatives with respect to x and t respectively. Superscripts e and p denote the elastic and plastic parts respectively.

The equations of motion, for no body forces, are given in the reference state by

$$\frac{\partial \sigma}{\partial x} = \rho \, \frac{\partial u}{\partial t} \qquad (3.2\text{-}1a)$$

$$\frac{\partial \tau}{\partial x} = \rho \, \frac{\partial v}{\partial t} \qquad (3.2\text{-}1b)$$

See Appendix 2 for a demonstration that the equations of motion take this form.

Let $U(\underset{\sim}{x}, t)$ and $V(\underset{\sim}{x}, t)$ respectively be the longitudinal and tangential displacements at time t of a cross-section initially at a distance x. Loading occurs at x = o. Then

$$\epsilon = U_x \qquad (3.2\text{-}2a)$$

$$u = U_t \qquad (3.2\text{-}2b)$$

$$\gamma = V_x \qquad (3.2\text{-}3a)$$

$$v = V_t \qquad (3.2\text{-}3b)$$

The sign convention to be used for compressive impact is that σ and ϵ represent compression, while positive

displacement U and velocity u represent motion in the negative x-direction. For tensile impacts these are reversed; then the same Equations (3.2-1) and (3.2-2) can be used for either compressive or tensile impact.

Differentiating Equation (3.2-2a) with respect to t and Equation (3.2-2b) with respect to x yields the following continuity equation

$$\epsilon_t = u_x \ . \tag{3.2-4a}$$

Similarly Equation (3.2-3) yields another continuity equation given by

$$\gamma_t = v_x \ . \tag{3.2-4b}$$

It is assumed that the total strain rate is separable into elastic and plastic parts. Thus

$$\epsilon_t = \epsilon_t^e + \epsilon_t^p \tag{3.2-5a}$$

and

$$\gamma_t = \gamma_t^e + \gamma_t^p \ , \tag{3.2-5b}$$

where the elastic parts are

$$\epsilon_t^e = \frac{1}{E} \sigma_t \tag{3.2-6a}$$

and

$$\gamma_t^e = \frac{1}{G} \tau_t \ , \tag{3.2-6b}$$

while the plastic strain rates, given by the plastic potential theory, are

$$\epsilon_t^p = \dot{\lambda} \frac{\partial f}{\partial \xi} = \dot{\lambda} \, \xi' \qquad \text{(3.2-7a)}$$

and

$$\gamma_t^p = \dot{\lambda} \frac{\partial f}{\partial \eta} = \dot{\lambda} \, (2\eta) \quad . \qquad \text{(3.2-7b)}$$

Here f is the yield function and $\dot{\lambda}$ is a scalar function, both defined in Chapter 2. The assumption of additivity of the elastic and plastic Lagrangian strain rates (instead of rate-of-deformation components) limits the applicability of the theory to small strains (less than about 0.05), as is explained in Appendix 2.

It is assumed that the material yields according to the Mises yield condition given by

$$f(\xi,\eta) \equiv \frac{3}{4} \, (\xi')^2 + \eta^2 - k^2 = 0 \quad . \qquad \text{(3.2-8)}$$

For the case of only two nonvanishing stress components dλ is much simplified; from Equation (2.4-19), $\dot{\lambda}$ is given by

$$\dot{\lambda} = H \, [\xi' \, \sigma_t + 2\eta \, \tau_t] \quad . \qquad \text{(3.2-9)}$$

Thus Equation (3.2-7) can be written as

$$\epsilon_t^p = \dot{\lambda} \; \xi' = H \; (\xi' \sigma_t + 2\eta \; \tau_t) \; \xi' \qquad (3.2\text{-}10a)$$

$$\gamma_t^p = \dot{\lambda}(2\eta) = H \; (\xi' \sigma_t + 2\eta \; \tau_t)(2\eta). \qquad (3.2\text{-}10b)$$

Substituting Equations (3.2-5) through (3.2-10) into Equation (3.2-4) gives

$$\frac{1}{E} \; \sigma_t + H \; (\xi' \; \sigma_t + 2\eta\tau_t)\xi' = u_x \qquad (3.2\text{-}11a)$$

$$\frac{1}{G} \; \tau_t + H \; (\xi' \sigma_t + 2\eta\tau_t) \; (2\eta) = v_x \; . \qquad (3.2\text{-}11b)$$

Then Equations (3.2-1) and (3.2-11) form a complete system of first order partial differential equations, which can be written in the matrix form

$$\underset{\sim}{A} \; \underset{\sim}{w}_t + \underset{\sim}{B} \; \underset{\sim}{w}_x = 0 \; , \qquad (3.2\text{-}12)$$

where $\underset{\sim}{w}$ is the vector

$$\underset{\sim}{w} = \begin{bmatrix} u \\ \sigma \\ v \\ \tau \end{bmatrix}$$

and $\underset{\sim}{A}$ and $\underset{\sim}{B}$ are the 4x4 square matrices given on the following page.

$$
\underset{\sim}{A} = \begin{bmatrix} \rho & 0 & 0 & 0 \\[2ex] 0 & [\frac{1}{E} + H(\xi')^2] & 0 & 2H\xi'\eta \\[2ex] 0 & 0 & \rho & 0 \\[2ex] 0 & 2H\xi'\eta & 0 & [\frac{1}{G} + 4H\eta^2] \end{bmatrix} ,
$$

$$
\underset{\sim}{B} = \begin{bmatrix} 0 & -1 & 0 & 0 \\[2ex] -1 & 0 & 0 & 0 \\[2ex] 0 & 0 & 0 & -1 \\[2ex] 0 & 0 & -1 & 0 \end{bmatrix}
$$

Note that $\underset{\sim}{A}$ and $\underset{\sim}{B}$ are square symmetric matrices. In the elastic region $H = 0$; therefore, $\underset{\sim}{A}$ becomes

$$
\underset{\sim}{A}^e = \begin{bmatrix} \rho & 0 & 0 & 0 \\[2ex] 0 & \frac{1}{E} & 0 & 0 \\[2ex] 0 & 0 & \rho & 0 \\[2ex] 0 & 0 & 0 & \frac{1}{G} \end{bmatrix}
$$

while $\underset{\sim}{B}$ remains the same.

The solution of Equation (3.2-12) will be carried out in Section 3.3 by the method of characteristics.

3.3 SOLUTION OF GOVERNING EQUATIONS

The system (3.2-12) is a quasilinear, symmetric, hyperbolic system of partial differential equations. From the theory of partial differential equations wave speeds, characteristic conditions and the simple wave solutions for this system of equations will be obtained in the following subsections.

3.3.1 Wave Speeds

The characteristic velocities c are the roots of the determinantal equation $|c\underset{\sim}{A}-\underset{\sim}{B}| = 0$ (see Appendix 1). Expansion of this determinant gives the quadratic equation,

$$L(\rho c^2)^2 - (M + N)\ \rho c^2 + 1 = 0\ , \qquad (3.3-1)$$

where

$$L = MN - S^2 \qquad M = \frac{1}{G} + 4H\ \eta^2$$

$$N = \frac{1}{E} + H\ (\xi')^2 \qquad S = 2H\ \xi'\ \eta\ . \qquad (3.3-2)$$

Solution of Equation (3.3-1) yields

$$\rho c^2 = \frac{(M+N) \pm [(M-N)^2 + 4S^2]^{\frac{1}{2}}}{2L} \qquad (3.3-3)$$

The positive sign in the numerator gives the fast wave speed c_f while the negative sign gives the slow wave speed c_s. Both c_f and c_s depend upon the state of stress and plastic deformation through Equations (3.3-2). For the elastic case both these wave speeds reduce to elastic bar velocities: c_f reduces to $c_o = \sqrt{E/\rho}$, while c_s reduces to $c_2 = \sqrt{G/\rho}$.

By rearranging Equation (3.3-1), we can write it as

$$D(c) \equiv H (\xi')^2 (c^2/c_2^2 - 1) \rho c^2$$
$$+ 4H\eta^2 (c^2/c_o^2 - 1) \rho c^2$$
$$+ (c^2/c_2^2 - 1) (c^2/c_o^2 - 1) = 0 , \qquad (3.3-4)$$

whence it is seen, since $0 < c_2 < c_o$ that

$$D(c_o) \geqslant 0 \qquad D(c_2) \leqslant 0 \qquad D(0) > 0 . \qquad (3.3-5)$$

Therefore, the roots c_f and c_s satisfy the inequalities

$$0 \leqslant c_s \leqslant c_2 \leqslant c_f \leqslant c_o . \qquad (3.3-6)$$

3.3.2   Characteristic Conditions

The characteristic condition along the characteristic dx = c dt is given (see Appendix 1) by

$$\underset{\sim}{\ell}^T \underset{\sim}{A} \, d\underset{\sim}{w} = 0 , \qquad (3.3-7)$$

where $\underset{\sim}{\ell}^T = [\ell_1, \ell_2, \ell_3, \ell_4]$ denotes the transpose of a left eigenvector of $(c\underset{\sim}{A} - \underset{\sim}{B})$. Because of the symmetry of $\underset{\sim}{A}$ and $\underset{\sim}{B}$, $\underset{\sim}{\ell}$ is also a right eigenvector of $(c\underset{\sim}{A} - \underset{\sim}{B})$. Thus

$$\ell^T (c\underset{\sim}{A} - \underset{\sim}{B}) = (c\underset{\sim}{A} - \underset{\sim}{B}) \underset{\sim}{\ell} = 0. \qquad (3.3-8)$$

Expansion of Equation (3.3-8) yields

$$\ell_1 \rho c + \ell_2 = 0 , \qquad (3.3-9a)$$

$$\ell_1 + Nc\ell_2 + Sc\ell_4 = 0 , \qquad (3.3-9b)$$

$$\rho c \ell_3 + \ell_4 = 0 , \qquad (3.3-9c)$$

$$Sc \ell_2 + \ell_3 + Mc\ell_4 = 0 . \qquad (3.3-9d)$$

Solution of any three of the above four equations gives (for that value of c) the eigenvector, which is determined only up to an arbitrary constant. Solution of Equations (3.3-9a, b, c) yields

$$\ell_1 = \ell_1 \qquad \ell_3 = \frac{1 - N\rho c^2}{S\rho c^2} \ell_1$$

$$\tag{3.3-10a}$$

$$\ell_2 = -\rho c \, \ell_1 \qquad \ell_4 = \frac{N\rho c^2 - 1}{S c} \ell_1$$

If we arbitrarily choose $\ell_1 = Sc$, we get

$$\underset{\sim}{\ell}^T = [Sc, \; -S\rho c^2, \; -Nc + \frac{1}{\rho c}, \; N\rho c^2 - 1] \tag{3.3-10b}$$

Instead, solving Equations (3.3-9a, c, d), we get an alternative choice

$$\underset{\sim}{\ell}^{T^*} = [\frac{1}{\rho c} - Mc, \; M\rho c^2 - 1, \; c, \; -S\rho c^2] \; , \tag{3.3-10c}$$

if we arbitrarily choose $\ell_3^* = Sc$. The elements ℓ_i^* are related to the elements ℓ_i by the equation $\ell_i^* = -Nc\ell_i$, as can be verified by using Equation (3.3-1).

A left eigenvector $\underset{\sim}{\ell}$ also determines a simple-wave solution, as follows.

3.3.3   Simple Waves

A simple wave solution is defined as the particular solution of Equation (3.2-12) in which the vector $\underset{\sim}{w}$ is a constant along each characteristic of a family of the characteristic lines. Since c is dependent on the stress

state, in a simple wave region the characteristic lines

belonging to the family are straight. Also from the

theory of characteristics (see Appendix 1), in a simple

wave region, as we go from one straight characteristic

to a neighboring one, $d\underset{\sim}{w}$ is given by

$$(c\underset{\sim}{A} - \underset{\sim}{B}) \, d\underset{\sim}{w} = 0 \ . \tag{3.3-11}$$

From Equations (3.3-8) and (3.3-11), we see that $\underset{\sim}{\ell}$ and

$d\underset{\sim}{w}$ are proportional. Therefore, with $\underset{\sim}{\ell}^T$ given by Equa-

tion (3.3-10b),

$$\frac{du}{sc} = \frac{d\sigma}{-s\rho c^2} = \frac{dv}{\frac{1}{\rho c}-Nc} = \frac{d\tau}{N\rho c^2-1} \tag{3.3-12}$$

From Equation (3.3-12) it immediately follows that

$$\frac{d\sigma}{d\tau} = \frac{s}{\frac{1}{\rho c^2} - N} \tag{3.3-13a}$$

The alternative form of $\underset{\sim}{\ell}^T$, given by Equation (3.3-10c),

yields

$$\frac{d\sigma}{d\tau} = \frac{\frac{1}{\rho c^2} - M}{s} \ . \tag{3.3-13b}$$

Other equalities of Equation (3.3-12) yield

$$\frac{dv}{d\tau} = \frac{du}{d\sigma} = -\frac{1}{\rho c} \ . \qquad\qquad (3.3\text{-}14)$$

Let Ψ denote the function giving the value of $\frac{d\sigma}{d\tau}$. We will consider the history of an individual particle, so that the path of integration from one characteristic to another will be along the line x = constant of the x,t-plane. It will be convenient to take the shear stress τ or the axial stress σ as the independent variable along this line, instead of the time t. The system of equations to be integrated then takes the form

$$\frac{d\sigma}{d\tau} = \Psi \qquad\qquad (3.3\text{-}15)$$

$$\frac{du}{d\tau} = -\frac{1}{\rho c}\Psi \qquad\qquad (3.3\text{-}16a)$$

$$\frac{dv}{d\tau} = -\frac{1}{\rho c} \qquad\qquad (3.3\text{-}16b)$$

to determine σ, u, and v as functions of τ.

The plastic strains ϵ^p and γ^p can be obtained by integrating the constitutive equations, Equations (3.2-11). Dividing Equation (3.2-11a) by σ_t and Equation (3.2-11b) by τ_t gives

$$\frac{1}{E} + H(\xi')^2 + 2H\eta\xi' \frac{d\tau}{d\sigma} = \frac{d\epsilon}{d\sigma} \qquad (3.3-17a)$$

$$\frac{1}{G} + 4H\eta^2 + 2H\eta\xi' \frac{d\sigma}{d\tau} = \frac{d\gamma}{d\tau} \qquad (3.3-17b)$$

along the line x = constant, since $u_x = \epsilon_t$ and $v_x = \gamma_t$ by Equations (3.2-4). If we substitute Equation (3.3-13b) in Equation (3.3-17a) we obtain

$$\frac{d\epsilon}{d\sigma} = \frac{1}{\rho c^2}$$

or, in terms of τ as the independent variable,

$$\frac{d\epsilon}{d\tau} = \frac{1}{\rho c^2} \Psi. \qquad (3.3-18a)$$

Similarly substituting for $\frac{d\sigma}{d\tau}$ in Equation (3.3-17b) yields

$$\frac{d\gamma}{d\tau} = \frac{1}{\rho c^2} \qquad (3.3-18b)$$

along the line x = constant in a simple wave region.

The translation of the center of the yield surface as the loading continues is obtained as follows. Since

$$d\sigma^* = b \, d\epsilon^p , \qquad (3.3-19a)$$

$$d\tau^* = b \, \frac{d\gamma^p}{2} , \qquad (3.3-19b)$$

we obtain

$$\frac{d\sigma^*}{d\tau^*} = \frac{2d\epsilon^p}{d\gamma^p} = \frac{2d\lambda\acute{\xi}}{d\lambda(2\eta)} = \frac{\acute{\xi}}{\eta} \ . \tag{3.3-20}$$

Also from Equations (3.3-18b) and (3.3-19b)

$$d\tau^* = \frac{b}{2}(d\gamma - d\gamma^e) = \frac{b}{2}(\frac{1}{\rho c^2} d\tau - \frac{d\tau}{G}) \ .$$

Hence

$$\frac{d\tau^*}{d\tau} = \frac{b}{2} \ (\frac{1}{\rho c^2} - \frac{1}{G}) \ . \tag{3.3-21}$$

If we substitute $b = \frac{2}{3} (1-m)g$, by Equation (2.4-4), and

$H = \frac{3}{4gk^2}$ in Equation (3.3-21), we obtain

$$\frac{d\tau^*}{d\tau} = \frac{1}{4Hk^2} (1-m) (\frac{1}{\rho c^2} - \frac{1}{G}) \ . \tag{3.3-22a}$$

From Equations (3.3-20) and (3.3-22a)

$$\frac{d\sigma^*}{d\tau} = \frac{1}{4Hk^2} (1-m) (\frac{1}{\rho c^2} - \frac{1}{G}) \frac{\acute{\xi}}{\eta} \ . \tag{3.3-22b}$$

Equations (3.3-15), (3.3-16), (3.3-18), and (3.3-22) form a complete set of simultaneous, first order, ordinary differential equations, which can be integrated numerically

for an assigned value of m, with c set equal to the expression for c_f in the fast simple wave or to the expression for c_s in the slow simple wave region. Results for various values of m and particular choices of the material parameters and loading conditions are given in Chapter 5 and the stress trajectory plots of Fig. 1 to Fig. 12.*

If the stress-strain curve has a continuous tangent at the yield stress, H will be zero at a point on the initial yield surface, and the right sides of Equations (3.3-22) are indeterminate. In Section 3.4 it is shown by L'Hospital's rule that the limiting values of $d\sigma^*/d\tau$ and $d\tau^*/d\tau$ as $H \to 0$ are given for a slow simple wave $(c_s \to c_2)$ by

$$\lim_{H \to 0} \frac{d\tau^*}{d\tau} = (1-m) \frac{n^2}{k^2} \qquad (3.3-23a)$$

$$\lim_{H \to 0} \frac{d\sigma^*}{d\tau} = (1-m) \frac{n\xi'}{k^2} \qquad (3.3-23b)$$

---

*For Figures 1 to 31 see Section 5.7.

3.4   PROPERTIES AND SLOPES OF STRESS
TRAJECTORIES FOR SIMPLE WAVES

In this section first of all some of the general

properties of the stress trajectories for simple wave so-

lutions will be discussed. Then, in order that numerical

integration of the equations obtained in Section 3.2 can

be carried out, the initial slopes of the stress trajec-

tories at the starting points of the integration process

will be established, because in some cases there are cer-

tain curves, e.g. the initial yield surface, where some

of the parameters may become unbounded or indeterminate

and thus not able to be handled numerically.

When the tube is initially unstressed, the plastic

simple wave stress trajectory in the σ, τ plane begins at

a point (σ^o, τ^o) on the initial yield curve (assumed in

this study to be the Mises yield ellipse $\sigma^2 + 3\tau^2 = 3k^2$).

If the impact loading is assumed to be a boundary stress

(σ^b, τ^b) applied instantaneously at $x = 0$ at time $t = 0$

and then maintained constant, there is an elastic wave

ahead of the plastic wave in which axial stress σ^o propa-

gates as a shock wave at a speed c_o. This is followed

by an elastic shear wave at speed c_2 propagating as a

jump in τ to the value τ^o, unless $\tau^o = 0$. If $\tau^o = 0$, a fast plastic simple wave of uniaxial stress σ follows the elastic wave. The stress trajectory for this fast simple wave begins at $(\sigma^o, 0)$ and moves along the σ-axis. If $\tau^o \neq 0$, there is no fast plastic simple wave for the case of no prestress; instead the elastic shear wave is followed by a slow plastic simple wave whose trajectory begins at (σ^o, τ^o) on the initial yield surface and leads to the final stress (σ^b, τ^b). When there is a uniaxial fast plastic wave (case $\tau^o = 0$, mentioned above) the fast wave may be followed immediately by a slow plastic wave of combined stress, whose trajectory leads from a point say $(\sigma^1, 0)$ on the σ-axis $(\sigma^1 \leqslant \sigma_c$, where σ_c is the critical point). Several slow wave trajectories for no initial prestress are shown in Fig. 1 to Fig. 3 , emanating either from a point (σ^o, τ^o) on the initial yield surface, or from a point on the σ-axis to the right of the initial yield surface. When (σ^b, τ^b) is given, the initial point (σ^o, τ^o) or $(\sigma^1, 0)$ for the slow wave stress trajectory leading to (σ^b, τ^b) is not known at first. The appropriate initial point for a given (σ^b, τ^b) can be located approximately by interpolating between two of the previously calculated trajectories.

When there is initial shear stress τ^1 beyond

the elastic limit, there is no initial elastic shock

wave but there is a fast plastic simple wave of combined

stress leading from $(0,\tau^1)$. Several examples of such fast

plastic waves are shown in Fig. 5 to Fig. 11. The fast

wave may be followed immediately by a slow wave, whose

stress trajectory begins at the end of the fast-wave tra-

jectory, as in Fig. 6, or in some cases the fast wave may

be separated from the slow wave by a jump in shear stress,

so that the slow wave stress trajectory emanates from a

point different from the end of the fast wave trajectory,

as in Fig. 7. These cases involving a shock wave separ-

ating the fast wave from the slow wave will be discussed

further in the results and discussion of Chapter 5. Here

we consider only the case that the slow-wave trajectory

begins at the point where the fast-wave trajectory ends,

and show that at such a point the slow-wave trajectory is

orthogonal to the fast-wave trajectory, as was demon-

strated by Clifton (1966) for the case of isotropic hard-

ening.

Equations (3.3-13) give the slopes of the stress

trajectories for the simple wave solutions. For the slow

simple wave the slope $(d\sigma/d\tau)$ given by Equation (3.3-13b) can be written as

$$\left(\frac{d\sigma}{d\tau}\right)_{c_s} = \frac{\frac{1}{\rho c_s^2} - M}{S} \quad , \tag{3.4-1}$$

where M and S are given by Equation (3.3-2) and $\frac{1}{\rho c_s^2}$ can be obtained by rearranging the quadratic Equation (3.3-1) into a quadratic for $\frac{1}{\rho c^2}$ as the variable as follows. Dividing Equation (3.3-1) by $(\rho c^2)^2$ gives

$$\frac{1}{(\rho c^2)^2} - (M+N)\frac{1}{\rho c^2} + L = 0 \quad . \tag{3.4-2}$$

Solution of the quadratic Equation (3.4-2) yields

$$\frac{1}{\rho c^2} = \frac{1}{2}\left\{(M+N) \pm \left[(M-N)^2 + 4S^2\right]^{\frac{1}{2}}\right\} \quad , \tag{3.4-3}$$

where the positive sign corresponds to the slow wave speed c_s while the negative sign yields the fast wave speed c_f. Therefore, at a point where a trajectory changes from a fast wave to a slow wave,

$$\frac{1}{\rho c_s^2} = -\frac{1}{\rho c_f^2} + (M+N) \quad . \tag{3.4-4}$$

Substituting Equation (3.4-4) into Equation (3.4-1) immediately yields

$$\left(\frac{d\sigma}{d\tau} \right)_{c_s} = \frac{N - \frac{1}{\rho c_f^2}}{S} \quad . \tag{3.4-5}$$

Now for the fast simple wave, the slope of the stress trajectory can be written by Equation (3.3-13a) as

$$\left(\frac{d\sigma}{d\tau} \right)_{c_f} = \frac{S}{\frac{1}{\rho c_f^2} - N} \quad . \tag{3.4-6}$$

Multiplying Equations (3.4-5) and (3.4-6) gives

$$\left(\frac{d\sigma}{d\tau} \right)_{c_s} \cdot \left(\frac{d\sigma}{d\tau} \right)_{c_f} = -1 \quad , \tag{3.4-7}$$

which implies that the simple wave stress trajectories for the fast waves and slow waves are orthogonal to each other, when they intersect for a particular stress history. In order that the numerical integration can be started, some of the limits evaluating the initial slopes of stress trajectories and other associated slopes will be evaluated next.

From Equation (3.3-2) we see that, since $S = 2H\xi'\eta$ vanishes whenever $H = 0$, $\xi' = 0$, or $\eta = 0$, the slow wave speed for these special cases is given by

$$\rho c_s^2 = \begin{cases} \dfrac{1}{M} & \text{if } M-N > 0 \\[2ex] \dfrac{1}{N} & \text{if } M-N < 0 \end{cases} \quad . \qquad (3.4\text{-}8)$$

The case $H = 0$ occurs for a point on the initial yield surface, if the uniaxial stress-strain curve has a con- tinuous slope at yield. For the case $H = 0$, we have $M = \dfrac{1}{G}$ and $N = \dfrac{1}{E}$, so that $(M-N) > 0$ and $\rho c_s^2 = \dfrac{1}{M}$. For the case $\xi' = 0$, we have $M-N = \dfrac{1}{G} + 4H\eta^2 - \dfrac{1}{E}$ and $\rho c_s^2 = \dfrac{1}{M}$. Finally, for the case $\eta = 0$, we have $M-N = \dfrac{1}{G} - \dfrac{1}{E} - H(\xi')^2$ and $(M-N) > 0$ for $H(\xi')^2 < \dfrac{1}{G} - \dfrac{1}{E}$, while $M-N < 0$ for $H(\xi')^2 > \dfrac{1}{G} - \dfrac{1}{E}$. We see that there is a critical point on the $\eta = 0$ axis where $H(\xi')^2 = \dfrac{1}{G} - \dfrac{1}{E}$. From Equation (3.2-11a), with $\eta = 0$ and $u_x = \epsilon_t$, we see that

$$\left[\dfrac{1}{E} + H(\xi')^2\right] \sigma_t = \epsilon_t \qquad (3.4\text{-}9)$$

Hence, if this critical point is reached by uniaxial loading, it represents the point on the uniaxial curve where $d\epsilon/d\sigma = \dfrac{1}{G}$ or where the slope of the uniaxial

tension curve equals G. This critical point is very important for the construction of simple wave trajectories, as the following discussion shows.

The quantity Ψ given by Equations (3.3-13) as

$$\Psi_s = \frac{S}{\frac{1}{\rho c_s^2} - N} \qquad (3.4\text{-}10a)$$

takes the form

$$\Psi_s = \frac{S}{M-N} \qquad (3.4\text{-}10b)$$

for M-N > 0 in the special cases H = 0, $\xi' = 0$, or $\eta = 0$. Hence, since S = 0 in these cases, we have $\Psi_s = 0$ in these special cases as long as (M-N) is positive. At the critical point mentioned above M-N = 0, and the expression for Ψ_s is indeterminate. For larger values of ξ (on η=0), we have M-N < 0 so that $\rho c_s^2 = \frac{1}{N}$ and the expression $\Psi_s = \frac{S}{\frac{1}{\rho c_s^2} - N}$ appears to be indeterminate at all points on the ξ axis to the right of the critical point. By using the alternative form for $\frac{d\sigma}{d\tau}$ in Equation (3.3-13), we see that

$$\frac{1}{\Psi_s} = \frac{d\tau}{d\sigma} = \frac{S}{\frac{1}{\rho c_s^2} - M} = \frac{S}{N-M} \qquad (3.4\text{-}11)$$

to the right of the critical point. This shows that $\frac{1}{\Psi} = 0$ at these points and that $\frac{d\tau}{d\sigma} = 0$ there. This implies that the only slow wave trajectory that can originate on the ξ axis to the right of the critical point is a wave of uniaxial tensile or compressive stress. Any combined-stress trajectory originating on the ξ-axis must originate to the left of the critical point or at the critical point. Trajectories originating to the left of the critical point offer no difficulty. For them the limiting value of Ψ as $\eta \rightarrow 0$ is zero. Hence trajectories departing from the $\eta = 0$ axis at points to the left of the critical point have a vertical tangent. It may, however, be noted that $c_f \rightarrow c_2$ as $\eta \rightarrow 0$. Therefore, the fast simple-wave, combined-stress trajectories in the σ, τ plane end at a point corresponding to $\eta = 0$. This point in the σ,τ plane does not correspond to $\tau = 0$ except for the case of m = 1.

At the critical point the slope of the trajectory is indeterminate. An infinite number of trajectories depart from the critical point with slopes anywhere between zero and infinity. Several trajectories will be computed by assuming different values of the initial slope, with particular choices of the material parameters.

Finally, before we start constructing these stress trajectories, we notice that $\dfrac{d\tau^*}{d\tau}$ given by Equation (3.3-22a) takes the indeterminate form $\dfrac{0}{0}$ for $H = 0$ (point on the initial yield surface) and thus requires the limiting value of the function to be determined. By L'Hospital's rule, this limit is evaluated as follows. By Equation (3.3-22a)

$$\left(\frac{d\tau^*}{d\tau} \right)_{c_s} = (1-m)\,\frac{1}{4Hk^2}\,\left(\frac{1}{\rho c_s^2} - \frac{1}{G} \right). \qquad (3.4\text{-}12)$$

Substituting in Equation (3.4-12) the value of ρc_s^2 given by Equation (3.3-3) we obtain

$$\left(\frac{d\tau^*}{d\tau} \right) = \frac{1-m}{4k^2}\,\frac{1}{H}\left[\frac{1}{2}\left\{ \left(\frac{1}{G} + 4H\eta^2 \right) + \left(\frac{1}{E} + H(\xi')^2 \right) \right.\right.$$

$$+ \left[\left(\frac{1}{G} - \frac{1}{E} + 4H\eta^2 - H(\xi')^2 \right)^2 \right.$$

$$\left.\left.\left. + 4(2H\eta\xi')^2 \right]^{\frac{1}{2}} \right\} - \frac{1}{G} \right]. \qquad (3.4\text{-}13)$$

Differentiating with respect to H the numerator and the denominator of the expression on the right in Equation (3.4-13), we obtain

$$\frac{d\tau^*}{d\tau} \to \frac{1-m}{8k^2} \left[4\eta^2 + (\xi')^2 \right.$$

$$+ \; \frac{\left[\left(\frac{1}{G} - \frac{1}{E}\right) + 4H\eta^2 - H(\xi')^2 \right]\left[4\eta^2 - (\xi')^2 \right] + 16H\eta^2(\xi')^2}{\left[\left(\frac{1}{G} - \frac{1}{E}\right) + 4H\eta^2 - H(\xi')^2 + 16H^2\eta^2 \; (\xi')^2 \right]^{\frac{1}{2}}}$$

as $H \to 0$. Hence the limiting value is

$$\underset{H \to 0}{\text{Lim}} \; \frac{d\tau^*}{d\tau} = \frac{1-m}{8k^2} \left[4\eta^2 + (\xi')^2 + \frac{\left(\frac{1}{G} - \frac{1}{E}\right)\left(4\eta^2 - (\xi')^2\right)}{\left(\frac{1}{G} - \frac{1}{E}\right)} \right]$$

or

$$\underset{H \to 0}{\text{Lim}} \; \frac{d\tau^*}{d\tau} = (1-m) \; \frac{\eta^2}{k^2} \; . \tag{3.4-14a}$$

From Equations (3.4-14a) and (3.3-20), we obtain

$$\underset{H \to 0}{\text{Lim}} \; \frac{d\sigma^*}{d\tau} = (1-m) \; \eta \; \frac{\xi'}{k^2} \; . \tag{3.4-14b}$$

Having evaluated the value of the slopes for critical points, we are now in a position to construct the stress trajectories. For various initial conditions and specific material properties the stress trajectories are plotted in Fig. 1 to Fig. 12.

CHAPTER 4

PLANE WAVES IN A HALF SPACE

4.1   INTRODUCTION

In the following Section 4.2 the equations that govern the motion of a loading plane wave in a half space of isotropic hardening material obeying the Mises yield condition are given. Similar equations were originally given by Bleich and Nelson (1965) for an elastic, ideally plastic material and later by Ting (Dec. 1968) for an isotropic hardening elastic, plastic material with a general yield condition $f(\sigma_{ij}) = k^2$. Ting and Nan (1968) considered combined pressure and shear loadings leading to simple waves and gave some simple-wave stress trajectories based on the Mises yield condition. In Sections 4.3 and 4.4 closed form solutions for the stress trajectories of simple waves, and a numerical solution for non-simple waves are obtained. These are applied to some boundary loadings not previously treated, including a case of compression and two independent shear loadings.

68

4.2   EQUATIONS GOVERNING THE MOTION

The basic equations governing wave propagation
in a general elastic, plastic material consist of a yield
condition defining the transition to the plastic state,
a set of constitutive equations relating stress, strain
and/or their rates, and the equations of motion. For the
most general plane wave propagating in a half space of
isotropic-hardening material governed by the Mises yield
condition, bounded by the plane $x = 0$, the above mentioned
basic equations are given below. Material coordinates
will be used (Lagrangian formulation) in the equations of
motion. Thus x is the initial coordinate of the particle.
Let $v_1(x,t)$, $v_2(x,t)$ and $v_3(x,t)$ be the x,y and z compon-
ents of the velocity of a particle, which are assumed to
be functions of x and t only. Let $\sigma_1(x,t)$ be the normal
stress component σ_{11} in the x-direction at any section x,
and let $\sigma_2(x,t)$ and $\sigma_3(x,t)$ be the lateral normal stresses
σ_{22} and σ_{33}. Also let $\tau_2(x,t)$ and $\tau_3(x,t)$ be the shear
stresses σ_{12} and σ_{13} at section x.

It is assumed that the normal strains ϵ_{22} and ϵ_{33}
in the lateral direction at the section x are zero. The
above assumption leads to the result

$$\sigma_2(x,t) = \sigma_3(x,t) \, , \qquad\qquad (4.2\text{-}1)$$

as follows. The elastic strain increments are given by the classical theory of elasticity as

$$\dot{\epsilon}^e_{ij} = \frac{1+\nu}{E}\,\dot{\sigma}_{ij} - \frac{\nu}{E}\,\delta_{ij}\dot{\sigma}_{pp} \, , \qquad\qquad (4.2\text{-}2)$$

where ν is Poisson's ratio and $\dot{\sigma}_{ij}$ are the time rates of the stress components σ_{ij}. By plastic potential theory with the Mises yield condition,

$$\dot{\epsilon}^p_{ij} = \dot{\lambda}\,\sigma'_{ij} \qquad\qquad (4.2\text{-}3)$$

where $\dot{\lambda}$ is a scalar function, and the prime on σ_{ij} denotes the deviatoric part of the stress component. Since the $d\epsilon_{ij}$ will be interpreted as increments of Lagrangian strain, rather than as the increments of natural strain, the assumption of additivity of elastic and plastic parts of the strain limits this treatment to small strains (less than about 0.05).

Equations (4.2-2) and (4.2-3) then yield

$$\dot{\epsilon}_{ij} = \dot{\epsilon}^e_{ij} + \dot{\epsilon}^p_{ij} = \frac{1+\nu}{E}\,\dot{\sigma}_{ij} - \frac{\nu}{E}\,\delta_{ij}\dot{\sigma}_{pp} + \dot{\lambda}\sigma'_{ij} \, .$$

$$(4.2\text{-}4)$$

For $\dot{\epsilon}_{11}$ and $\dot{\epsilon}_{22}$ this gives

$$\dot{\epsilon}_{22} = 0 = \frac{1}{E} [\dot{\sigma}_{22} - \nu(\dot{\sigma}_{11} + \dot{\sigma}_{33})] + \dot{\lambda}\sigma'_{22} . \qquad (4.2-5)$$

$$\dot{\epsilon}_{33} = 0 = \frac{1}{E} [\dot{\sigma}_{33} - \nu(\dot{\sigma}_{11} + \dot{\sigma}_{22})] + \dot{\lambda}\sigma'_{33} . \qquad (4.2-6)$$

Subtracting Equations (4.2-5) and (4.2-6) yields

$$\frac{1+\nu}{E} (\dot{\sigma}_{22} - \dot{\sigma}_{33}) + \dot{\lambda}(\sigma'_{22} - \sigma'_{33}) = 0. \qquad (4.2-7)$$

As long as the material remains elastic, we have $\dot{\lambda} = 0$ and hence $\dot{\sigma}_{22} = \dot{\sigma}_{33}$. If the material is initially stress free, it follows that at yield $\sigma_{22} = \sigma_{33}$, whence $\sigma'_{22} - \sigma'_{33} = 0$ at yield. Hence Equation (4.2-7) shows that $\sigma_{22} - \sigma_{33}$ remains equal to zero during the deformation.

In the notation defined at the beginning of this section, the equations of motion in material coordinates can be written as

$$\sigma_{1x} = \rho v_{1t} \qquad (4.2-8a)$$

$$\tau_{2x} = \rho v_{2t} \qquad (4.2-8b)$$

$$\tau_{3x} = \rho v_{3t} \qquad (4.2-8c)$$

where the letter subscripts x and t denote partial derivatives. (See Appendix 2 for a demonstration that in this problem the Lagrangian equations of motion take this form.) Under the assumption of isotropic hardening, the Mises yield condition $f(\sigma_{ij}) = k^2$ can be written as

$$\frac{(\sigma_1 - \sigma_2)^2}{3} + \tau_2^2 + \tau_3^2 = k^2 , \qquad (4.2-9)$$

where k, the yield stress in pure shear, is the single parameter defining the hardening. For isotropic hardening, the scalar function $\dot{\lambda}$ of Equation (4.2-3) is

$$\dot{\lambda} = H\dot{f} , \qquad (4.2-10)$$

where H(k) is a function of the accumulated effective plastic strain or of the plastic work done, which may be expressed as a function of k during loading, and $\dot{f} = \sigma_j \sigma_{jt}'$. See Equations (2.4-17) to (2.4-20). Recall from Chapter 2, that

$$H(k) = \frac{3}{4gk^2} \text{ for loading } [f = k^2, \text{ and } \dot{f} \geqslant 0]$$

$$(4.2-11a)$$

$$H = 0 \text{ for unloading } [f \leqslant k^2, \text{ and/or } \dot{f} < 0]$$

$$(4.2-11b)$$

where $g = d\bar{\sigma}/d\bar{\epsilon}^p$ for isotropic hardening. The slope g of the universal stress-strain curve is really a function of the accumulated effective plastic strain $\int d\bar{\epsilon}^p$, but during loading $\sqrt{3}k = \bar{\sigma} = F[\int d\bar{\epsilon}^p]$. Hence g may be considered a function of k during loading.

For the half space problem under consideration, Equations (4.2-4) represent four constitutive equations. Note that

$$\epsilon_{22} = \epsilon_{33} = 0 \qquad\qquad (4.2\text{-}12)$$

and that the continuity requirements give

$$v_{1x} = \epsilon_{11t} \qquad\qquad (4.2\text{-}13a)$$

$$v_{2x} = 2\epsilon_{12t} = \gamma_{12t} \qquad\qquad (4.2\text{-}13b)$$

$$v_{3x} = 2\epsilon_{13t} = \gamma_{13t}. \qquad\qquad (4.2\text{-}13c)$$

The constitutive equations, Equations (4.2-4), take the following form when $\dot{\lambda}$ is given by Equation (4.2-10) and the strain rates are replaced by velocity gradients by using the continuity equations, Equations (4.2-13),

$$\frac{1}{E}\sigma_{1t} - \frac{2\nu}{E}\sigma_{2t} \qquad\qquad (4.2\text{-}14a)$$

$$+ H\,[s\sigma_{1t} - s\sigma_{2t} + 2\tau_2\tau_{2t} + 2\tau_3\tau_{3t}]\,(s) = v_{1x}$$

$$\frac{-2\nu}{E} \sigma_{1t} + \frac{2(1-\nu)}{E} \sigma_{2t} \qquad\qquad\qquad (4.2\text{-}14b)$$

$$+ H[s\sigma_{1t} - s\sigma_{2t} + 2\tau_2\tau_{2t} + 2\tau_3\tau_{3t}] \; (-s) = 0$$

$$\frac{1}{G} \tau_{2t} + 2H[s\sigma_{1t} - s\sigma_{2t} + 2\tau_2\tau_{2t} + 2\tau_3\tau_{3t}] \; (\tau_2) = v_{2x} \qquad (4.2\text{-}14c)$$

$$\frac{1}{G} \tau_{3t} + 2H[s\sigma_{1t} - s\sigma_{2t} + 2\tau_2\tau_{2t} + 2\tau_3\tau_{3t}] \; (\tau_3) = v_{3x} \qquad (4.2\text{-}14d)$$

where

$$s = \frac{2}{3} (\sigma_1 - \sigma_2) \; . \qquad\qquad\qquad (4.2\text{-}15)$$

Note that $\sigma_1' = s$, while $\sigma_2' = \sigma_3' = -\frac{1}{2} s$. The four Equations (4.2-14) form with the three equations of motion, Equations (4.2-8), a set of seven first order partial differential equations for the seven functions v_1, v_2, v_3, σ_1, σ_2, τ_2 and τ_3 for the plane wave propagating into a half space. These equations differ from those given by Ting (Dec. 1968) for the general plane wave only in that the specific choice of the yield condition as the Mises yield condition has furnished the explicit form for $\dot{\lambda}$.

The seven equations may be written in matrix form as

$$\underset{\sim}{A} \; \underset{\sim}{w}_t + \underset{\sim}{B} \; \underset{\sim}{w}_x = 0 \qquad\qquad\qquad (4.2\text{-}16)$$

where $\underset{\sim}{w}$ is the vector given by

$$\underset{\sim}{w}^{T} = [v_1, \; v_2, \; v_3, \; \sigma_1, \; \sigma_2, \; \tau_2, \; \tau_3] \; , \qquad (4.2\text{-}17)$$

and $\underset{\sim}{A}$ and $\underset{\sim}{B}$ are the 7 X 7 square matrices given below.

$$\underset{\sim}{A} = \begin{bmatrix} \rho \underset{\sim}{I}_3 & \underset{\sim}{0} \\ \underset{\sim}{0} & \underset{\sim}{S} \end{bmatrix} \qquad (4.2\text{-}18)$$

where $\underset{\sim 3}{I}$ is a 3 X 3 unit matrix and $\underset{\sim}{S}$ is the 4 X 4 matrix:

$$\underset{\sim}{S} = \begin{bmatrix} \left[\dfrac{1}{E} + Hs^2\right] & \left[\dfrac{-2\nu}{E} - Hs^2\right] & 2H\tau_2 s & 2H\tau_3 s \\[2ex] \left[\dfrac{-2\nu}{E} - Hs^2\right] & \left[\dfrac{2(1-\nu)}{E} + Hs^2\right] & -2H\tau_2 s & -2H\tau_3 s \\[2ex] 2H\tau_2 s & -2H\tau_2 s & \left[\dfrac{1}{G} + 4H\tau_2^2\right] & 4H\tau_2\tau_3 \\[2ex] 2H\tau_3 s & -2H\tau_3 s & 4H\tau_2\tau_3 & \left[\dfrac{1}{G} + 4H\tau_3^2\right] \end{bmatrix} .(4.2\text{-}19)$$

The matrix $\underset{\sim}{B}$ is

$$\underset{\sim}{B} = \begin{bmatrix} \underset{\sim}{0} & \underset{\sim}{M} \\ \underset{\sim}{M}^{T} & \underset{\sim}{0} \end{bmatrix} \qquad (4.2\text{-}20)$$

where

$$\underset{\sim}{M} = \begin{bmatrix} 1 & 0 & 0 & 0 \\ 0 & 0 & 1 & 0 \\ 0 & 0 & 0 & 1 \end{bmatrix}. \qquad (4.2-21)$$

Alternatively the matrix $\underset{\sim}{S}$ can be written as

$$\underset{\sim}{S} = \underset{\sim}{S}^e + H\underset{\sim}{\nabla f}(\underset{\sim}{\nabla f})^T \qquad (4.2-22)$$

where $\underset{\sim}{S}^e$ is obtained by setting $H = 0$ in $\underset{\sim}{S}$ and thus corresponds to the elastic case, and $\underset{\sim}{\nabla f}$ is the gradient of the yield function f, while $(\underset{\sim}{\nabla f})^T$ represents its transpose.

$$(\underset{\sim}{\nabla f})^T = [s, \ -s, \ 2\tau_2, \ 2\tau_3] \qquad (4.2-23)$$

The solution of the system of Equations (4.2-16) will be carried out by the method of characteristics in Section 4.3.

4.3   SOLUTION OF THE GOVERNING EQUATIONS

In the following subsections the simple wave solutions of the system of equations given by Equation (4,2-16) will be obtained. Subsection (4.3.1) will determine the wave speeds, while Subsection (4.3.2) will discuss the characteristic conditions. Simple wave solutions will be obtained in Subsection 4.3.2.

4.3.1 Wave Speeds

In this subsection the solution for the wave speeds for the system of equations (4.2-16) will be carried out by the method of characteristics (see Appendix 1). The wave velocities c are the roots of the 7 X 7 determinantal equation $|c\underset{\sim}{A}-\underset{\sim}{B}| = 0$. The order of the determinant can be lowered as follows. The matrix $(c\underset{\sim}{A}-\underset{\sim}{B})$ can be written as a product of two partitioned matrices

$$(c\underset{\sim}{A}-\underset{\sim}{B}) = \begin{bmatrix} \rho c\underset{\sim}{I}_3 & \underset{\sim}{M} \\ \underset{\sim}{M}^T & c\underset{\sim}{S} \end{bmatrix} = \begin{bmatrix} \rho c\underset{\sim}{I}_3 & \underset{\sim}{0} \\ \underset{\sim}{M}^T & \underset{\sim}{D} \end{bmatrix} \begin{bmatrix} \underset{\sim}{I}_3 & (1/\rho c)\underset{\sim}{M} \\ \underset{\sim}{0} & (1/\rho c)\underset{\sim}{I}_4 \end{bmatrix} \tag{4.3-1}$$

where $\underset{\sim}{M}$ and $\underset{\sim}{S}$ are the matrices defined in Equations (4.2-19) and (4.2-21), $\underset{\sim}{I}_3$ is a 3 X 3 unit matrix, and $\underset{\sim}{D}$ is given by

$$\underset{\sim}{D} = \rho c^2 \underset{\sim}{S} - \underset{\sim}{M}^T \underset{\sim}{M} . \qquad (4.3-2)$$

The determinant of the product of two square matrices is the product of the two determinants of the individual matrices, and the determinant of a triangular square matrix is the product of its diagonal elements. Therefore, Equation (4.3-1) yields the characteristic equation

$$\left| c\underset{\sim}{A} - \underset{\sim}{B} \right| = \frac{1}{\rho c} \left| \underset{\sim}{D} \right| = 0 , \qquad (4.3-3)$$

where $\left| \underset{\sim}{D} \right|$ is a 4 X 4 determinant.

The determinant can be further simplified by following a procedure suggested by Ting (Dec. 1968). Combining Equations (4.2-22) and (4.3-2) yields

$$\underset{\sim}{D} = \rho c^2 [\underset{\sim}{S}^e + H \underset{\sim}{\nabla f} (\underset{\sim}{\nabla f})^T] - \underset{\sim}{M}^T \underset{\sim}{M} \qquad (4.3-4a)$$

or

$$\underset{\sim}{D} = \underset{\sim}{D}^e + H\rho c^2 \underset{\sim}{\nabla f} (\underset{\sim}{\nabla f})^T \qquad (4.3-4b)$$

where

$$\underset{\sim}{D}^e = \rho c^2 \underset{\sim}{S}^e - \underset{\sim}{M}^T \underset{\sim}{M} . \qquad (4.3-5)$$

Ting (Dec. 1968) showed that if $\underset{\sim}{P}$ is an $\underset{\sim}{r} \times \underset{\sim}{r}$ matrix,

g and $\underset{\sim}{h}$ are column vectors with r elements, and "a" is

a scalar, then the determinant of the matrix $\underset{\sim}{P} + a \underset{\sim}{h} \underset{\sim}{g}^T$

is equal to the determinant of $\underset{\sim}{P}$ plus a $\underset{\sim}{h}^T \underset{\sim}{P}^* \underset{\sim}{g}$, where $\underset{\sim}{P}^*$

is the transpose of the adjoint of $\underset{\sim}{P}$, i.e. the element

P^*_{ij} in $\underset{\sim}{P}^*$ is the cofactor of the element P_{ij} in $\underset{\sim}{P}$. For

the problem of interest   the adjoint matrix is symmetric.

Thus

$$|\underset{\sim}{D}| = |\underset{\sim}{D}^e| + \rho c^2 \, H(\underset{\sim}{\nabla f})^T (\underset{\sim}{D}^e)^* (\underset{\sim}{\nabla f}) \qquad (4.3\text{-}6)$$

where $(\underset{\sim}{D}^e)^*$ is the adjoint of $\underset{\sim}{D}^e$. The 4 X 4 matrix $\underset{\sim}{D}^e$

has only six nonzero elements:

$$D^e_{11} = \frac{\rho c^2}{E} - 1 \qquad D^e_{22} = \frac{2(1-\nu)}{E} \rho c^2$$

$$(4.3\text{-}7)$$

$$D^e_{33} = D^e_{44} = \frac{\rho c^2}{G} - 1 \qquad D^e_{12} = D^e_{21} = \frac{-2\nu}{E} \rho c^2 \ .$$

The adjoint matrix $(\underset{\sim}{D}^e)^*$ has the following six nonzero

elements

$$(D^e)^*_{11} = \frac{2(1-\nu)}{E} \rho c^2 \left(\frac{\rho c^2}{G} - 1\right)^2 \qquad (D^e)^*_{22} = \left(\frac{\rho c^2}{E} - 1\right)\left(\frac{\rho c^2}{G} - 1\right)$$

$$(D^e)^*_{33} = (D^e)^*_{44} = \left(\frac{\rho c^2}{G} - 1\right)\left[\frac{\rho c^2}{G} \frac{1-2\nu}{2} - (1-\nu)\right]\frac{2\rho c^2}{E}$$

$$(D^e)^*_{12} = (D^e)^*_{21} = \frac{2\nu}{E} \rho c^2 \left(\frac{\rho c^2}{G} - 1\right)^2 . \qquad (4.3\text{-}8)$$

Hence Equations (4.3-3) and (4.3-6) yield

$$\frac{1}{\rho c}|\underset{\sim}{D}| \equiv c\left(\frac{\rho c^2}{G} - 1\right)\left\{ \frac{2}{E}\left(\frac{\rho c^2}{G} - 1\right)\left[\frac{\rho c^2}{G} \frac{1-2\nu}{2} - (1-\nu)\right] \right.$$

$$+ H s^2 \left(\frac{\rho c^2}{G} - 1\right)\left[\frac{3(1-2\nu)}{E} \rho c^2 - 1\right] + 8H\tau^2\left[\frac{\rho c^2}{G} \frac{1-2\nu}{2}\right.$$

$$\left.\left. - (1-\nu)\right]\right\} = 0 \qquad (4.3\text{-}9)$$

where $\tau^2 = \tau_2^2 + \tau_3^2$. Evidently $c = 0$ and $c = \pm c_2$ are roots of the equation, where $c_2 = \sqrt{G/\rho}$ is the elastic shear wave speed.

The remaining roots are given by the equation obtained by dividing through by Hc $(\frac{\rho c^2}{G} - 1)$. The resulting equation is denoted as $D(c) = 0$ below. It has been transformed by substituting $G = \rho c_2^2$, noting that

$$\frac{c_1^2}{c_2^2} = \frac{2(1-v)}{1-2v} \qquad (4.3\text{-}10)$$

where c_1 is the dilational elastic wave speed, and by eliminating Poisson's ratio v from the resulting equation by introducing the parameter β defined by Bleich and Nelson (1965) as

$$\beta = \frac{2(1+v)}{1-2v} \ . \qquad (4.3\text{-}11)$$

After some algebraic manipulation, the reduced equation below is obtained.

$$D(c) \equiv \left(\frac{3}{\beta} \frac{c^2}{c_2^2} - 1 \right) \left(\frac{c^2}{c_2^2} - 1 \right) s^2 + \frac{4}{\beta} \tau^2 \frac{c^2}{c_2^2} \left(\frac{c^2}{c_2^2} - \frac{c_1^2}{c_2^2} \right)$$

$$+ \frac{3}{\beta+1} \frac{1}{HE} \left(\frac{c^2}{c_2^2} - 1 \right) \left(\frac{c^2}{c_2^2} - \frac{c_1^2}{c_2^2} \right) = 0 \ . \qquad (4.3\text{-}12)$$

This is the same equation as was obtained by Ting and Nan (1968) for compression and a single shear τ with the Mises yield condition (except for a minor difference in notation for the parameter H).

As Ting and Nan have pointed out, it can be easily seen from Equation (4.3-12) that

$$D(c_1) \geqslant 0 \qquad D(c_2) \leqslant 0 \qquad D(o) \geqslant 0 \ , \qquad (4.3\text{-}13)$$

whence the roots $\pm c_f$ and $\pm c_s$ of Equation (4.3-12) satisfy the inequalities

$$0 \leqslant c_s \leqslant c_2 \leqslant c_f \leqslant c_1 \ . \qquad (4.3\text{-}14)$$

4.3.2 Characteristic Conditions

The characteristic condition along the characteristic of slope c is given (see Appendix 1) by

$$\underset{\sim}{\ell}^T \underset{\sim}{A} \ d\underset{\sim}{w} = 0 \ , \qquad (4.3\text{-}15)$$

where $\underset{\sim}{\ell}$ is a column vector obtained from

$$\underset{\sim}{\ell}^T (c\underset{\sim}{A} - \underset{\sim}{B}) = 0 \ . \qquad (4.3\text{-}16)$$

If $\ell_1, \ell_2, \ldots \ell_7$ are the elements of the column vector $\underset{\sim}{\ell}$, Equation (4.3-16) gives the set of seven homogeneous simultaneous equations,

$$c\rho\ell_1 + \ell_4 = 0 \qquad\qquad (4.3\text{-}17)$$

$$c\rho\ell_2 + \ell_6 = 0 \qquad\qquad (4.3\text{-}18)$$

$$c\rho\ell_3 + \ell_7 = 0 \qquad\qquad (4.3\text{-}19)$$

$$\frac{1}{c}\ell_1 + (\frac{1}{E} + Hs^2)\ell_4 - (\frac{2\nu}{E} + Hs^2)\ell_5 + 2s\tau_2 H\ell_6 + 2s\tau_3 H\ell_7 = 0$$
$$(4.3\text{-}20)$$

$$-(\frac{2\nu}{E} + Hs^2)\ell_4 + (\frac{2(1-\nu)}{E} + Hs^2)\ell_5 - 2s\tau_2 H\ell_6 - 2s\tau_3 H\ell_7 = 0$$
$$(4.3\text{-}21)$$

$$\frac{1}{c}\ell_2 + 2s\tau_2 H\ell_4 - 2s\tau_2 H\ell_5 + (\frac{1}{G} + 4\tau_2^2 H)\ell_6 + 4\tau_2\tau_3 H\ell_7 = 0$$
$$(4.3\text{-}22)$$

$$\frac{1}{c}\ell_3 + 2s\tau_3 H\ell_4 - 2s\tau_3 H\ell_5 + 4\tau_2\tau_3 H\ell_6 + (\frac{1}{G} + 4\tau_3^2 H)\ell_7 = 0 ,$$
$$(4.3\text{-}23)$$

and $\underset{\sim}{\ell}$ can be obtained up to an arbitrary constant by solving any six of the above seven equations. We arbitrarily drop Equation (4.3-20) from the set. Then solving the remaining set of six equations yields (up to an arbitrary constant) the following vector $\underset{\sim}{\ell}$.

$$\underset{\sim}{\ell}^T = [\Psi, \ 1, \ \tau_3/\tau_2, \ -\rho c\Psi, \ \Phi, \ -\rho c, \ -\rho c\tau_3/\tau_2] , \qquad (4.3\text{-}24)$$

where

$$\Psi = -\frac{\tau^2}{s\tau_2}\frac{c_1^2}{c_2^2} - \frac{s\beta}{4\tau_2}\left(1 + \frac{\beta+4}{3\beta GHs^2}\right)\left(1 - \frac{c_2^2}{c^2}\right) \qquad (4.3\text{-}25)$$

$$\Phi = \frac{\beta-2}{3}\frac{\tau^2}{s\tau_2}\rho c + \frac{\rho cs\beta}{4\tau_2}\left(1 - \frac{\beta-2}{3\beta GHs^2}\right)\left(1 - \frac{c_2^2}{c^2}\right) \qquad (4.3\text{-}26)$$

and

$$\tau^2 = \tau_2^2 + \tau_3^2 . \qquad (4.3\text{-}27)$$

By means of Equation (4.3-12) and Equations (4.3-25)
through (4.3-27) Ψ and Φ can alternatively be written as

$$\Psi = \frac{s}{\tau_2}\frac{c^2 - c_2^2}{c^2 - c_1^2} \qquad (4.3\text{-}28)$$

$$\Phi = \frac{\rho s}{2\tau_2 c}\frac{(c^2 - c_2^2)(c^2 - \beta c_2^2)}{(c^2 - c_1^2)} . \qquad (4.3\text{-}29)$$

Substituting Equations (4.3-24) through (4.3-29) in Equa-
tions (4.3-15) yields the characteristic conditions along
each characteristic of slope c given by Equation (4.3-9).
After some algebraic manipulations the resulting equation
takes the following form.

$$E\tau_2(\Psi dv_1 + dv_2) + E\tau_3 dv_3 - \left\{ \left[\frac{3}{2} EHs^2 + \frac{3\beta}{2(\beta+1)} - \frac{\beta c_2^2}{2c^2} EHs^2 \right.\right.$$

$$\left.\left. - \frac{\beta-2}{\beta+1} \beta \frac{c_2^2}{2c^2} \right] c\Psi\tau_2 + 2EHc\tau_2^2 s + 2EHc\tau_3^2 s \right\} d\sigma_1$$

$$+ \left\{ \left[\frac{3}{2} EHs^2 + \frac{3\beta}{2(\beta+1)} - \frac{\beta c_2^2}{2c^2} EHs^2 - \frac{\beta+4}{\beta+1} \beta \frac{c^2}{2c^2} \right] c\Psi\tau_2 \right.$$

$$+ 2EHc\tau_2^2 s + 2EHc\tau_3^2 s \right\} d\sigma_2 - \left\{ (3-\beta\frac{c_2^2}{c^2}) EH\tau_2 sc\Psi \right.$$

$$+ (\frac{E}{G} + 4EH\tau_2^2 + 4EH\tau_3^2) c \right\} d\tau_2 - \left\{ (3-\beta\frac{c_2^2}{c^2}) EH\tau_3 sc\Psi \right.$$

$$+ (\frac{E}{G} + 4EH\tau_2^2 + 4EH\tau_3^2) c \right\} d\tau_3 = 0 \qquad (4.3\text{-}30)$$

This is the characteristic condition, an interior differential equation governing along each characteristic when the appropriate c for that characteristic is used.

A left eigenvector $\underset{\sim}{\ell}$ also determines a simple wave solution of the system of equations (4.2-16), as given below in Subsection (4.3.3).

4.3.3   Simple Waves

In Appendix 1 it is shown that in a simple wave region, if we go from one straight characteristic to a

neighboring one, the elements of the increment $d\underset{\sim}{w}$ in the solution are proportional to the elements of $\underset{\sim}{\ell}$. Thus

$$\frac{dv_1}{\Psi} = \frac{dv_2}{1} = \frac{dv_3}{\tau_3/\tau_2} = \frac{d\sigma_1}{-\rho c \Psi} = \frac{d\sigma_2}{\phi} = \frac{d\tau_3}{-\rho c \tau_3/\tau_2} \qquad (4.3\text{-}31)$$

with the understanding that if any denominator in Equation (4.3-31) vanishes, so does the corresponding numerator. In particular if we put $\tau_3 = 0$ and $\tau_2 = \tau$, Equation (4.3-31) reduces to the form given by Ting and Nan (1968).

Note that the last equality in Equation (4.3-31) implies

$$d\tau_2/\tau_2 = d\tau_3/\tau_3 . \qquad (4.3\text{-}32)$$

Integration of Equation (4.3-32) yields $\tau_3 = \gamma\tau_2$ where γ is a constant. Hence any plastic simple wave involves radial loading from the origin in the τ_2,τ_3-plane. This would seem to imply that there is no solution based on simple waves which could not be reduced by a rotation of the coordinate axes to the results of Ting and Nan for loading by compression and a single shear. We shall see, however, in Section 5.3 that the constant γ associated with the fast simple wave need not be the same as that

associated with the slow simple wave, and that the tran-
sition from one τ_2, τ_3-plane to another involves discon-
tinuities in τ_2 and τ_3 propagating at the elastic shear
wave speed c_2.

Equation (4.3-31) also implies

$$\frac{d(\sigma_1 - \sigma_2)}{d\tau_2} = \frac{\rho c \Psi + \Phi}{\rho c} . \qquad (4.3-33)$$

Substituting for Ψ and Φ from Equations (4.3-28) and
(4.3-29) into Equation (4.3-33) furnishes the following
expression, where $s = \frac{2}{3}(\sigma_1 - \sigma_2)$,

$$\frac{ds}{d\tau_2} = \frac{s}{3\tau_2} \frac{(c^2 - c_2^2)(3c^2 - \beta c_2^2)}{c^2(c^2 - c_1^2)} \qquad (4.3\text{-}34a)$$

or alternatively

$$\frac{ds}{d\tau_2} = -\frac{4}{3}\frac{\tau^2}{s\tau_2} - \frac{1}{3GHs\tau_2}\left(1 - \frac{c_2^2}{c^2}\right) . \qquad (4.3\text{-}34b)$$

We shall see that, as a consequence of Equation (4.3-37)
below, Equations (4.3-34a) and (4.3-34b), respectively,
can be written as

$$\frac{ds}{d\tau} = \frac{s}{3\tau} \frac{(c^2 - c_2^2)(3c^2 - \beta c_2^2)}{c^2(c^2 - c_1^2)} \qquad (4.3\text{-}34c)$$

or alternatively

$$\frac{ds}{d\tau} = -\frac{4}{3}\frac{\tau}{s} - \frac{1}{3GHs\tau} . \qquad (4.3\text{-}34d)$$

Equation (4.3-31) gives

$$\frac{d\sigma_1}{d\tau_2} = \frac{s}{\tau_2} \frac{c^2 - c_2^2}{c^2 - c_1^2} , \qquad (4.3\text{-}35a)$$

which, by virtue of Equation (4.3-37) below, can be written alternatively as

$$\frac{d\sigma_1}{d\tau} = \frac{s}{\tau} \frac{c^2 - c_2^2}{c^2 - c_1^2} . \qquad (4.3\text{-}35b)$$

Since $\tau_3 = \gamma\tau_2$ in a simple wave, by Equation (4.3-32),

$$\tau = \sqrt{\tau_2^2 + \tau_3^2} = \sqrt{1 + \gamma^2}\, \tau_2 \qquad (4.3\text{-}36)$$

for $\tau_2 > 0$. Hence

$$\frac{d\tau_2}{\tau_2} = \frac{d\tau_3}{\tau_3} = \frac{d\tau}{\tau} . \qquad (4.3\text{-}37)$$

Equations (4.3-34) and (4.3-35a) can thus be written in the alternative forms of Equations (4.3-34c), (4.3-34d), and (4.3-35b) given above. Equations (4.3-34d) and (4.3-35b) are identical to the equations given by Ting and Nan for the single shear compression loading. Since the right side of Equation (4.3-34d) is a function of s and τ only (since c depends only on s and τ), that equation is uncoupled and can be integrated independently to give a one-parameter family of s-τ curves, as Ting and Nan showed. When the resulting s as a function of τ is substituted into Equation (4.3-35b), that equation can be integrated by a numerical quadrature, with an additive constant of integration. The additivity of the integration constant shows that for any one curve in the s,τ-plane the family of curves in the σ_1,τ-plane can be obtained by translating one member of the family in the σ_1-direction.

Integration of Equations (4.3-34) and (4.3-35) gives the stress history experienced by a particle in the simple wave region. Numerical integration results for several such particles with various initial and boundary conditions are shown in Figures 13 to 14, and discussed in Section 5.3. Additional properties of simple

wave solutions in a half space have been discussed by Ting and Nan (1968). When the half space is initially prestressed, the simple wave solution for such a case is different, as is discussed in detail in Section 5.3.

4.4 NUMERICAL SOLUTIONS FOR NONSIMPLE WAVES

In the preceding sections, the characteristics and characteristic conditions for the system of equations (4.2-16) have been obtained. Closed form solutions (i.e. simple wave solutions by numerical quadrature) can be obtained for suitable boundary conditions. In this section, the characteristic conditions will be integrated for a boundary condition which does not give a simple wave solution. Closed form solutions are not possible and thus the characteristic conditions given in the incremental form will be integrated numerically. Equation (4.3-15) represents the increment $d\underset{\sim}{w}$ of vector $\underset{\sim}{w}$ along a characteristic with wave speed c, where Equation (4.3-9) gives the values of c. For simplicity, numerical solution is sought here only for cases where one compressive load and one shear load act on the

boundary $x = 0$ of the half space under consideration.

Therefore, by setting $\tau_3 = 0$ and $\tau_2 = \tau$ in Equation

(4.3-30) the incremental relations, after some algebraic

manipulations, can be written as follows.

$$
Ec\Psi \; dv_1 + Ec \; dv_2 - \left\{ \left[\frac{3\beta c^2}{2(\beta+1)} + (3c^2-\beta c_2^2) \frac{EHs^2}{2} - \frac{\beta(\beta-2)}{2(\beta+1)} c_2^2 \right] \Psi \right.
$$

$$
\left. + 2EHc^2\tau s \right\} d\sigma_1 + \left\{ \left[\frac{3\beta c^2}{2(\beta+1)} + (3c^2-\beta c_2^2) \frac{EHs^2}{2} - \frac{\beta(\beta+4)}{2(\beta+1)} c_2^2 \right] \Psi \right.
$$

$$
\left. + 2EHc^2\tau s \right\} d\sigma_2 - \left\{ (3c^2-\beta c_2^2) \; EH\tau s\Psi + (\frac{E}{G} + 4EH\tau^2)c^2 \right\} d\tau = 0 .
$$

$$(4.4-1)$$

And, after rearrangement of terms, Equation (4.3-9) or the

reduced Equation (4.3-12) can be written as

$$
c\left[\frac{3}{\beta} s^2 + \frac{4\tau^2}{\beta} + \frac{3}{EH(\beta+1)} \right] \left(\frac{c^2}{c_2^2}\right)^2 - c\left[\frac{\beta+3}{\beta} s^2 + \frac{4c_1^2}{c_2^2} \frac{\tau^2}{\beta} \right.
$$

$$
\left. + \frac{\beta+7}{(\beta+1)EH} \right] \left(\frac{c^2}{c_2^2}\right) + c\left[s^2 + \frac{3}{(\beta+1)EH} \frac{c_1^2}{c_2^2} \right] = 0 . \quad (4.4-2)
$$

$c = 0$ is evidently a root of Equation (4.4-2); the other

four roots are

$$
c = \pm \; c_f \quad \text{and} \quad c = \pm \; c_s ,
$$

which can be obtained by solving the quadratic equation left after cancelling c from Equation (4.4-2). Then for the five values of c, Equation (4.4-1) yields a set of five simultaneous equations for the increments of the five elements of the vector $\underset{\sim}{w}$. A systematic scheme to compute these increments will be discussed here.

Vitiello and Clifton (1967) developed an explicit difference scheme for the case of a thin-walled tube problem. In their scheme the solution of a system of difference equations of the type of Equation (4.4-1) at a time $t + \Delta t$ is obtained as an explicit function of the solution at time t. Here Δt is the time increment for the difference grid (see Fig. 20). Equation (4.4-1) may be abbreviated as

$$\alpha_{ij} dw_j = 0 \quad \text{for} \quad i = 1 \text{ to } 5 \qquad (4.4-3)$$

along the characteristic whose wave speed is c_i. (In Fig. 20, $c_5 = 0$ gives the vertical line QP). The coefficients α_{ij} depend on the state of stress and the wave speed. Following Vitiello and Clifton (1967), we approximate all the coefficients α_{ij} for the difference scheme by their values at Q, i.e. by the values calculated using

the known stress values at Q, and obtain the values w_i at points Q_i by linear interpolation along the horizontal grid line through mesh points Q', Q, Q'' after locating Q_1, Q_2, Q_3, Q_4 by approximating the characteristic segments $Q_i P$ by straight lines of slope $dx/dt = c_i$, where the c_i are evaluated at Q. If λ denotes the mesh ratio $\Delta t/\Delta x$, then the interpolation gives

$$w_j(Q_i) = w_j(Q) + \lambda c_i(Q)[w_j(Q') - w_j(Q)] \quad \text{for } i = 1,2 \qquad (4.4\text{-}4a)$$

$$w_j(Q_i) = w_j(Q) + \lambda c_i(Q)[w_j(Q) - w_j(Q'')] \quad \text{for } i = 3,4 \qquad (4.4\text{-}4b)$$

and

$$w_j(Q_i) = w_j(Q) \quad \text{for } i = 5 . \qquad (4.4\text{-}4c)$$

Substituting Equations (4.4-4) into Equations (4.4-3) gives

$$\alpha_{ij}(Q)[w_j(P) - w_j(Q)] = \lambda c_i(Q)\alpha_{ij}(Q)[w_j(Q') - w_j(Q)] \quad \text{for } i = 1,2$$
$$\qquad (4.4\text{-}5a)$$

$$\alpha_{ij}(Q)[w_j(P) - w_j(Q)] = \lambda c_i(Q)\alpha_{ij}(Q)[w_j(Q) - w_j(Q'')] \quad \text{for } i = 3,4$$
$$\qquad (4.4\text{-}5b)$$

$$\alpha_{ij}(Q)[w_j(P) - w_j(Q)] = 0 \quad \text{for } i = 5 . \qquad (4.4\text{-}5c)$$

Solution at P is found by solving Equations (4.4-5), a
set of five simultaneous linear algebraic equations for
the five unknown values $w_i(P)$.

A more sophisticated iterative procedure could
be used with the coefficients $\alpha_{ij}^{(n)}$ for the nth iteration
approximated (see Nan (1968)) by

$$\alpha_{ij}^{(n)} = \frac{1}{2} [\alpha_{ij}^{(n-1)}(Q_i) + \alpha_{ij}^{(n-1)}(P)] ,$$

or by some other average value instead of using all coef-
ficients evaluated at Q. No such sophisticated procedure
was attempted. According to Vitiello and Clifton (1967),
theorems of the theory of numerical analysis imply that
the exact difference solution converges to the exact so-
lution $\underset{\sim}{w}$ of the differential equation in the maximum norm
with an error that is $O(\Delta x)$, provided the functions in-
volved are Lipschitz continuous and that the mesh ratio
$\Delta x/\Delta t \geqslant c_{max}$. This mesh ratio restriction is also that
required as a necessary condition that the domain of de-
pendence of the difference equations must include the do-
main of dependence of the differential equations. Vitiello
and Clifton (1967) pointed out that the convergence for
plastic wave propagation problems is, however, not always

assured because discontinuities at wave fronts and bound-

aries between elastic and plastic regions violate the

smoothness assumptions. But in some numerical experi-

ments they found good agreement between the solutions

and the numerical quadratures of simple wave solutions.

CHAPTER 5

APPLICATIONS AND RESULTS

5.1   SIMPLE WAVE SOLUTIONS FOR
THIN-WALLED TUBE

In Clifton's (1966) solutions for the simple wave

stress trajectories for a thin-walled tube of isotropic

hardening material, loaded by combined tension-torsion

impact idealized as an assumed instantaneous application

of uniform stress (σ^b, τ^b) at the boundary x = 0 (applied

at t = 0 and held constant thereafter), the slow simple

wave trajectory of σ versus τ, leading to the final values

(σ^b, τ^b) for any particle, could be constructed by backward

integration of Equation (3.3-15) from the final values

(σ^b, τ^b), since the right-hand side Ψ is a function only

of σ and τ. See Fig. 3* for several such trajectories.

If this trajectory leads back to a point on the initial

yield curve of σ versus τ, then the impact on an initially

stress-free tube produces only the slow simple wave fol-

lowing the elastic jumps in σ (traveling at the elastic

---

*Figures 1 to 31 are given at the end of this chapter.

bar-wave speed c_o) and in τ (traveling at the elastic

shear-wave speed c_2). When the backward-integrated slow-

wave trajectory leads back to a point on the σ-axis out-

side the initial yield locus, then a fast simple wave of

uniaxial stress σ precedes the slow simple wave. When

the bar is prestressed in shear into the plastic range

before impact, there is also a fast wave of combined

stress, which is constructed by forward integration from

the initial condition $(0,\tau^1)$ point until it intersects

the slow wave leading to (σ^b,τ^b) at a point (σ^o,τ^o) out-

side the initial yield locus. In this case the slow-wave

trajectory initiates at this intersection point (σ^o,τ^o)

instead of on the initial locus, but from the intersec-

tion point to the final point (σ^b,τ^b) the slow-wave tra-

jectory is the same as it would have been without the

prestress, when the hardening is purely isotropic.

For kinematic hardening or combined kinematic

and isotropic hardening the solution is more complicated.

Because the function Ψ on the right-hand side of Equation

(3.3-15) depends in these cases on the location of the

center of the yield surface and on the accumulated effec-

tive plastic strain, the slow-wave σ,τ-trajectory cannot

be constructed by backward integration from (σ^b, τ^b). It

is necessary to construct it by forward integration, so

that the motion of the yield-surface center and the accum-

ulated effective strain can be calculated by following

the history of the deformation. For a given choice of

the hardening parameter m other than the isotropic hard-

ening choice m = 1, it is not too difficult to construct

a slow wave trajectory by forward integration beginning

at some point on the initial yield surface (no plastic

prestress), but it is not known in advance what starting

point should be used for the trajectory leading to arbi-

trary prescribed constant boundary stresses (σ^b, τ^b) at

the impact end x = 0. It is therefore necessary to con-

struct a family of slow-wave trajectories starting from

a sequence of points on the initial yield locus. Then

the member of that family leading to the prescribed

(σ^b, τ^b) point is selected. Since in practice only a

finite number of such slow-wave trajectories will be

constructed, it may be necessary to interpolate between

them, or to use an interative construction to converge

on the desired trajectory leading to arbitrary prescribed

(σ^b, τ^b). The complexity is compounded when there is

initial prestress beyond yield, since because of the deformation in the combined-stress fast simple wave, the plastic strain and the yield-surface center location at the intersection of the fast wave trajectory with a previously constructed slow-wave trajectory (leading to (σ^b, τ^b) from a point on the initial yield locus) are not in general the same as the plastic strain and the yield-surface center of the previously constructed slow simple wave at the intersection point. Thus the slow simple wave leading to (σ^b, τ^b) will be different for different prestress conditions when the hardening is not isotropic. We shall consider first some examples where the tube is initially stress free and then some cases where the tube is initially stressed beyond yield.

Numerical integration of the simultaneous first-order ordinary differential Equations (3.3-15), (3.3-16), (3.3-18), and (3.3-22) can be carried out by any of the standard methods. A fourth order Runge-Kutta method was used here. The standard computer program to carry out the integration was obtained from the Michigan State University Computer Laboratory, Program Documentation No. 00000035, March 64. The Runge-Kutta method has the

advantages that it is self starting and stable and pro-
vides good accuracy. It keeps no account of the error
estimate, but changing the step size to different values
and then comparing the results gives an estimate of the
accuracy of the method.

To illustrate the procedure outlined in Chapters
2 and 3, specific examples with prescribed initial and
boundary conditions that result in simple-wave solutions
for the thin-walled tube will be discussed for different
values of the hardening parameter m. The material, for
which the simple wave stress trajectories are shown in
Figures 1 to 12, was assumed to have the following
stress-strain curve in simple tension, the same stress-
strain curve as was used by Clifton (1966).

$$\epsilon^P = 0.403 \times 10^{-8} (\sigma - \sigma_Y)^{1.732} \qquad (5.1\text{-}1)$$

where $\sigma_y = 1750$ psi. is the initial yield stress in ten-
sion. Hence, in uniaxial tension,

$$\frac{d\sigma}{d\epsilon^P} = 78410 \; \frac{1}{(\epsilon^P)^{0.4226}} . \qquad (5.1\text{-}2)$$

For a uniaxial tension test, $d\epsilon^p = \overline{d\epsilon}^p$ and thus $\epsilon^p = \int \overline{d\epsilon}^p$.

Therefore, for a general three-dimensional deformation state, Equation (5.1-2) implies

$$g = 78410 \ \frac{1}{\left[\int \overline{d\epsilon}^p\right]^{0.4226}} \tag{5.1-3}$$

and g is a monotonically decreasing function of $\int \overline{d\epsilon}^p$.

The value of Poisson's ratio v and Young's modulus E are assumed to be 0.33 and 10^7 psi., respectively.

5.2 EXAMPLES OF COMBINED TENSION-TORSION IMPACTS ON THE THIN-WALLED TUBE

Consider a semi-infinite thin-walled tube initially at rest and unstressed, which is given simultaneously instantaneous compressive and torsion impacts causing uniformly distributed boundary normal and shear stresses σ^b and τ^b respectively on the end x = 0, which remain constant for t > 0. A family of slow-wave trajectories is constructed for each of the choices m = 0, m = 0.5, and m = 1 of the hardening parameter. The choice m = 0, corresponding to the purely kinematic

hardening case, gives the trajectories of Fig. 2. The
choice m = 1 corresponding to the purely isotropic hard-
ening case previously solved by Clifton (1966) gives the
trajectories of Fig. 1, while the choice m = 0.5 is a
combination of both isotropic and kinematic hardening.
Fig. 3 shows the network of simple wave stress trajec-
tories for m = 0.5.

Figure 4 shows examples of the relative differ-
ence in the stress history experienced by a particle at
x = constant, due to the different choices of material
hardening parameter m. This figure is constructed by
choosing an appropriate stress trajectory from each of
the networks for m = 0, m = 0.5, and m = 1 and then
plotting on a single graph.

Now consider the case of a thin-walled tube ini-
tially stressed with static shear load causing positive
shear stress τ^1 greater than the yield stress of the tube
in shear, which is then given simultaneously instantan-
eous compressive and torsion impacts causing uniformly
distributed boundary normal and shear stresses σ^b and τ^b,
respectively, constant for t > 0 at the end x = 0. As
was noted earlier, complexity of constructing simple wave

solutions is greater when there is an initial prestress
beyond yield. For each initial condition of prestress
a fast wave stress trajectory is obtained for each of
the choices m = 0, m = 0.5, and m = 1 of the hardening
parameter. From a series of points on any one of these
fast-wave trajectories a series of slow-wave trajectories
is constructed by forward integration with the initial
conditions of stress, yield-surface center and accumu-
lated effective plastic strain for each slow wave of the
series given by the values of those quantities at the
starting point of that slow-wave trajectory on the fast-
wave trajectory. All of the slow wave trajectories
starting from any one fast-wave trajectory are constructed
with the same value of the hardening parameter m as was
used for that fast wave. Figures 5 to 10 show several
such fast-wave stress trajectories and a family of slow-
wave stress trajectories originating from each fast-wave
stress trajectory. For the particular choice of m = 1,
i.e. corresponding to pure isotropic hardening, a family
of slow-wave stress trajectories originating from each
fast-wave stress trajectory is not necessary because for
that case the stress trajectories in the σ, τ-plane are

explicit functions of σ and τ only and thus the slow

simple wave stress trajectories need only be constructed

originating from the initial yield surface.

As was pointed out earlier in Section 3.4, each

member of the family of fast-wave trajectories in the

σ,τ-plane will end at a point corresponding to $\eta = 0$,

and $c = c_2$. For positive initial stress τ^1, the point

in the σ,τ plane corresponding to $\eta = 0$, and $c = c_2$ will

be for some positive value of τ, say $\tau = \tau^d$, except in

the case $m = 1$ for which $\tau^d = 0$. The slow-wave trajec-

tory from the end of the fast-wave trajectory is a hori-

zontal straight line in the σ,τ-plane, with $\tau = \tau^d$, as

is shown in Fig. 9 . If the boundary condition τ^b is

such that $\tau^b < \tau^d$, then there is no slow-wave trajectory

leading from a point on the fast-wave trajectory to

(σ^b,τ^b). Instead there will be a jump in shear stress

from a point on the fast-wave trajectory to a point on

the slow-wave trajectory; this jump propagates at the

elastic shear wave speed c_2. The point on the fast-wave

trajectory from which the jump occurs is not known in

advance when arbitrary boundary conditions (σ^b,τ^b) are

prescribed with $\tau^b < \tau^d$. Just as it was necessary to

construct a family of slow-wave trajectories emanating

from a series of points on the fast-wave trajectory and

to interpolate between them to find the slow-wave trajec-

tory leading to a given point (σ^b, τ^b) with $\tau^b > \tau^d$, it

is now necessary to construct a family of trajectories

for which the slow-wave trajectory is separated from the

fast-wave trajectory by a jump in τ.

The value of this jump in τ is determined by the

yield condition just before the jump, where k has the

current value determined by the hardening up to the jump.

In the ξ, η-plane the jump is represented as a vertical

line from a point on the upper boundary of the ellipse

$\xi^2 + 3\eta^2 = 3k^2$ to a point on the lower boundary, a jump

in η by the amount $-2\eta^f$, if η^f is the value of η in the

fast-wave just before the jump. Since the jump across

the interior of the yield curve represents an elastic

change, there is no hardening associated with the jump.

Hence the yield curve center (σ^*, τ^*) and the $\int \overline{d\epsilon}^p$ are

unchanged. This means that the jump in τ in the σ, τ-

plane is also of amount $-2\eta^f$ from the point (σ^f, τ^f) on

the fast-wave trajectory to $(\sigma^f, \tau^f - 2\eta^f)$ at the beginning

of the slow-wave trajectory. A slow-wave trajectory

starting from $(\sigma^f, \tau^f - 2\eta^f)$ is then constructed for a series of points (σ^f, τ^f) on the fast-wave trajectory, with initial values of σ^*, τ^* and $\int \overline{d\epsilon}^p$ for each such slow wave given by the values of these parameters at (σ^f, τ^f). Figures 7 to 8 show several examples of such trajectories involving a jump in τ.

When the hardening is isotropic, no jump occurs in τ when both τ^l and τ^b are positive; only when τ^b is negative (for positive τ^l) does the jump followed by additional plastic deformation occur with isotropic hardening, since then $\tau^b < \tau^d = 0$. Also when the boundary loading is elastic, i.e. $(\sigma^b)^2 + 3(\tau^b)^2 \leqslant 3k^2$, the jump in shear occurs but then for this elastic boundary loading there is no combined-stress slow wave incorporating any additional plastic strain. A case of elastic boundary loading demonstrating the jump in shear for the isotropic hardening case is shown in Fig. 11. Ting and Nan (1968) discussed the possibility of such jumps for plane waves in a half space in the case of isotropic hardening. Because of the jump, there is a qualitative difference between the predictions of kinematic or combined kinematic and isotropic hardening and the predictions of isotropic hardening, for $0 \leqslant \tau^b < \tau^d$.

5.3   SIMPLE WAVE SOLUTIONS FOR HALF SPACE

Construction of stress trajectories for plane plastic simple-wave regions in a half space of isotropic hardening material loaded by one compression and two shears reduces to the case of one compression and one shear previously obtained by Ting and Nan (1968) when the half space is initially unstressed. But the construction procedure changes when the half space is pre-stressed statically with a shear component in one direction while the shear part of the impact with two shear stress components τ_2^b and τ_3^b has a resultant shear stress τ^b in a different direction. Such simple wave solutions will be considered in the later part of this section.

The stress trajectories for plane waves in a half space are four-dimensional trajectories in σ_1, σ_2, τ_2, τ_3-space. But, for a simple wave, we have $\tau_3 = \gamma\tau_2$, and it is possible to discuss each simple wave in the three-dimensional σ_1, σ_2, τ-subspace, where $\tau^2 = \tau_2^2 + \tau_3^2 = (1 + \gamma^2)\tau_2^2$, as was pointed out in Section 4.3. This three-dimensional stress trajectory in σ_1, σ_2, τ-space is conveniently represented by its projections onto two nonparallel planes, for example onto the σ_1,τ-plane and

onto the $(\sigma_1 - \sigma_2), \tau$-plane as in Figures 13 to 14. The material properties assumed for these examples are the same as those assumed by Ting and Nan (1968). The hardening parameter H is assumed during loading to be related to the current value of the shear yield stress k by the equation

$$H = \frac{7.5}{k^2} \left(\frac{k}{k_o} - 1\right)^{\frac{1}{2}}.$$

The initial shear yield stress k_o, and the elastic modulus E and Poisson's ratio v are assumed to be

$$k_o = 1000 \text{ psi.}, \quad E = 10^7 \text{ psi.}, \quad v = 0.25 \ (\beta = 5).$$

Ting and Nan (1968) obtained similar stress paths for $\beta = 5$ for one compression and one shear. They also gave solutions for $\beta = 2.25$ and observed that the character of the solutions changes somewhat at $\beta = 3$ $(v = 0.125)$.

Consider the case of a half space with no initial prestress, subjected to uniformly distributed step-function impact loads in compression σ_1^b and two shear stress components τ_2^b and τ_3^b such that the deformations are non-elastic. In this case the two shear stress components

will reduce to a single shear stress $\tau^b = \left[(\tau_2^b)^2 + (\tau_3^b)^2 \right]^{\frac{1}{2}}$.

The admissible stress paths in the σ_1,τ-plane and $(\sigma_1-\sigma_2)$, τ-plane for such a case would either be like odgb´ or like odeb´´ in Figures 13 and 14. For the path odeb´´ there is only a slow simple wave following the elastic jumps in σ_1 and s (traveling at the dilatational-wave-speed c_1) and in τ (traveling at the elastic shear—wave speed c_2). For the path odgb´, a fast simple wave of zero shear stress precedes the slow simple wave. Figures 16 and 17 show the simple wave solutions in the x,t-plane for the two cases considered above.

Now consider the case when the half space is statically prestressed beyond yield with two shear stress components τ_2^1 and τ_3^1 which have resultant shear stress τ^1, and then uniform step-function impact loads of one compressive stress σ_1^b and two shear stress components τ_2^b and τ_3^b, with resultant shear stress τ^b, are applied on the boundary x = 0 of the half space. If γ denotes the ratio of shear stress components, then let $\gamma^b = \tau_3^b/\tau_2^b$ denote the ratio of boundary shear stress components, while the initial value of $\gamma^1 = \tau_3^1/\tau_2^1$.

First consider the case when $\gamma^1 = \gamma^b$. This is
again equivalent to the case considered by Ting and Nan
(1968) of one compression load and one shear load. As
was pointed out in Subsection 4.3.3, the stress trajec-
tories for slow simple waves in the σ_1, τ plane may be
given an arbitrary rigid body displacement in the σ_1-
direction, corresponding to the additive integration
constant. The need for this is apparent from Figures
13 and 14, because the intersections of the fast-wave
stress trajectory pqr and the calculated slow-wave stress-
trajectory eb$^{\smile}$c does not have the same shear ordinate in
both the figures, which are supposed to be projections of
the same stress trajectory in the σ_1, σ_2, τ-space. There-
fore, for the case of initial static prestress of shear
τ^1, each slow-wave stress trajectory in the σ_1, τ-plane
must be given a horizontal displacement (i.e. parallel
to the σ_1-axis) by an amount such that the intersection
of the slow wave stress trajectory, with the fast-wave
stress trajectory has the same shear stress ordinate in
both the projection planes. For different values of pre-
stress τ^1, the amount of translation of the slow-wave
stress trajectory in the σ_1, τ-plane will be different.

Fig. 15 shows the modified network of stress trajectories in the σ_1, τ-plane for one such prestress case in shear.

Now consider the case when $\gamma^b \neq \gamma^1$. In this case too the slow-wave trajectories in the σ_1, τ-plane need modification as described for when $\gamma^b = \gamma^1$. But Equation (4.3-32) implies radial loading in τ_2, τ_3-plane in simple wave regions (so that γ remains constant during plastic loading). However, it is conceivable that an elastic jump may occur in γ, traveling at elastic shear wave speed c_2. Such a jump is only possible at the end of a fast simple wave or at the end of a constant-state region following the fast simple wave. Therefore, $\gamma = \gamma^1$ remains constant in the fast-wave and constant-state regions, and $\gamma = \gamma^b$ remains constant in the constant-state region following the jump and in the slow simple-wave region. A jump in γ implies a jump in both τ_2 and τ_3. Fig. 18 shows one such example in the x,t-plane. The corresponding stress trajectory could be obtained from Figures 14 and 15.

5.4   NONSIMPLE WAVE SOLUTION
FOR A HALF SPACE

Only one example of numerical integration of the

characteristic conditions obtained in Section 4.4 has

been worked out, for a half space, subjected to compres-

sion and one shear loading. For simplicity, the boundary

and initial conditions were chosen to avoid discontinu-

ities in the stresses, except at the leading wave front.

The half-space was assumed statically prestressed in shear

to a value τ_0 below yield. Then at time t = 0 the bound-

ary x = 0 was assumed loaded suddenly in compression to

a value $(\sigma_1)_0$ such that yield is just reached at $(\sigma_1)_0$,

τ_0. For t > 0 the boundary tractions both increase lin-

early with time. Specific numerical values of τ_0 = 200

psi. and $(\sigma_1)_0$ = 2575 psi. were chosen for the illustra-

tion. With this type of loading the leading wave is an

elastic shock wave, a jump in σ_1 from zero to $(\sigma_1)_0$,

propagating at the elastic dilatational wave speed c_1.

Immediately above this line in the x,t-plane the stress

state is uniform with $\sigma_1 = (\sigma_1)_0$, $\tau = \tau_0$. The plastic

wave region above the line x = $c_1 t$ has the following

initial conditions

$$v_1(x, x/c_1) = -(\sigma_1)_o/\rho c_1, \quad v_2(x, x/c_1) = 0.0$$

$$\text{for } x \geqslant 0$$

$$\sigma_1(x, x/c_1) = (\sigma_1)_o, \quad \tau(x, x/c_1) = \tau_o.$$

The boundary conditions on $x = 0$ in the half space are

$$\sigma_1(0,t) = (\sigma_1)_o + 10^9 t$$

$$\tau(0,t) = \tau_o + 0.25 \times 10^9 t$$

for stress in psi. and time in seconds. The increment

in the time step is given by $\Delta t = \Delta x/c_1$. For the above

example, solutions were obtained with different values

of grid size $\Delta x = 0.05$ in., 0.025 in., and 0.0125 in.

in order to see the effect of change in grid size.

Figures 21 and 22 demonstrate the stress profiles at

$t \approx 2.5$ microseconds and the stress histories exper-

ienced by particles originally at $x = 0.3$ in. and $x = 0.7$

in. For the example considered, $c_1 = 2.174 \times 10^5$ in./sec.,

and therefore, with the final value of $\Delta x = 0.0125$ in.

the final time-increment size was $\Delta t = \Delta x/c_1 \approx 0.57$

micro seconds.

The integration process was terminated after a

time period equal to the time that would be required for

an elastic dilatational wave traveling at speed c_1 to pass through a 3/2 in. thick plate. This choice was made arbitrarily. For the mesh size of $\Delta x = 0.0125$ in., there were 7140 grid points to calculate, and the total computation time on the CDC 3600 computer was 2 min. 30 sec.

The numerical results obtained are presented in Figures 23 to 28 as velocity and stress histories at different sections, x-constant, and as velocity and stress profiles at different time intervals. Projections of stress trajectories in the σ_1, τ and ($\sigma_1 - \sigma_2$), τ-planes are shown in Fig. 29 for particles initially located at $x = 0.5$ in., and $x = 1.0$ in. Fig. 30 shows level lines for various constant values of σ_1, v_1, τ, and v_2 in the x,t-plane. Despite the fact that this is not a simple wave it is observed that the level lines are all straight. Each level line of σ_1 is also a level line of v_1, and each level line of τ is a level line of v_2. Further comment on this unanticipated result is given in Section 5.5.3. The slopes dx/dt of the level lines of σ_1 and v_1 are denoted by $\underline{a}$ while the slopes of the level lines of τ and v_2 are denoted by $\underline{b}$. Fig. 31 shows a plot of $\underline{a}$ versus σ_1 and $\underline{b}$ versus τ.

5.5   DISCUSSION OF RESULTS

5.5.1   Comparison of Different
Hardening Assumption Results
for Tension-Torsion Impact
on Thin-Walled Tube

The relative differences, caused by varying the
hardening parameter m, in the simple-wave stress histories
experienced by a particle in a thin-walled tube depend on
the ratio σ^b/τ^b of the impact boundary normal and shear
stresses and on the initial state of the tube. For no
initial prestress and for σ^b/τ^b less than about one, the
relative differences in the stress history for a given
boundary condition are not significant, as is evidenced
by Fig. 4. These differences still remain small when the
tube is prestressed with a static shear stress beyond
yield, if the ratio of impact boundary normal and shear
stresses remains small. Significant differences begin
to occur when σ^b/τ^b is large.

For the case of initial static prestress beyond
yield, the differences may even become qualitative as
well as quantitative. Fig. 12 demonstrates these dif-
ferences in the stress history for certain boundary and

initial conditions. In the case shown in Fig. 12, for m = 1 or m = 0.5 the simple wave solution in the x,t-plane consists of a fast simple wave, a constant state region and a slow simple wave region, while for m = 0 (purely kinematic hardening), following the constant state region a jump occurs in shear stress, traveling at the elastic shear speed c_2. Such a jump can also occur for m = 0.5, but for conditions with positive shear stress such a jump followed by a plastic loading is never predicted by the isotropic hardening assumption. This qualitative difference in the predictions by the kinematic hardening assumption (or by the combined kinematic and isotropic hardening assumption) from the predictions by the isotropic hardening assumption could be an important factor, if experimental studies confirm or fail to confirm the existence of such a jump in shear stress for suitable impacts on a tube prestressed in shear.

When there is no prestress, such qualitative differences do not appear, but the quantitative difference becomes noticeable when the impact σ^b/τ^b increases beyond unity. In Fig. 4 the quantitative differences in

the stress histories when the tube is initially stress free and the ratio of the impact boundary normal and shear stresses is large, are shown. When the tube is prestressed with normal stress beyond the critical point, and then loaded with normal and shear impact loads, the phenomenon of unloading predicted by the isotropic hardening assumption is repeated by kinematic hardening and combined kinematic and isotropic hardening, but again the process of constructing simple wave solutions is more difficult than it is in the isotropic hardening cases. This unloading phenomenon has been previously predicted by Clifton for isotropic hardening, as follows.

As Clifton (1966) showed, when an isotropic-hardening tube is prestressed in uniaxial normal stress beyond the critical point (the point where the slope $d\sigma/d\epsilon$ of the uniaxial stress-strain curve equals the elastic shear modulus G) and then loaded with normal and shear impact loads, an elastic wave precedes the combined-stress plastic wave. This elastic wave consists of a jump decrease in σ traveling at speed c_o followed by a jump increase in τ traveling at speed c_2.

After these two elastic waves have passed, the stress point is at the proper (σ^o, τ^o) value to begin a slow-wave trajectory leading to (σ^b, τ^b) from a point on the (hardened) yield locus that passes through the prestress point $(\sigma^1, 0)$. When the hardening is kinematic hardening or combined kinematic and isotropic hardening, a similar unloading phenomenon occurs, but the analysis is more complex because of the greater history dependence. No examples for such a case have been worked out here. It would be necessary to construct a family of slow-wave trajectories leading from various points (σ^o, τ^o) on the hardened yield locus. For isotropic hardening case the slow-wave trajectory could be constructed by backward integration from (σ^b, τ^b) to determine the beginning point (σ^o, τ^o) on the hardened yield locus, but this is not possible with the other hardening assumptions.

5.5.2 Simple Waves in Isotropic Hardening Half Space

The simple wave solutions with one compression and two shear impact step-function loadings on the boundary of a half space of isotropic hardening material

reduce to the case of one compression and one shear im-
pact step-function loadings when $\gamma^1 = \gamma^b$. Then $\tau_3 = \gamma\tau_2$,
and all plastic simple-wave stress histories are radial
in the τ_2, τ_3-plane. A rotation of the coordinate axes
then reduces the problem to the case of loading by com-
pression and a single shear previously treated by Ting
and Nan (1968).

For the cases when $\gamma^1 \neq \gamma^b$, an elastic jump in γ
traveling at the elastic shear wave speed c_2 occurs. In
these cases the stress history is not radial with a single
τ_3/τ_2 ratio, but the fast simple wave is radial with one
τ_3/τ_2 ratio while the slow simple wave is radial with an-
other τ_3/τ_2 ratio after the jump in γ. (There are also,
as a rule, constant state regions in the x,t-plane pre-
ceding and following the $x = c_2 t$ wave front.) These
cases cannot be reduced by a rotation of the coordinate
axes to the cases treated by Ting and Nan. But the
stress-trajectory projections onto the σ_1,τ-plane and
the $(\sigma_1-\sigma_2)$,τ-plane $(\tau^2 = \tau_2^2 + \tau_3^2)$, belong to the fami-
lies of trajectories computed for compression and one
shear. Therefore, all simple wave solutions for one
compression and two shear loadings for a half space of

isotropic hardening material can be constructed from
stress trajectories like those already obtained by Ting
and Nan (1968) for the case of compression loading and
one shear loading.

The simple-wave solutions reveal the possibility
that elastic unloading regions can occur in the interior
even when the dynamic boundary tractions are increasing,
so that the final (σ^b, τ^b) point lies outside the (hard-
ened) yield locus. Similarly plastic loading regions
may occur even when the boundary loading is elastic.
This suggests that unforeseen elastic and plastic load-
ings and possible discontinuities may also occur with
nonsimple waves. When they do occur they will make the
numerical integration procedures difficult.

5.5.3   Nonsimple Waves in
          Isotropic Hardening
          Half Space

Stress histories and stress profiles obtained
for different values of Δx show that a further reduction
in the mesh size is needed to obtain a more accurate so-
lution. But the difference method used to approximate
the system of partial differential equations itself needs

improvements. Therefore, it was felt that reducing the grid size to still a smaller value would waste computer time without contributing much to the accuracy of the solution.

The surprising result that the level lines of σ_1, v_1, τ, and v_2 from the numerical solution are all straight raises some interesting questions about the possibility of finding analytic solutions, or at least solutions obtained by quadratures instead of by the step-by-step numerical integration of the hyperbolic system of equations. Since the surprising result was only discovered during the final stage of preparing this manuscript, no investigation of these possibilities has yet been made. Because only one numerical example has been worked out, it is not possible to make any generalizations about what other boundary conditions would lead to straight level lines.

This is not a simple wave solution, since both σ_1 and τ are not constant along the same level line, and the level lines are not in general characteristics of the governing hyperbolic system. But the compressional wave and the shear wave appear as though they were uncoupled,

122

since the level line of σ_1 is also a level line of v_1,
and the level line of τ is also a level line of v_2.
Such uncoupling was not expected because the governing
constitutive equations are coupled.

Nonsimple wave solutions for several different
boundary conditions on a half space have been reported
by Nan (1968), but he did not show any level lines.

5.6   CONCLUSIONS AND RECOMMENDATIONS FOR FURTHER RESEARCH

The present study has been carried out with a
view of predicting material behaviors under combined
stresses, offering to experimentalists the possibility
of a qualitative difference in the results due to dif-
ferent material behaviors and different boundary condi-
tions.

For some loadings the kinematic hardening and
combined kinematic and isotropic hardening assumptions
lead to predictions qualitatively different from the
predictions of isotropic hardening. This opens the pos-
sibility of experimental verifications.

The simple wave solutions with kinematic hardening and combined kinematic and isotropic hardening are more complex to construct than with the isotropic hardening assumption. The difficulty is a result of the history-dependence of the hardening even during continuous loading. This difficulty will likely persist with any other history-dependent hardening theories.

Nonsimple wave solutions might not be much more difficult with history-dependent hardening assumptions, since the numerical integration follows the history anyway. But the numerical integration procedures should be used with caution, since unforeseen discontinuities and elastic regions may occur. Not enough examples of nonsimple waves have been worked out to permit generalizations.

Although simple waves in an isotropic hardening half space loaded by compression and two independent shears cannot always be reduced by a rotation of axes to the compression and one shear case treated by Ting and Nan (1968), the stress trajectories they obtained can be adapted to give the solution for the more general case.

The nonsimple wave solution obtained for the particular example in this study offers a possibility of closed-form solutions because the level lines of the solution are straight and the compressional and shear waves appear to be uncoupled. But it should be noted that not enough has been done to make any definite conclusions. This possiblity of closed-form nonsimple wave solutions should certainly be a subject for further research.

Many details of error analysis and convergence in the numerical procedure also remain to be investigated, as well as techniques for handling unloading waves and reflections from the opposite face when the half space is replaced by a plate of finite thickness.

This subject of dynamic plasticity with combined stresses has drawn the attention of research workers only very recently. A few simple examples, such as the thin-walled tube and the half space, have been solved for certain simple boundary conditions and material behaviors. The phenomena predicted by these examples need to be confirmed or contradicted by experimental studies. Rapid progress in this direction may not occur because of the difficulties of the combined-stress experiments. Only

one experimental investigation has been reported so far,
by Lipkin and Clifton (1968), who were able to confirm
the existence of fast waves and slow waves in tests on
tubes.

In the meantime, solutions for more boundary
value problems need to be obtained, and, if possible,
procedures worked out to handle the cases where unfore-
seen unloading occurs.

5.7   GRAPHICAL DISPLAY OF RESULTS

Figures 1 to 31 are given on the following pages
in this section to display the results obtained for the
boundary value problems of the thin-walled tube and the
half space.

*Initial yield surface
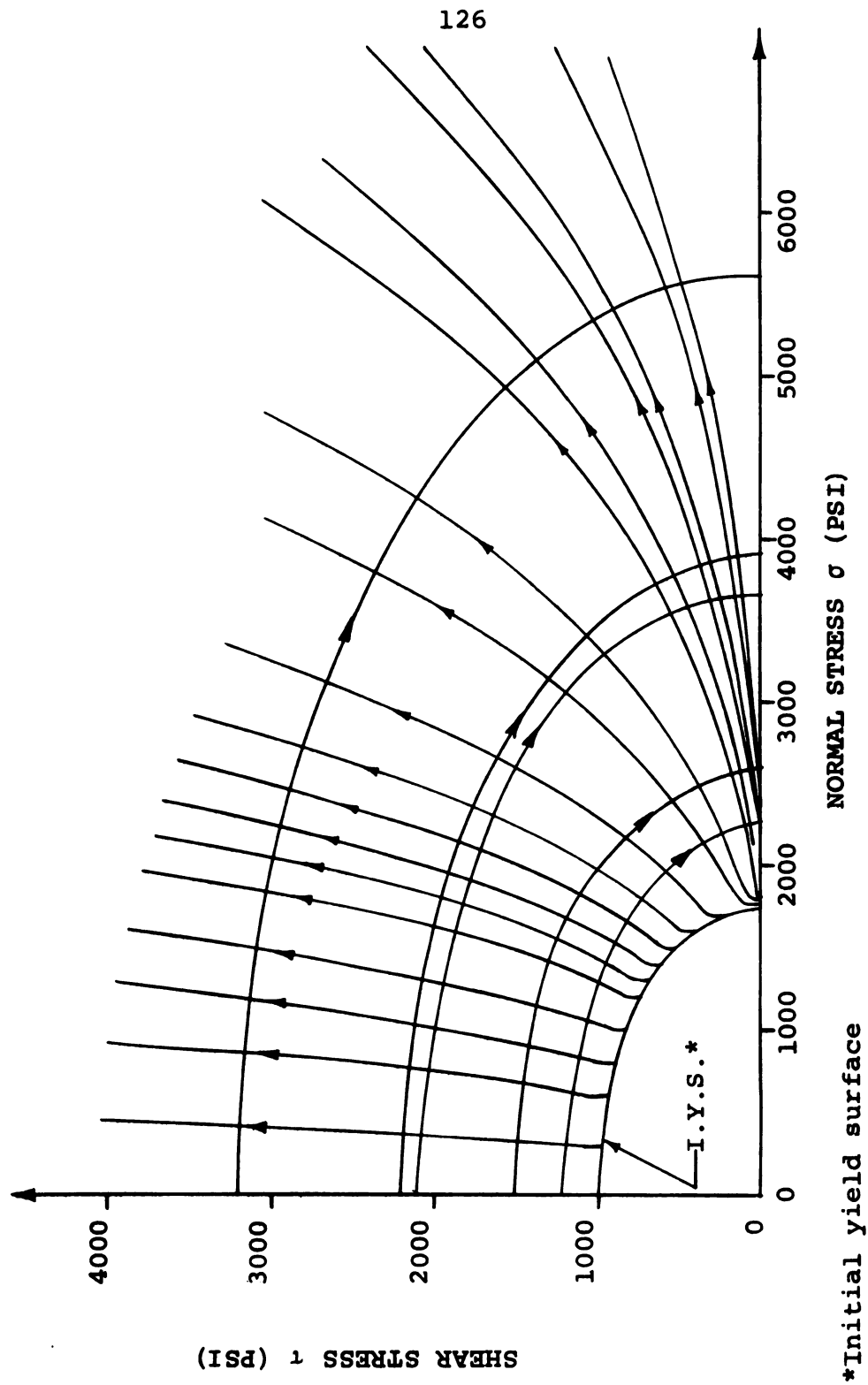
Fig.1.--Slow Simple Wave Stress Paths for a Nonprestressed Tube (m = 1.0)
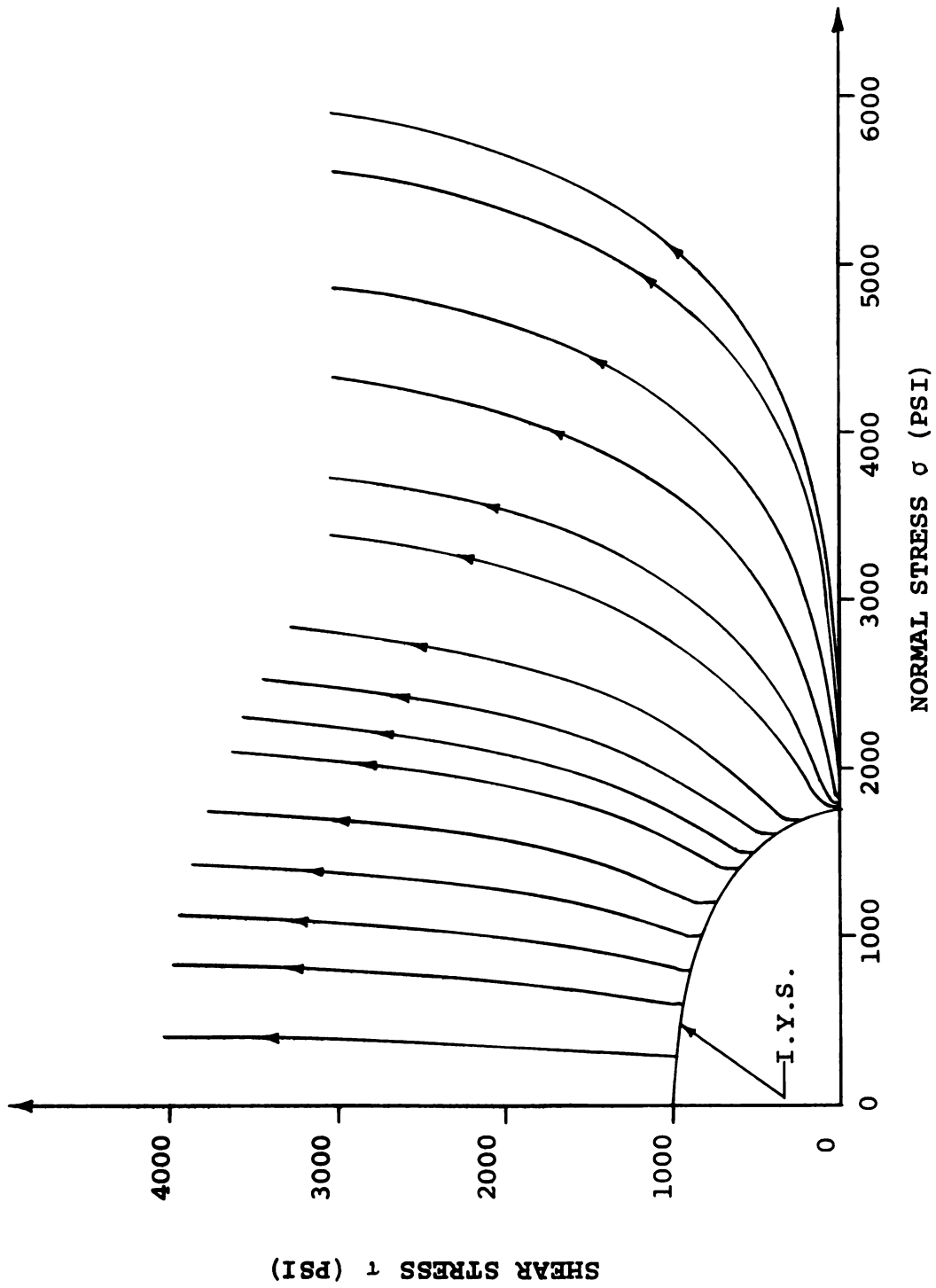
Fig. 2.--Slow Simple Wave Stress Paths for Nonprestressed Tube (m = 0.0)
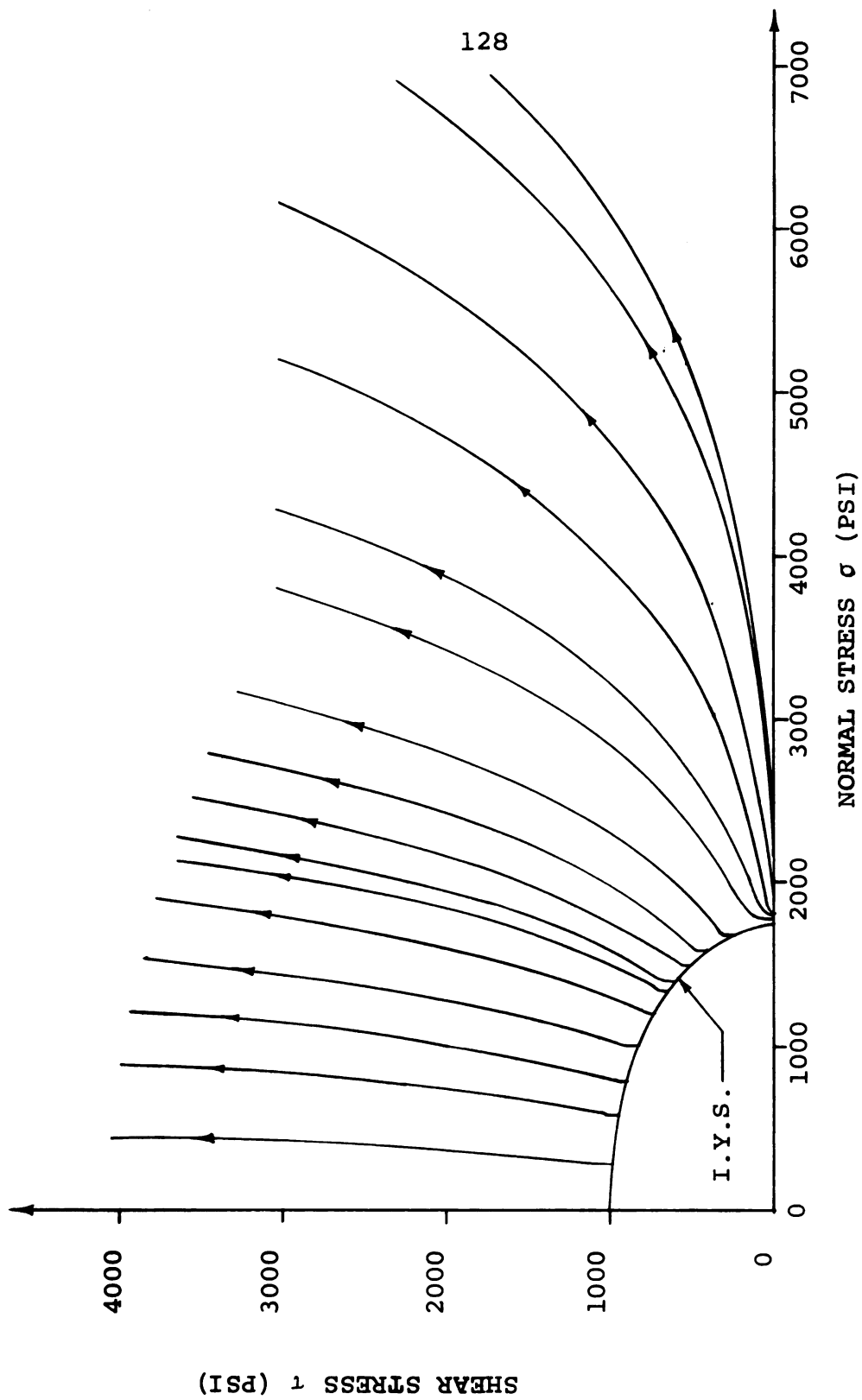
Fig. 3.--Slow Simple Wave Stress Paths for Nonprestressed Tube (m = 0.5)
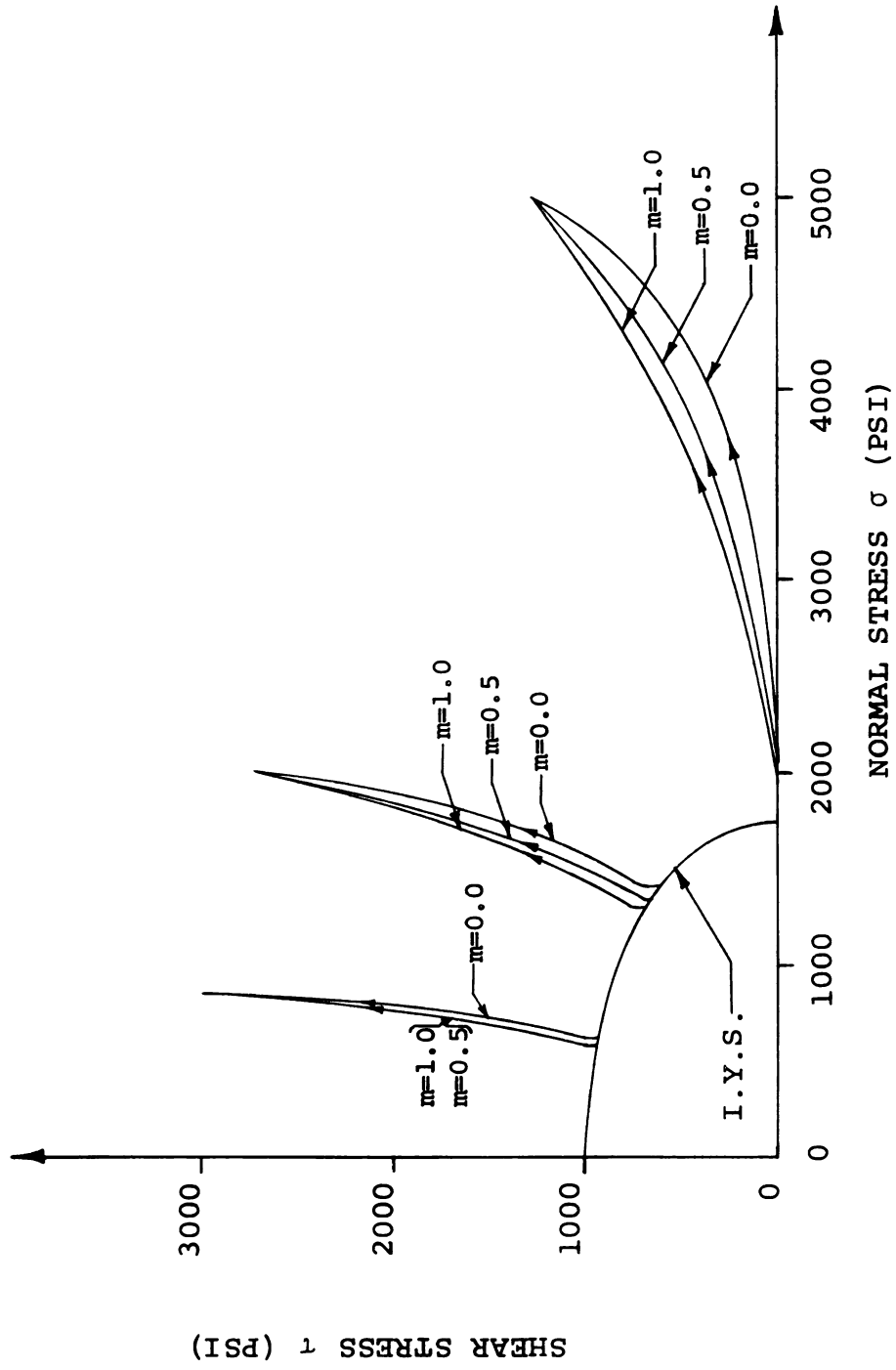
Fig. 4.--Particle Stress Paths in a Tube
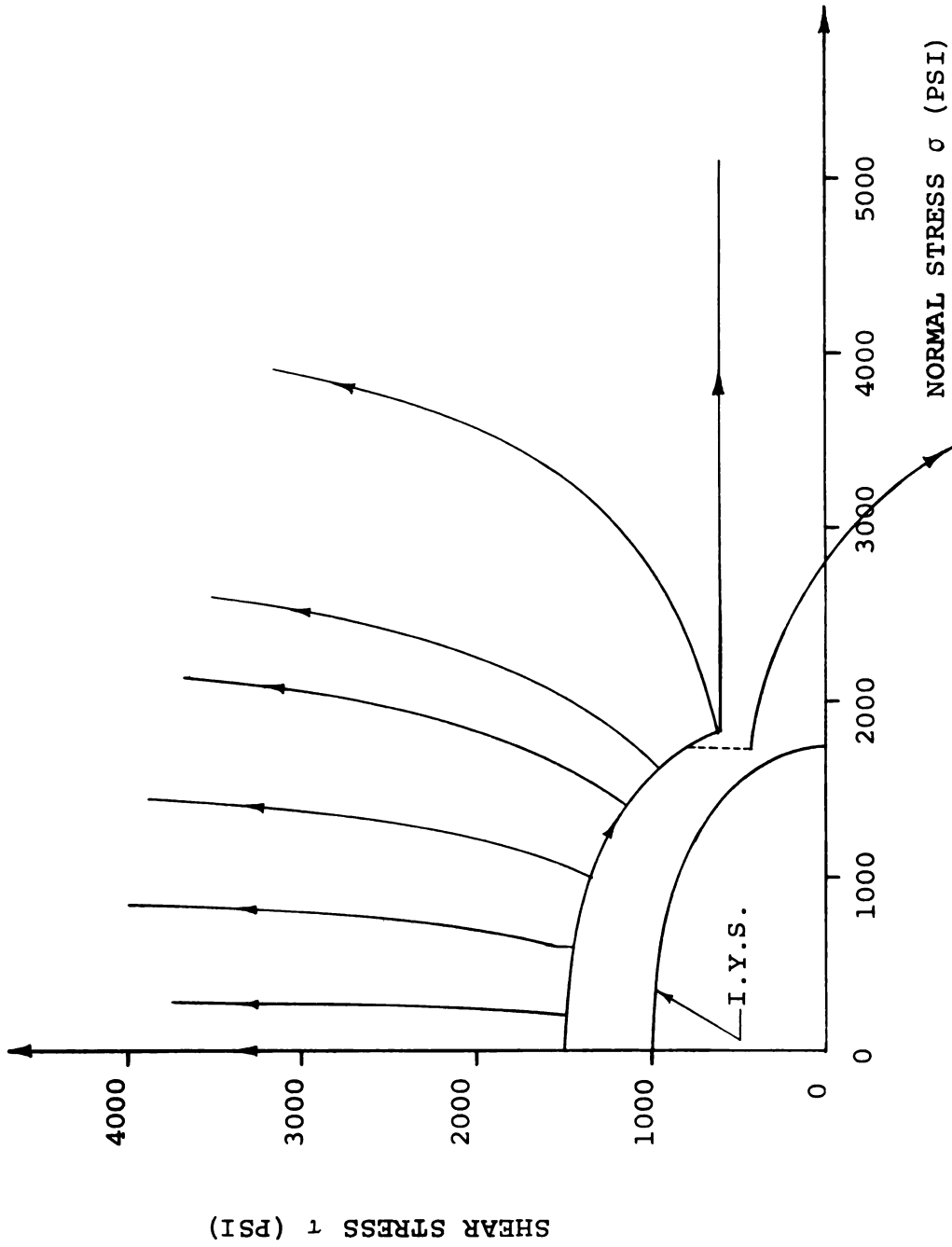
Fig. 5.--Simple Wave Stress Paths for Prestressed Tube (m = 0.0)
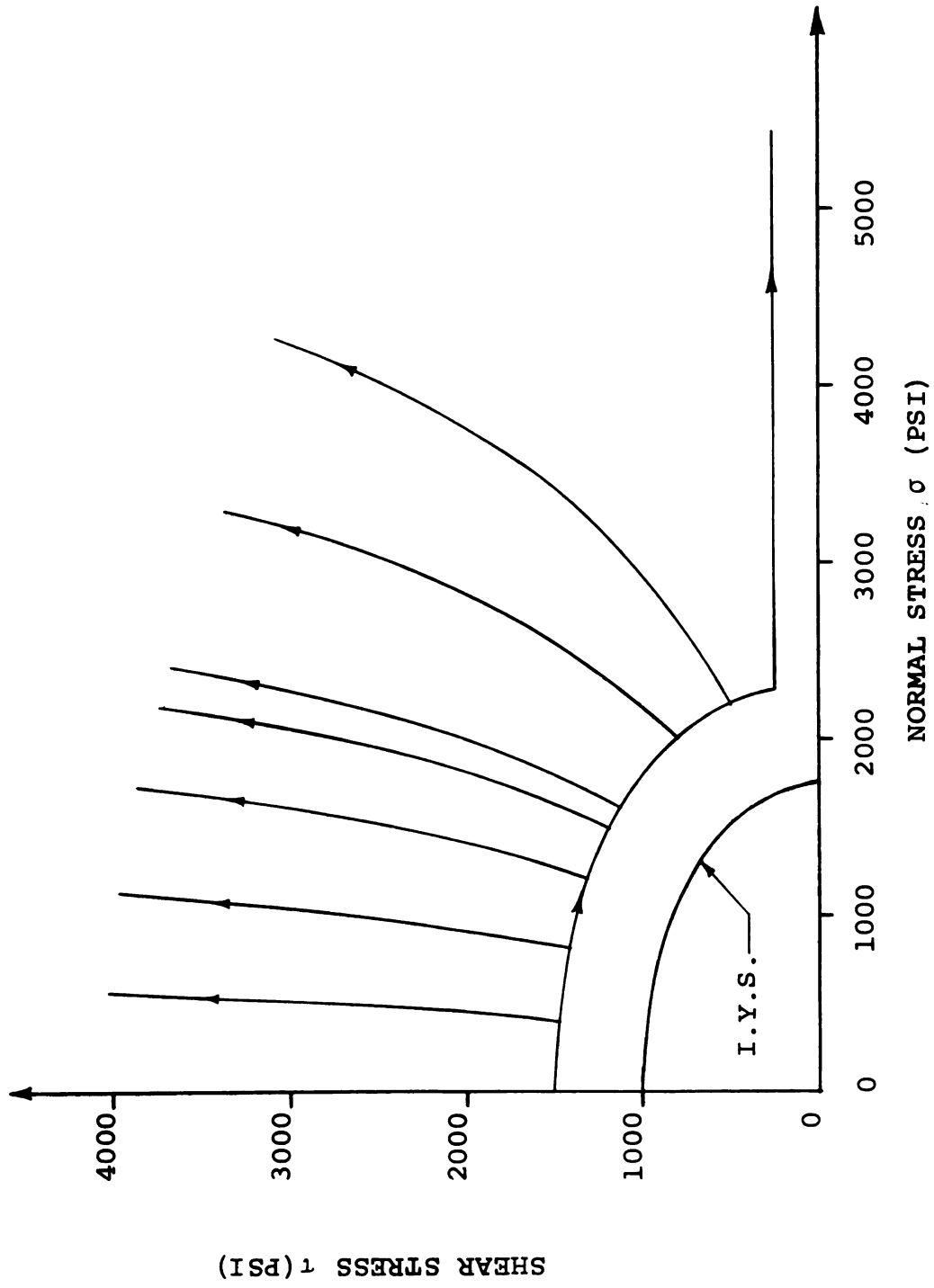
Fig. 6.--Simple Wave Stress Paths for Prestressed Tube (m = 0.5)
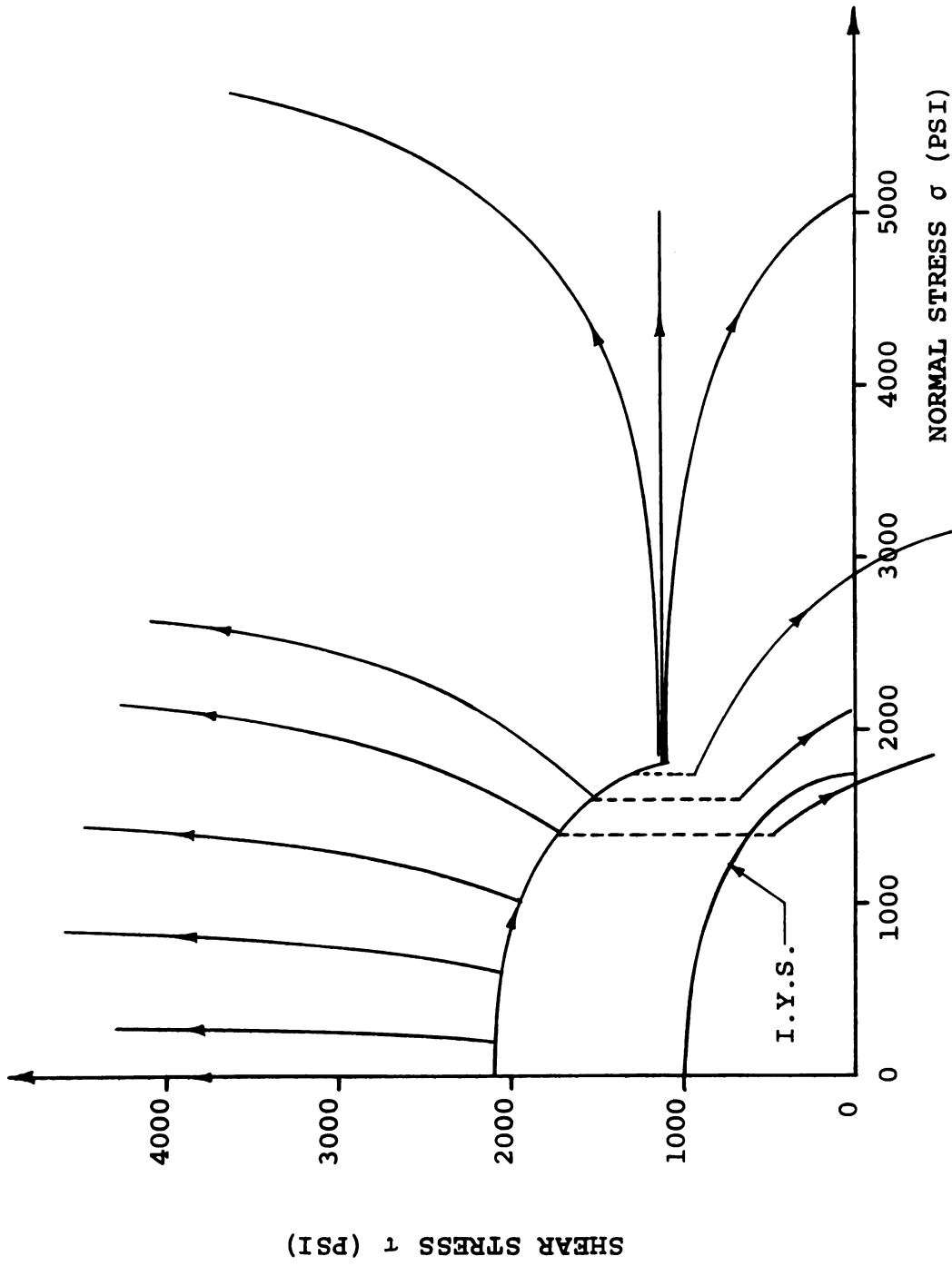
Fig. 7.--Simple Wave Stress Paths for Prestressed Tube (m = 0.0)
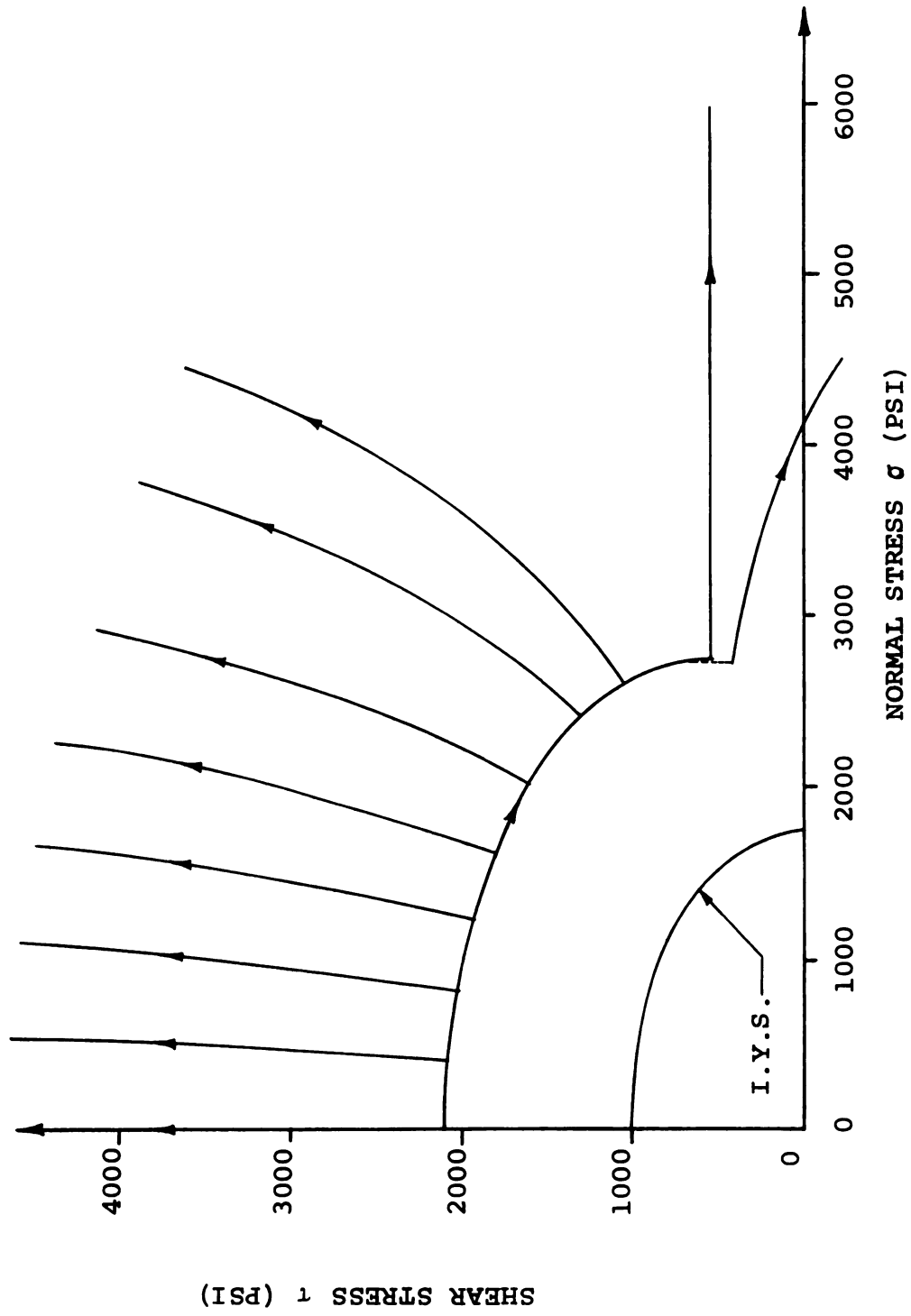
Fig. 8.--Simple Wave Stress Paths for Prestressed Tube (m = 0.5)
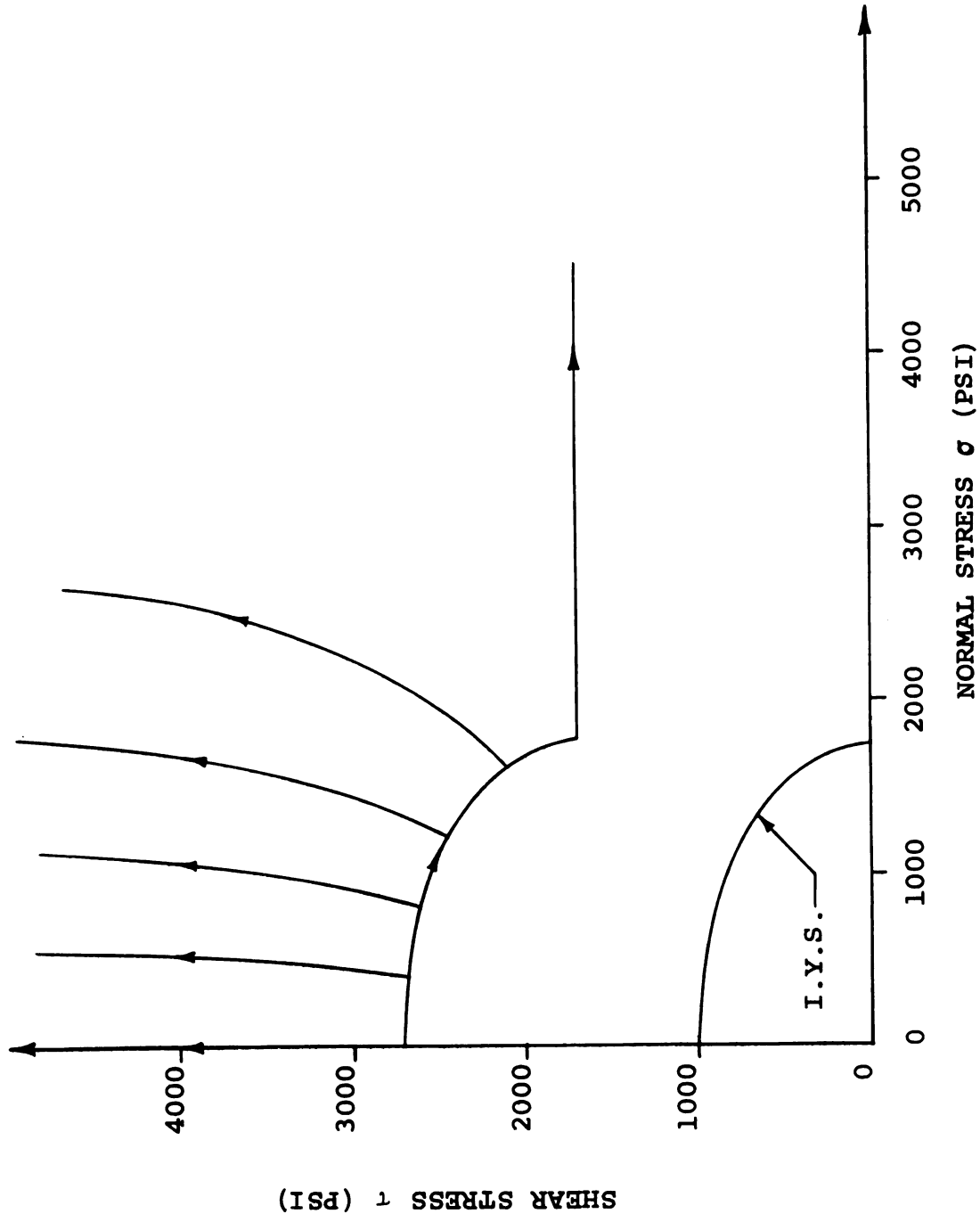
Fig. 9.--Simple Wave Stress Paths for Prestressed Tube (m = 0.0)
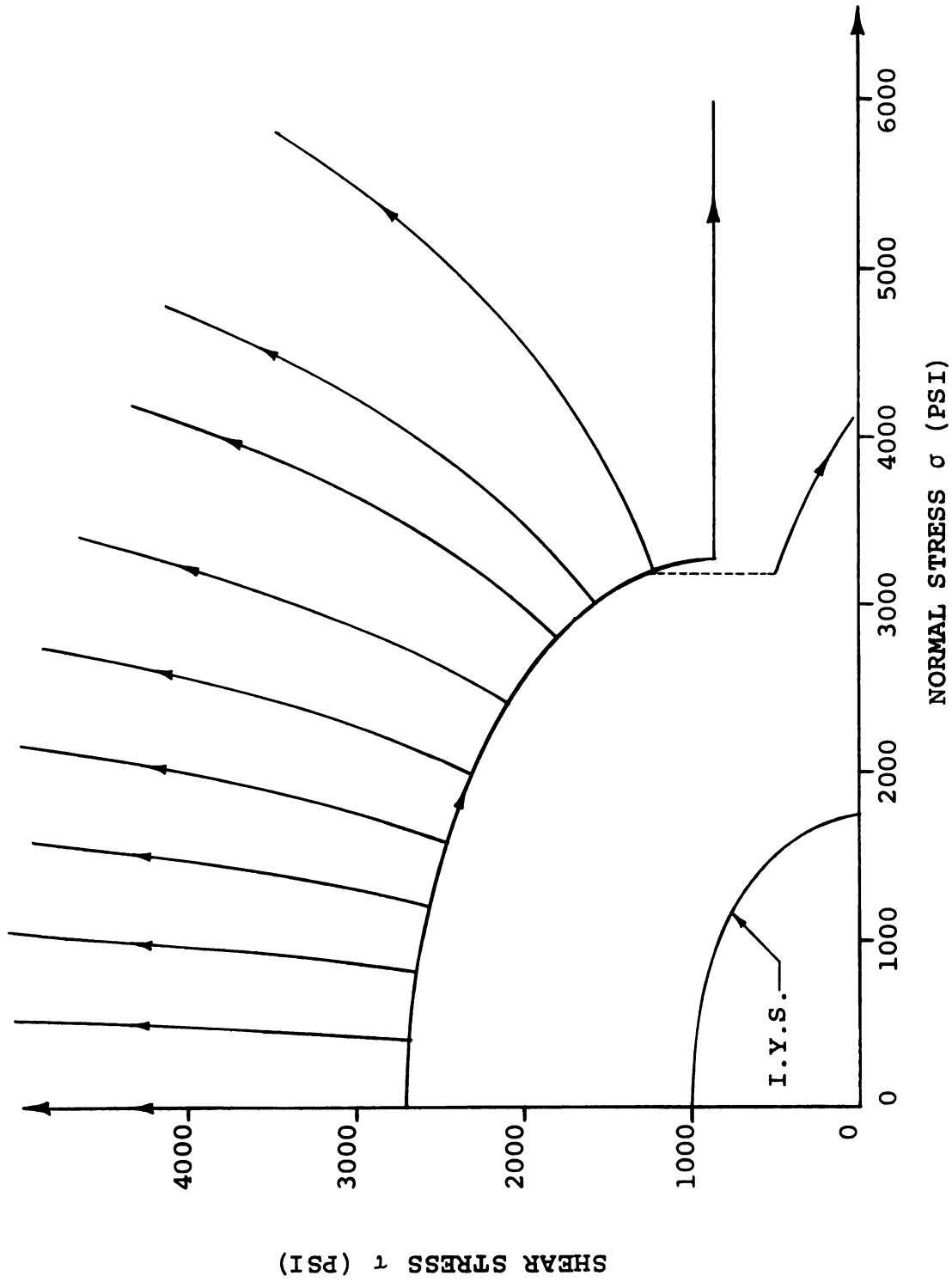
Fig. 10.--Simple Wave Stress Paths for Prestressed Tube (m = 0.5)
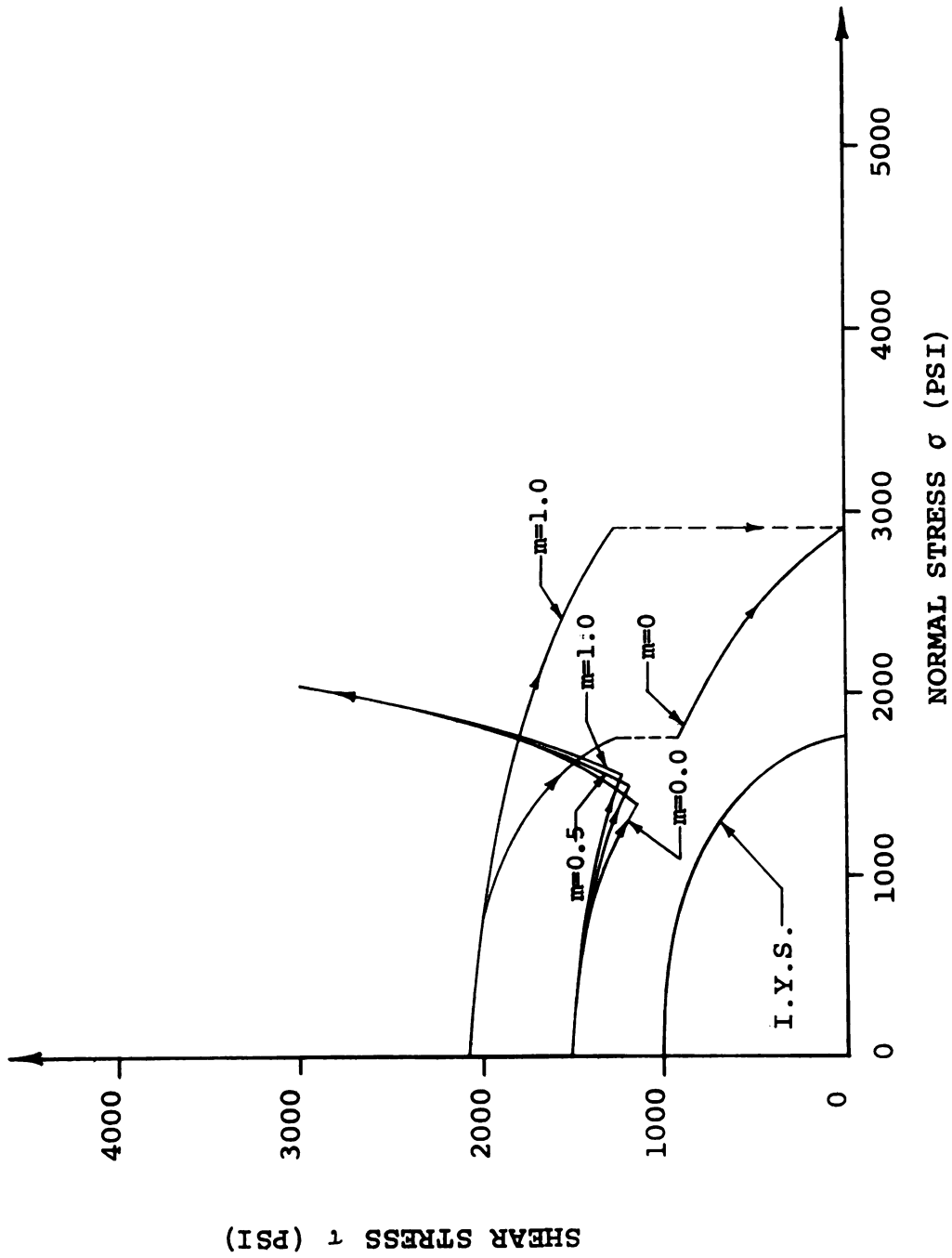
Fig. 11.--Particle Stress Paths in a Tube
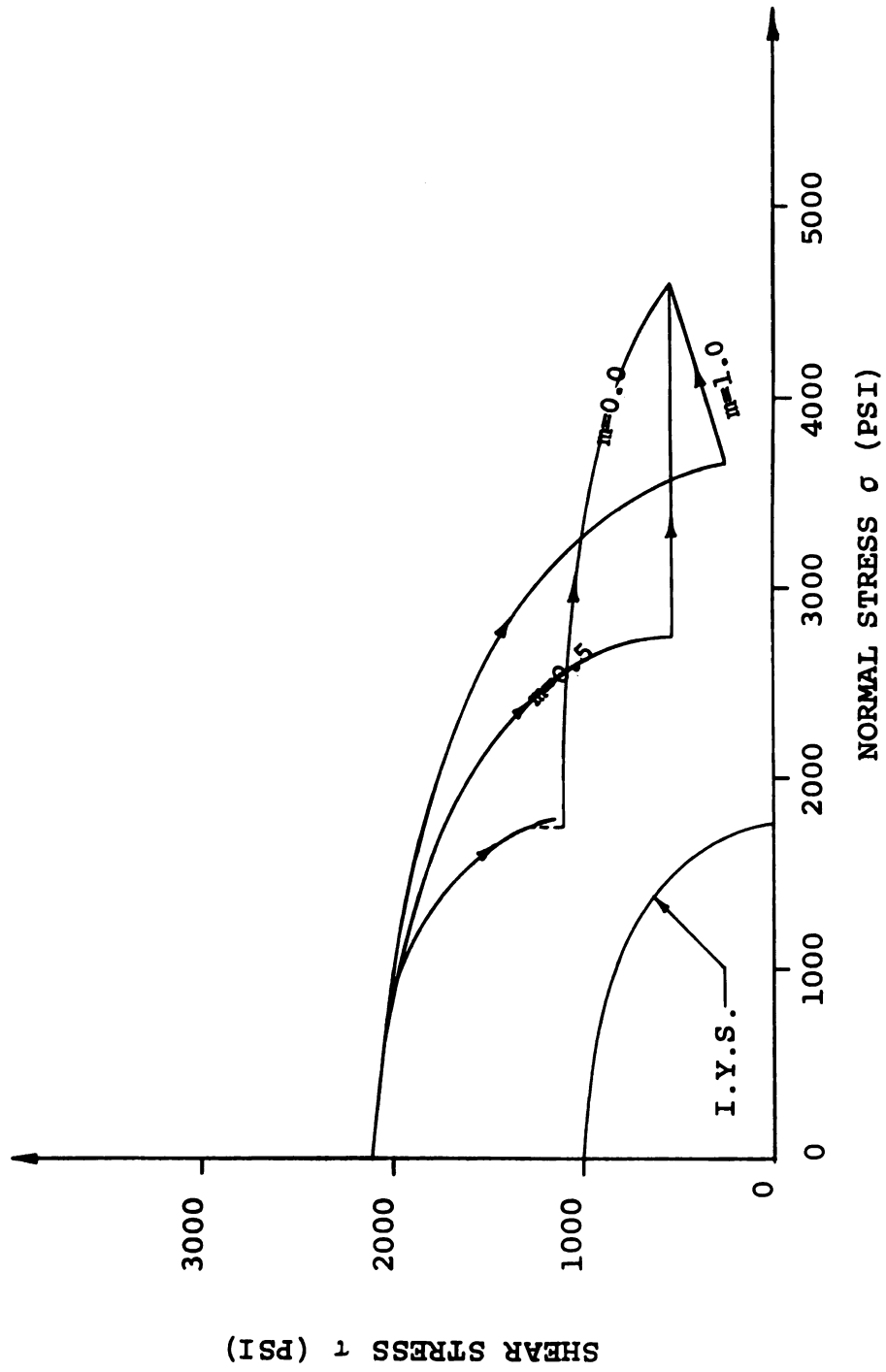
Fig. 12.--Particle Stress Paths in a Tube
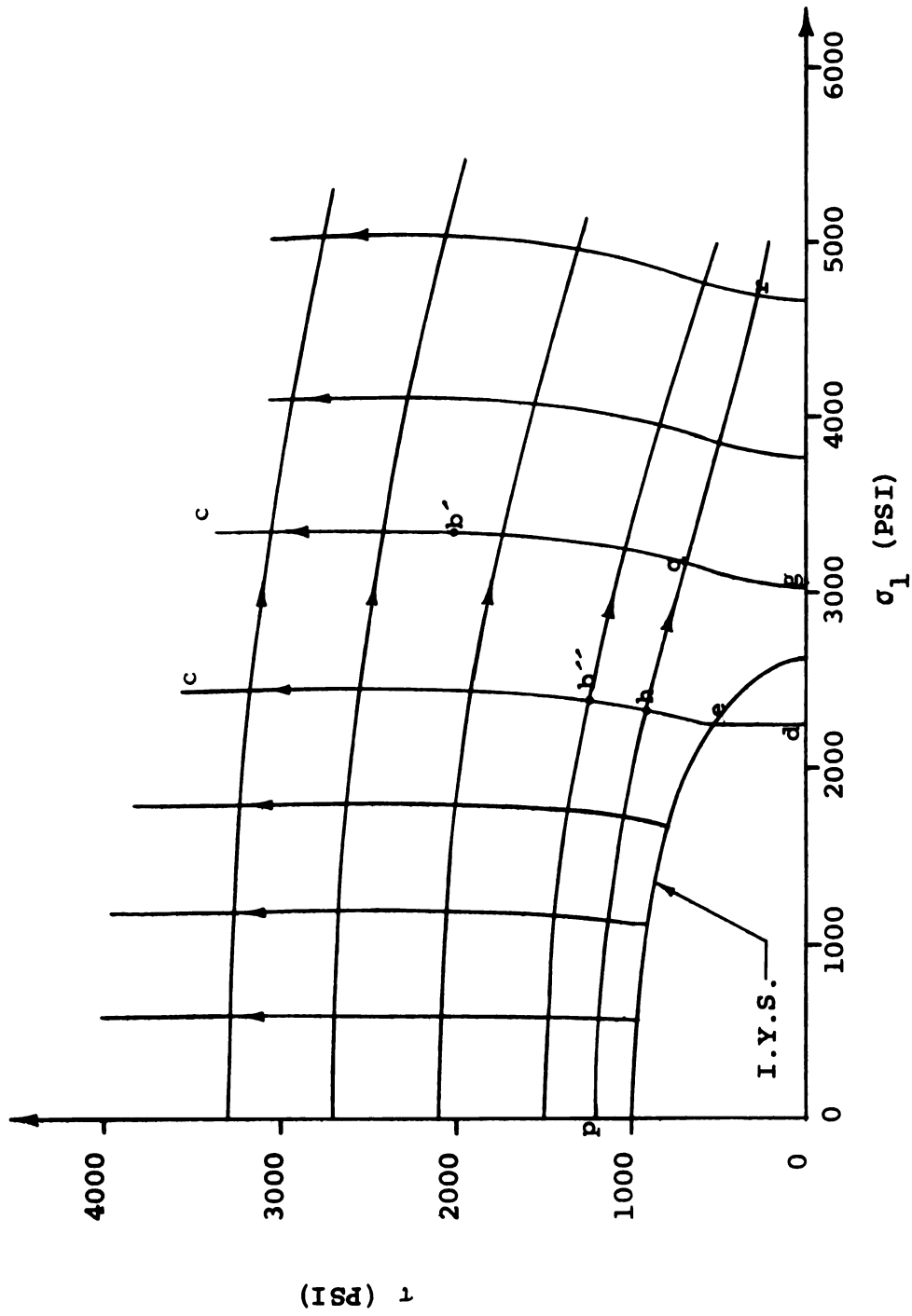
Fig. 13.--Simple Wave Stress Paths for a Half Space
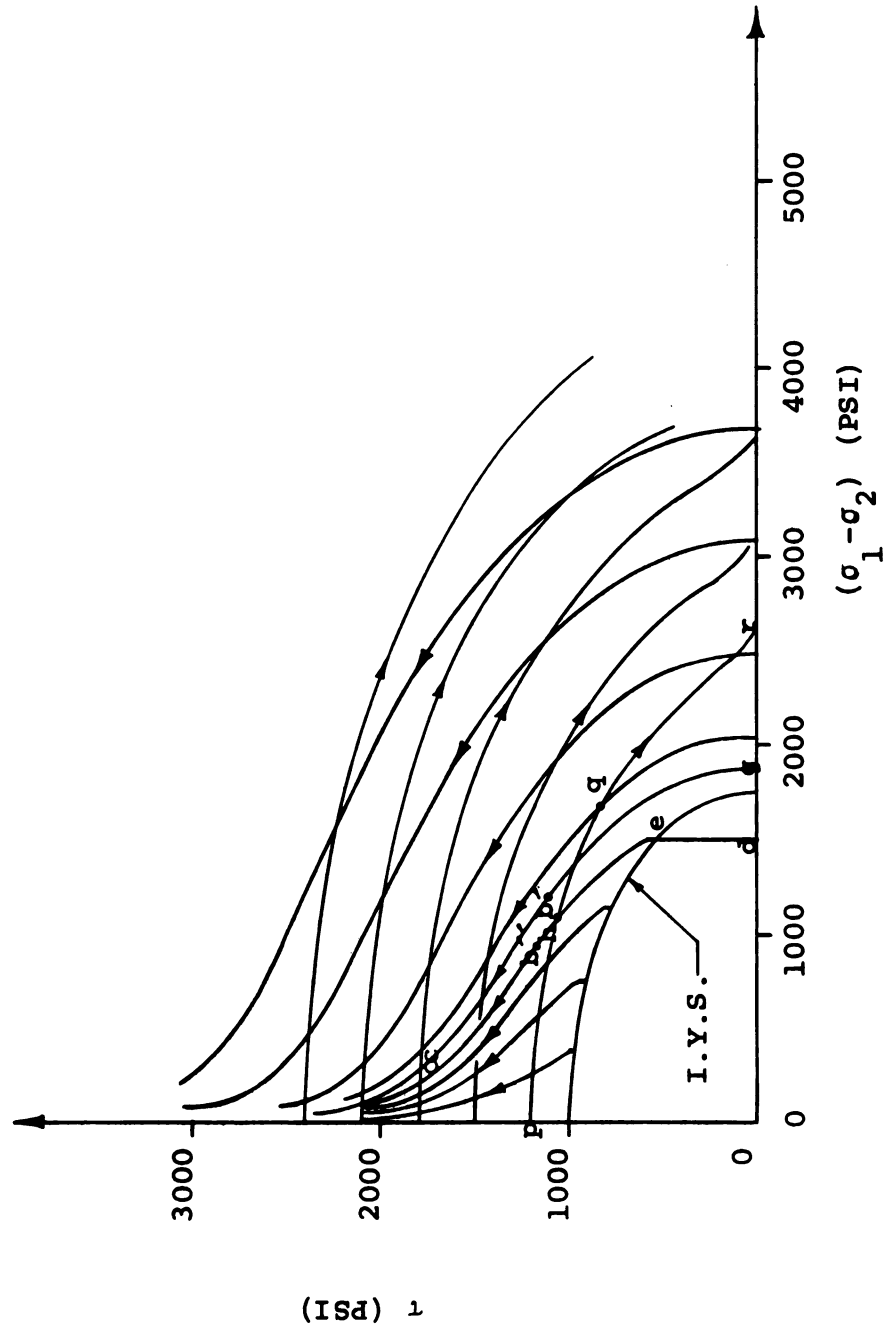
Fig. 14.--Simple Wave Stress Paths for a Half Space
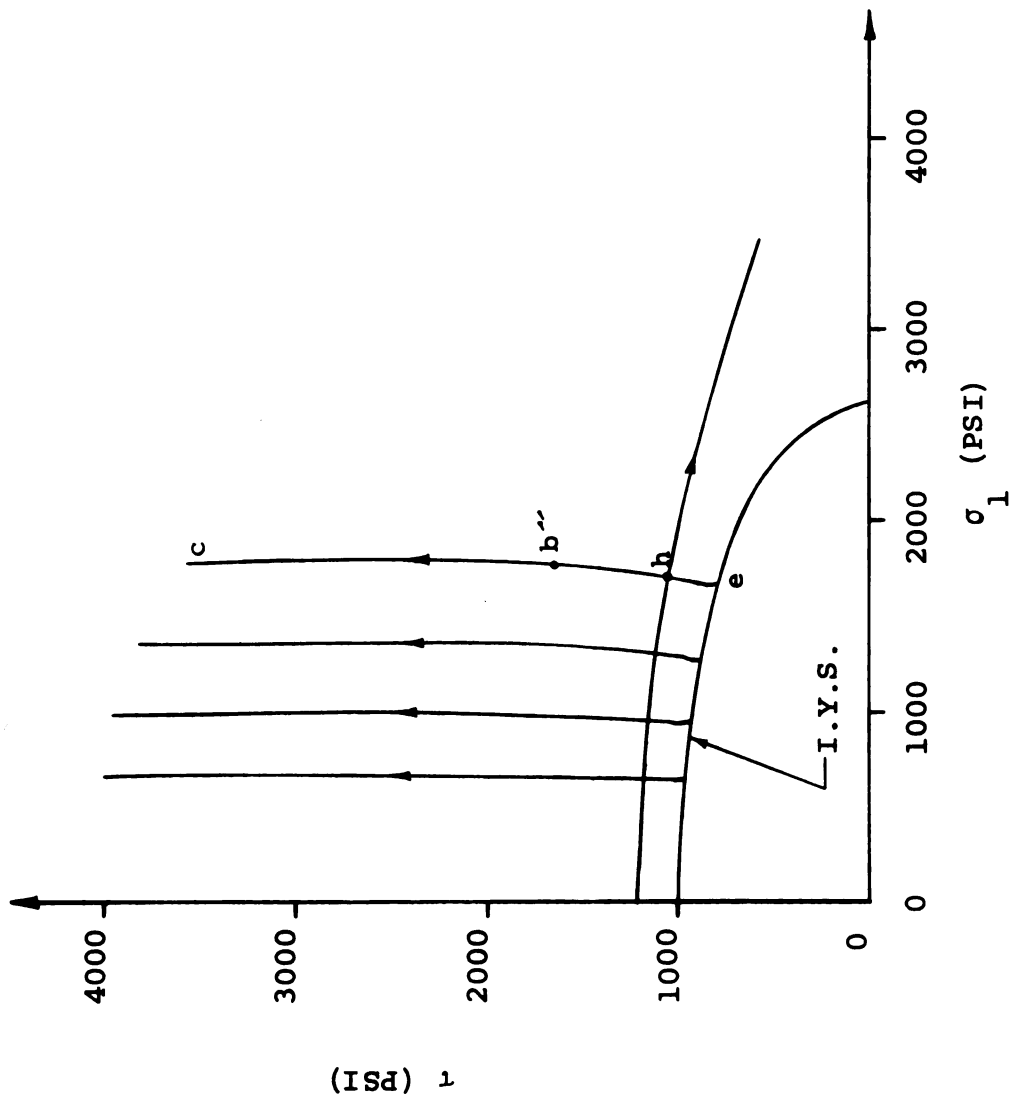
Fig. 15.--Modified Simple Wave Stress Paths for a Half Space
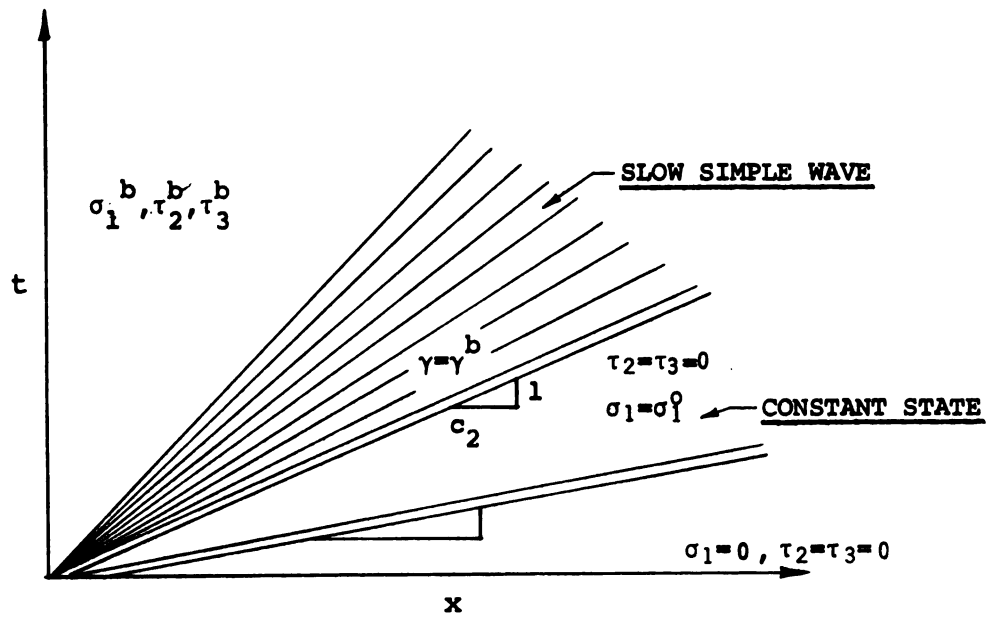
Fig. 16.--Simple Wave Solution, No Prestress, No Fast Wave
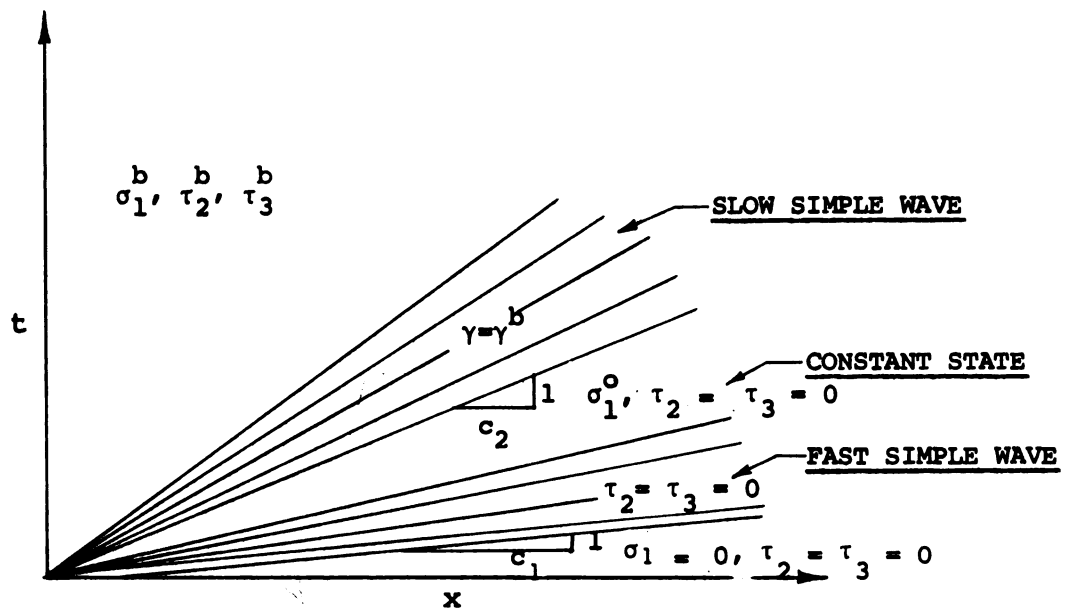
Fig. 17.--Simple Wave Solution, No Prestress
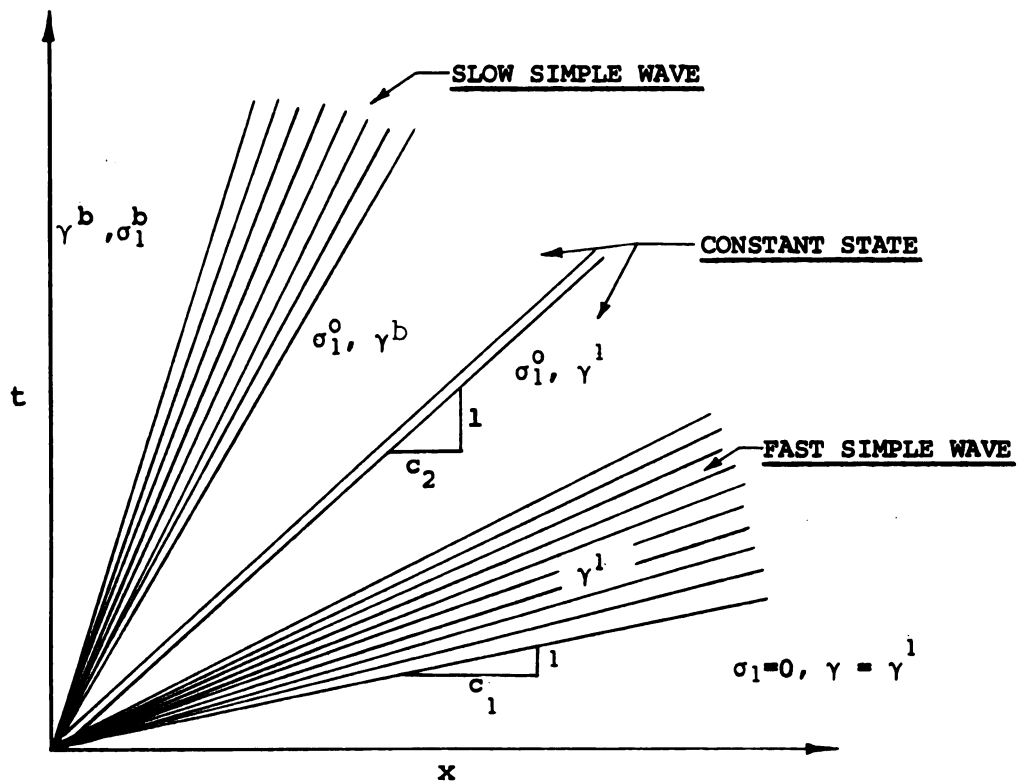
Fig. 18.--Simple Wave Solution With Jump in γ
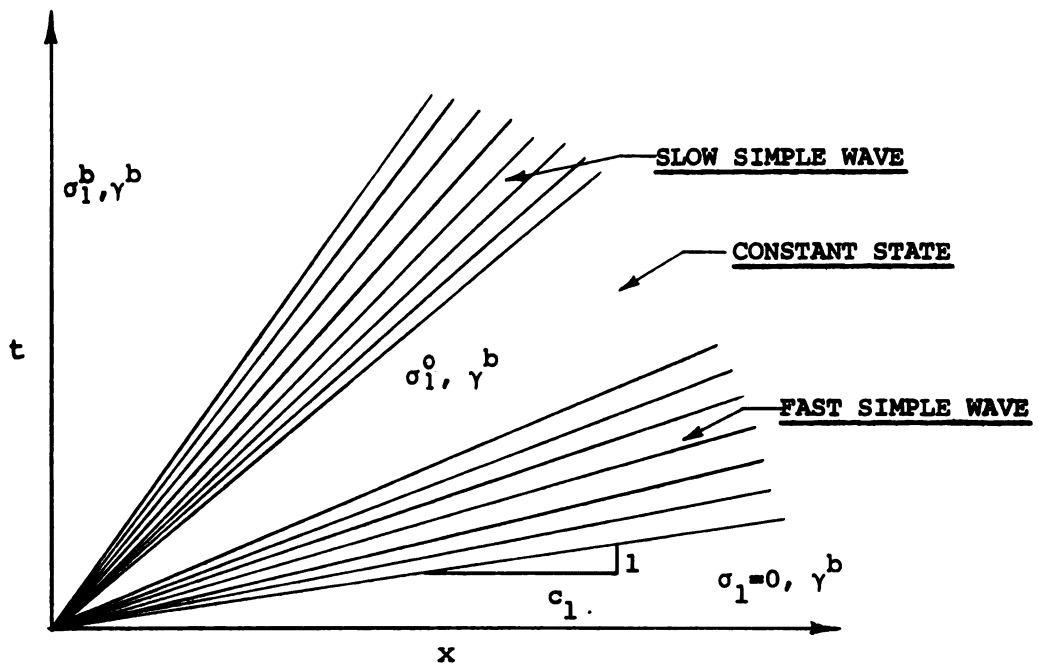
Fig. 19.--Simple Wave Solution With Constant γ
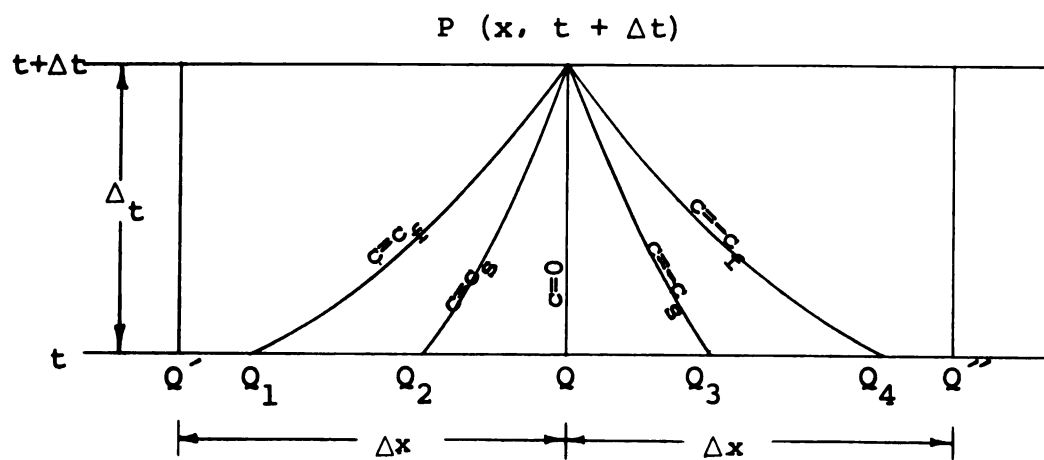
Fig. 20a.--Interior Grid Point P
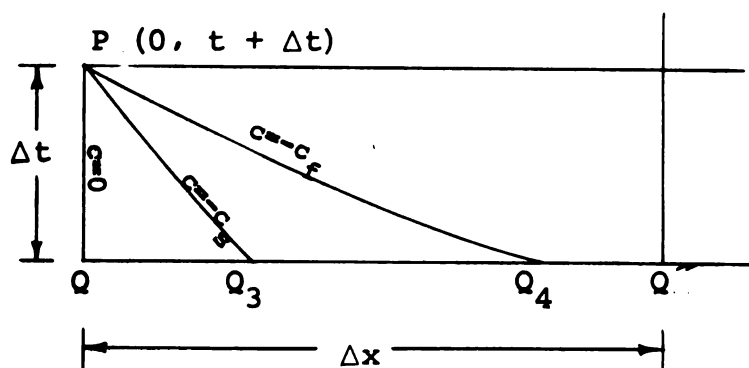
Fig. 20b.--Boundary Grid Point P
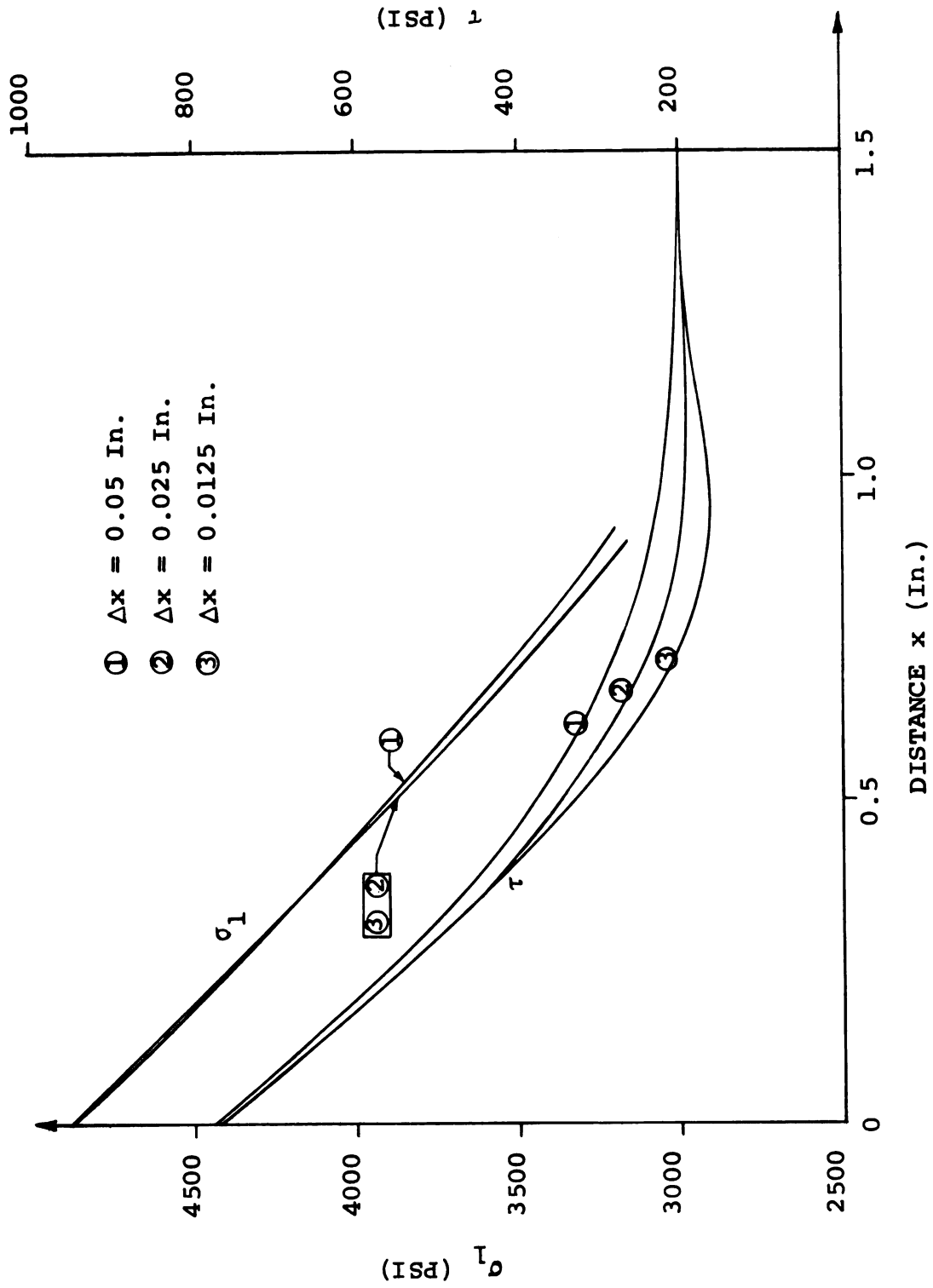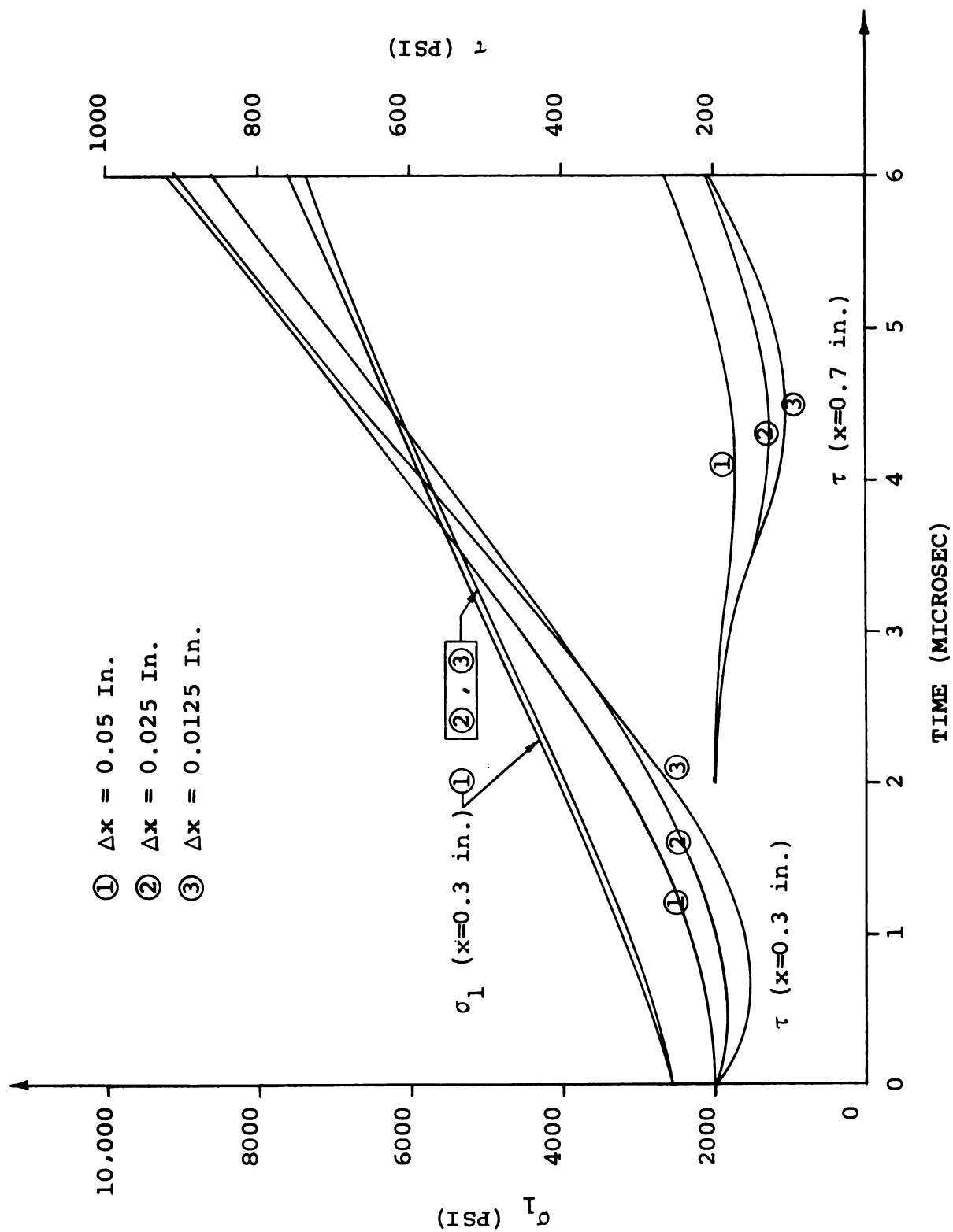
Fig. 21.--Stress Profile at t ≈ 2.25 microsec.

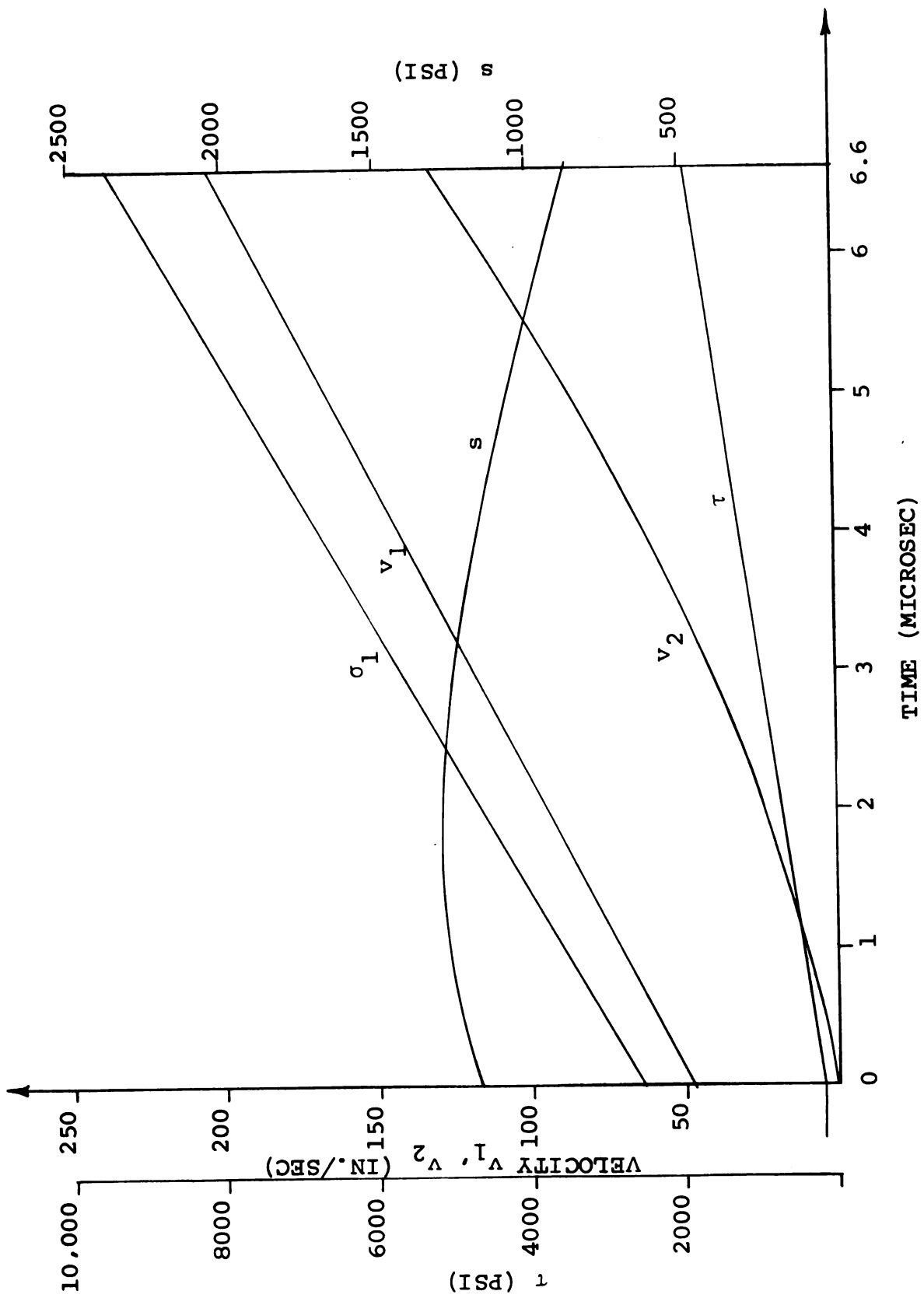Fig. 22.--Stress Histories of σ_1 at $x = 0.3$ in. and τ at $x = 0.3$ in. and $x = 0.7$ in.
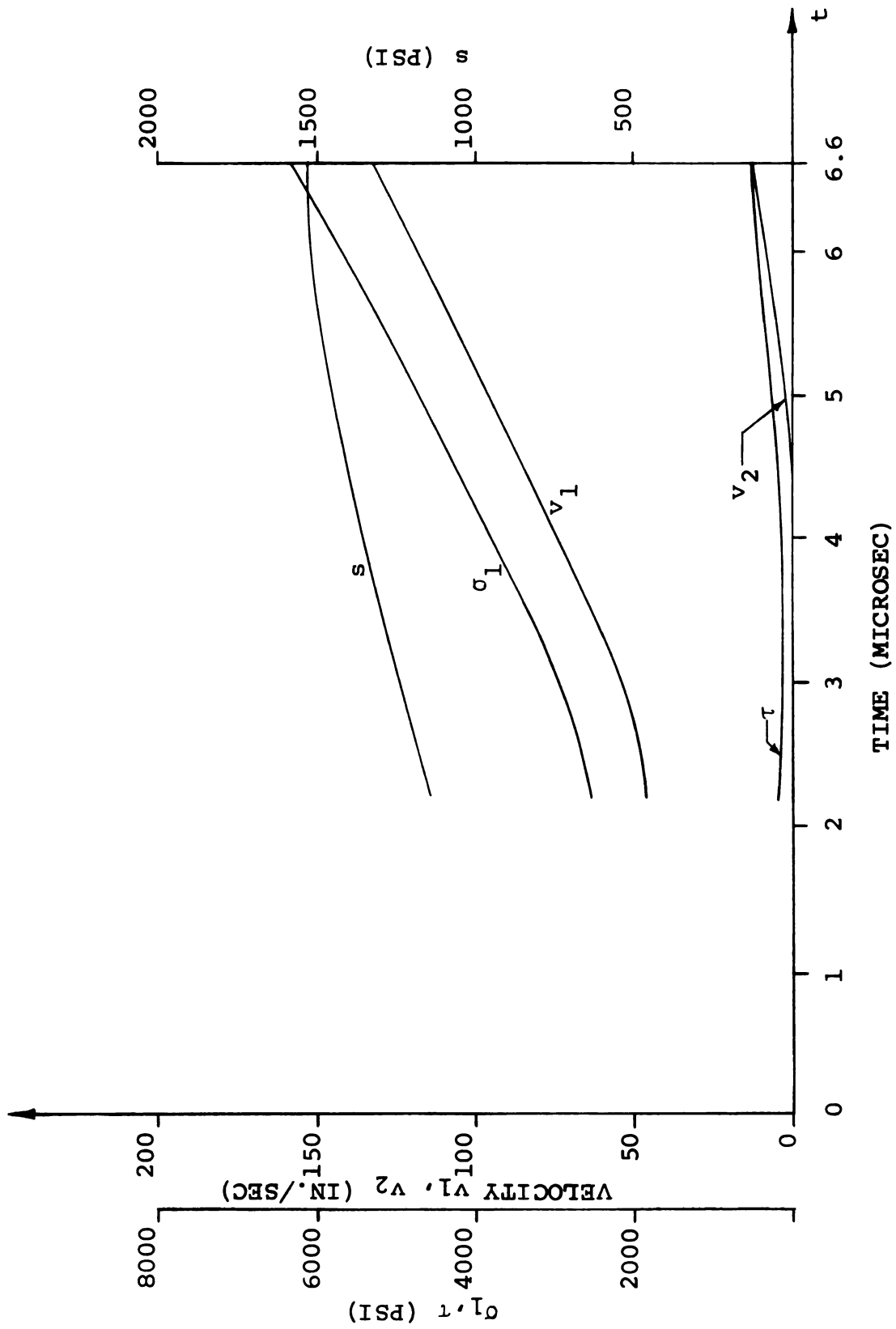
Fig. 23.--Stress and Velocity Histories at x = 0. in.
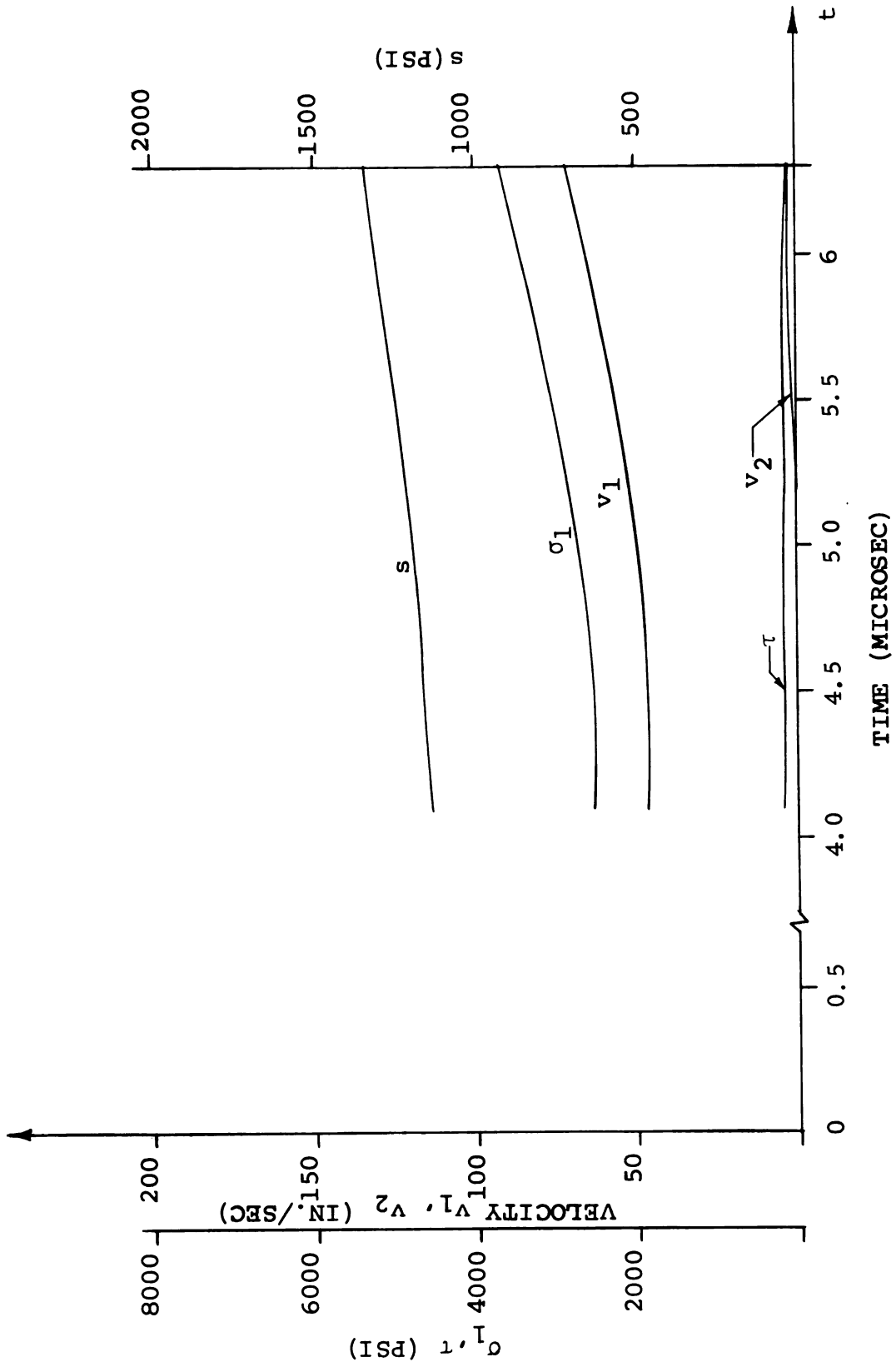
Fig. 24.--Stress and Velocity Histories at x = 0.5 in.

Fig. 25.--Stress and Velocity Histories at x = 1.0 in.

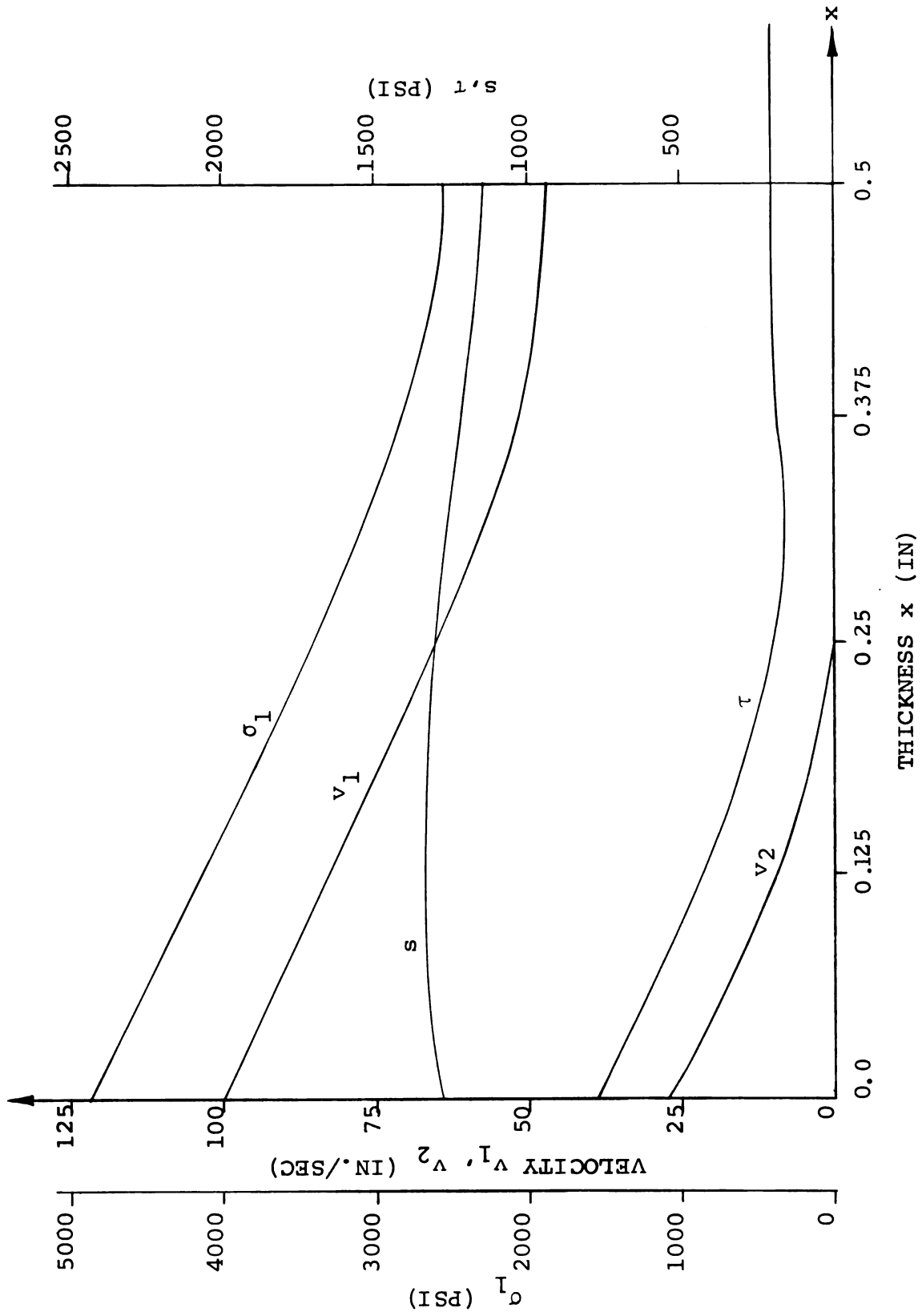Fig. 26.--Stress and Velocity Profiles at t ≈ 2.5 MICROSEC
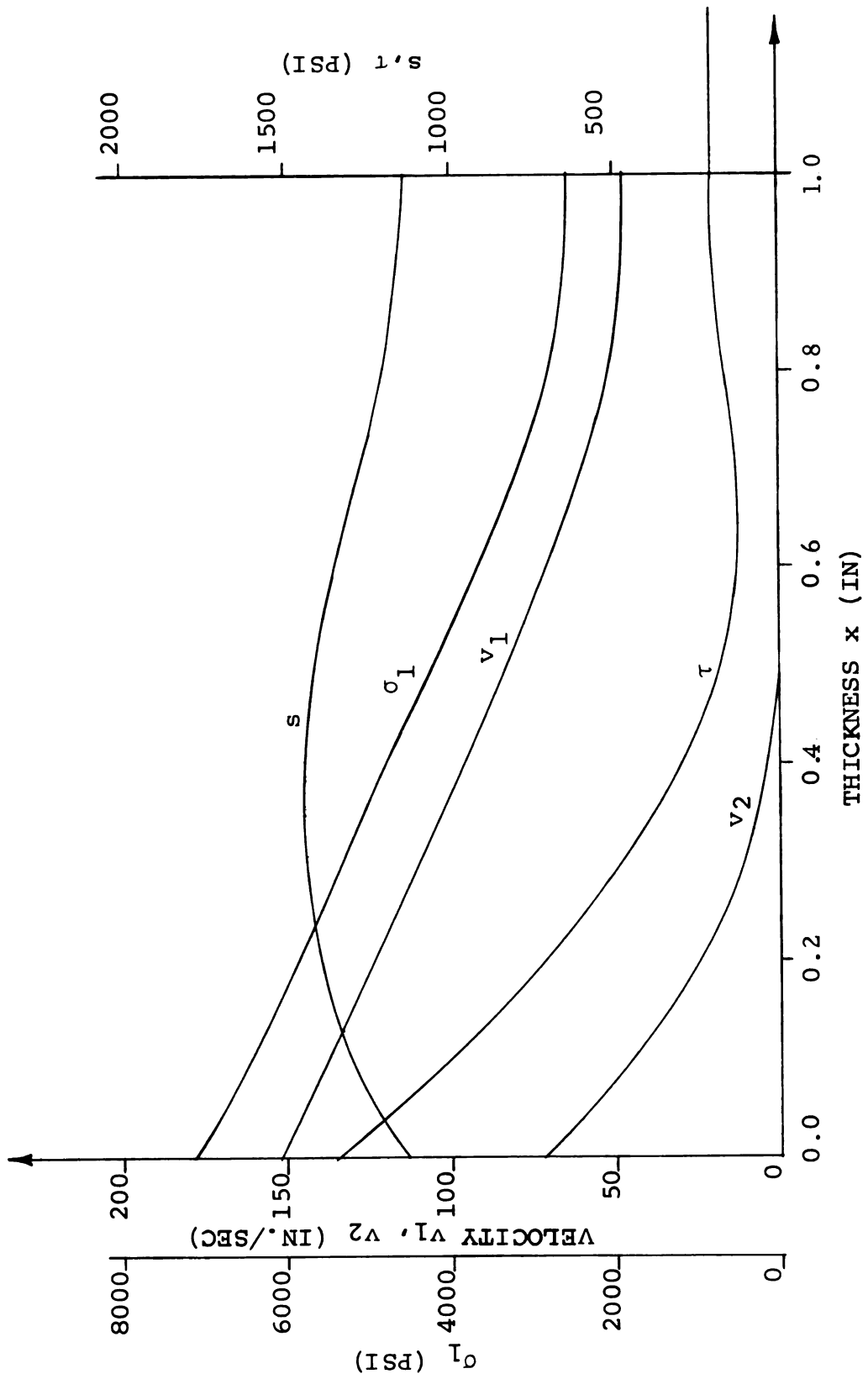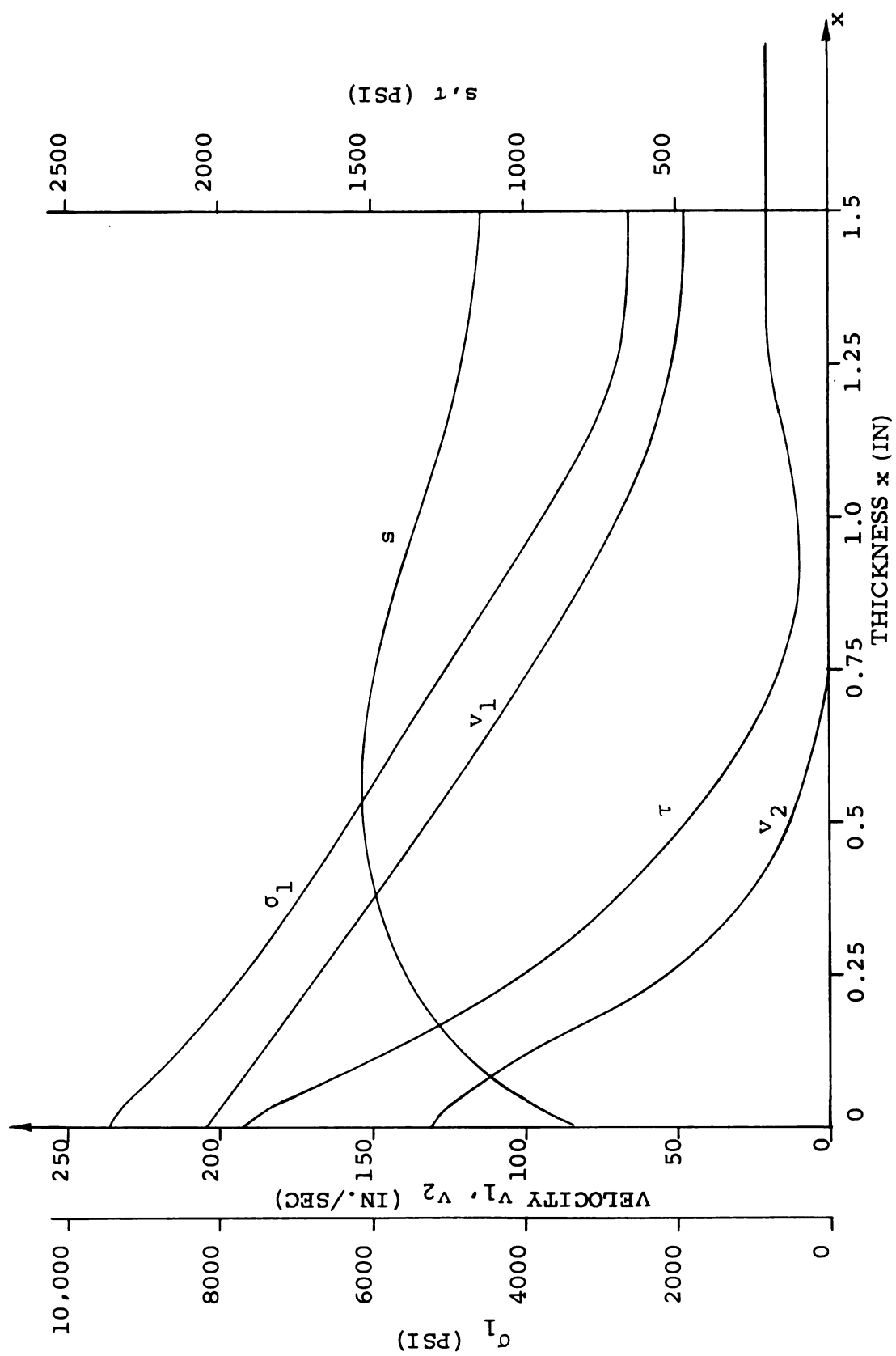
Fig. 27.--Stress and Velocity Profiles at t ≈ 5 MICROSEC

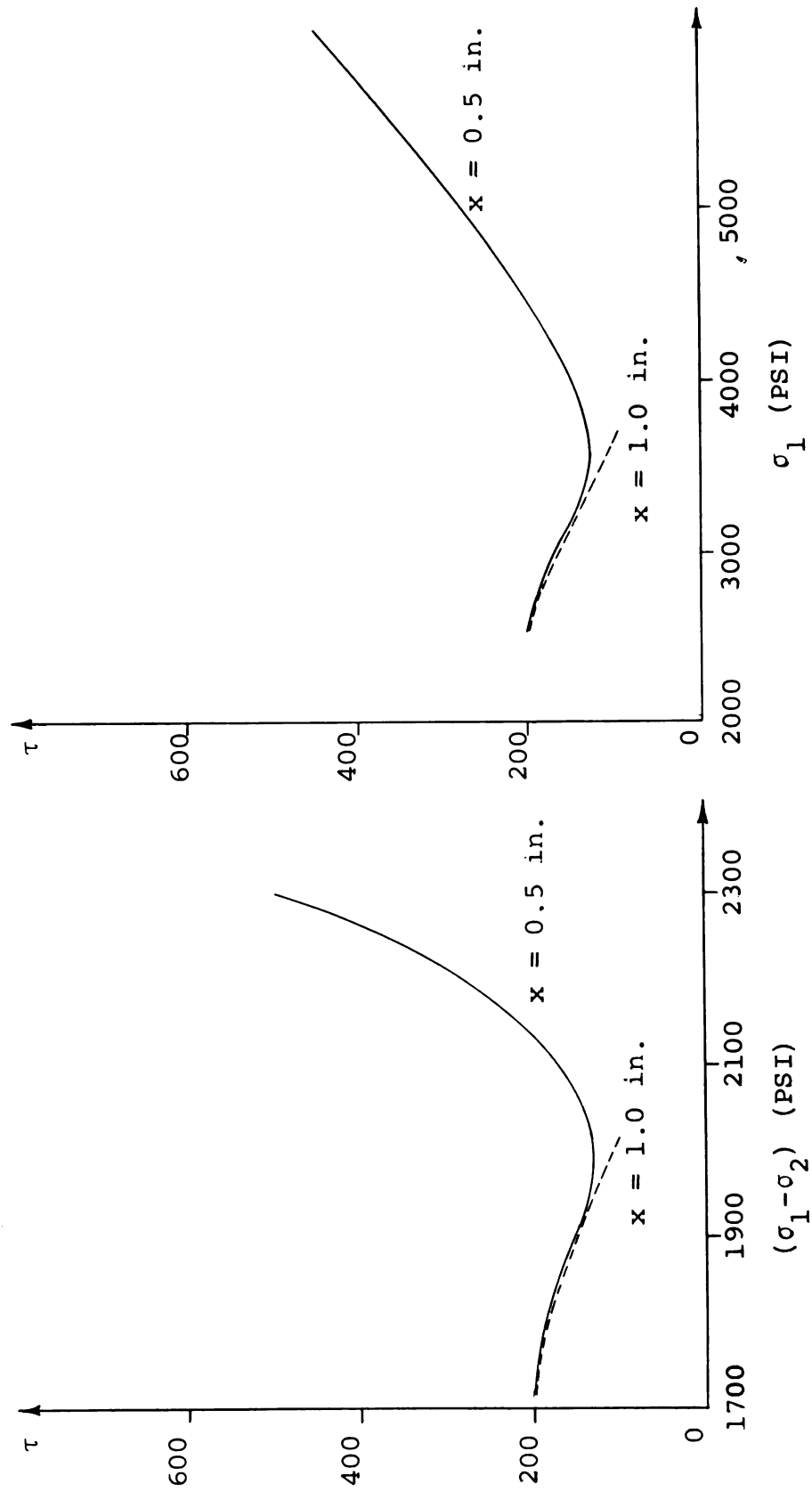Fig. 28.--Stress and Velocity Profiles at t ≈ 7 MICROSEC

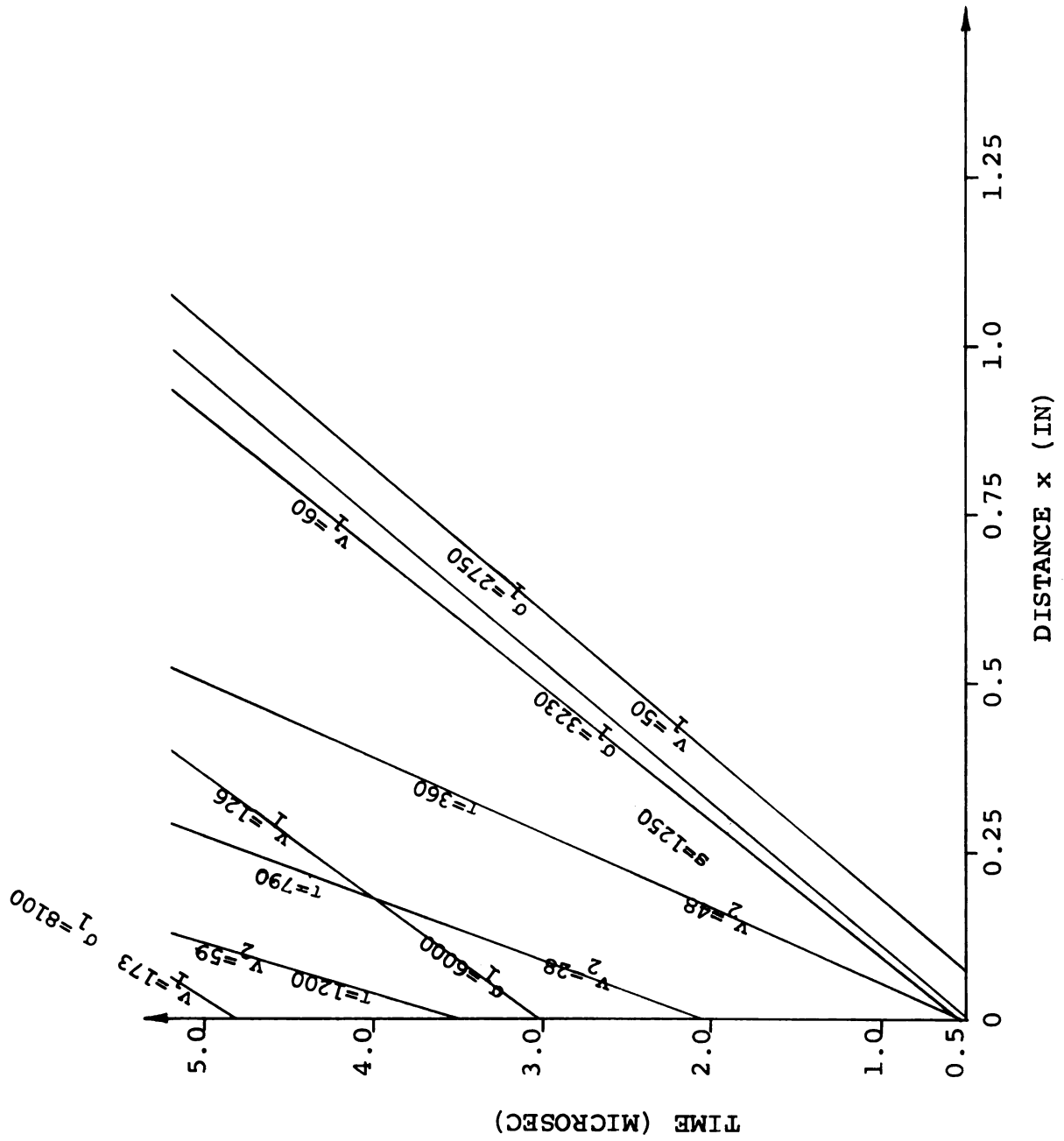Fig. 29.--Nonsimple Wave Stress Trajectories

Fig. 30.--Stress and Velocity Level Lines

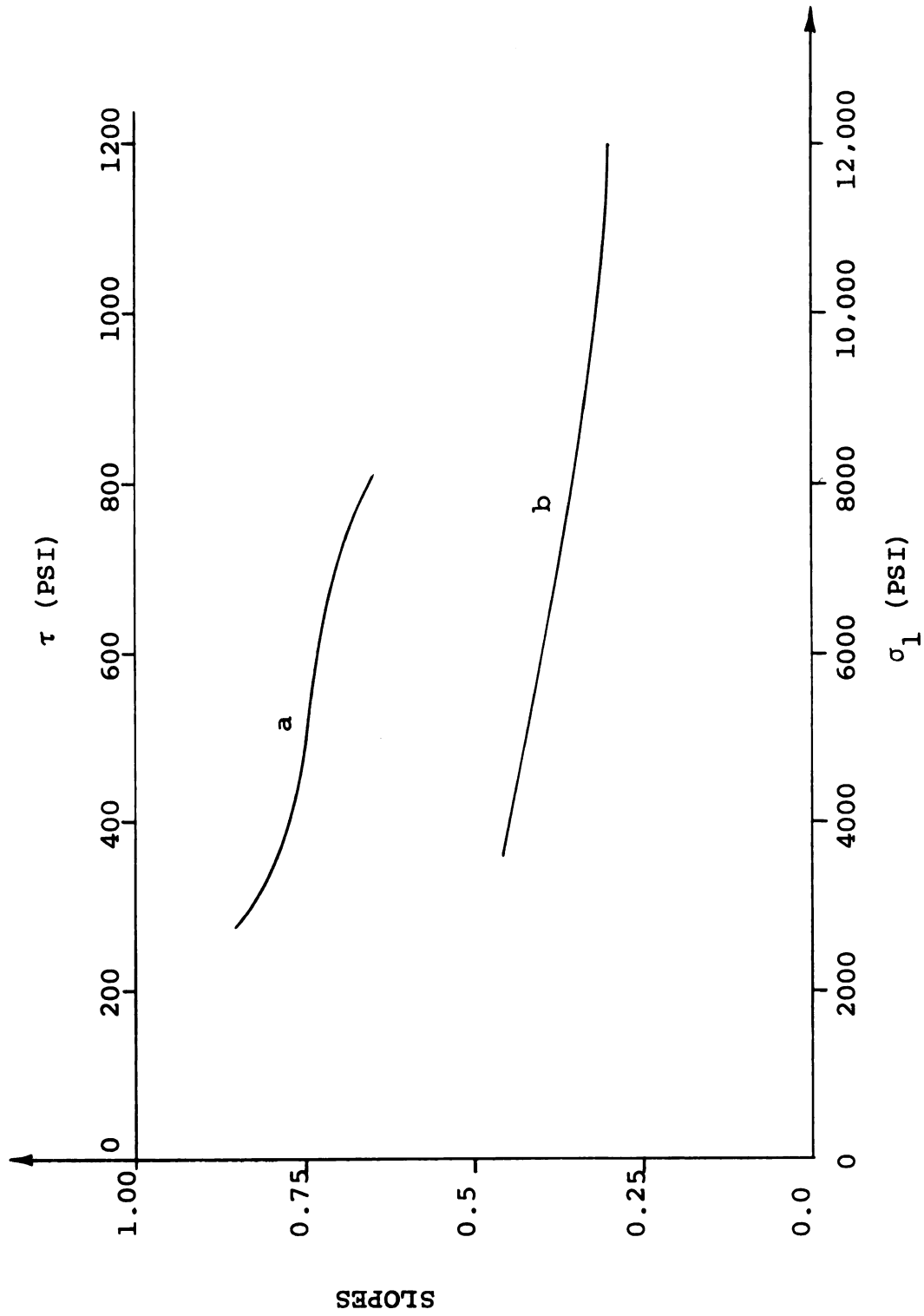Fig. 31.--Slope a of σ_1 and v_1 Level Lines Versus σ_1 and Slope b of τ and v_2 level lines versus $\frac{1}{\tau}$

APPENDIX 1

THEORY OF PARTIAL DIFFERENTIAL EQUATIONS*

A1.1   METHOD OF CHARACTERISTICS

The method of characteristics for solving quasi-linear, hyperbolic system of first order partial differential equations involves choosing appropriate directions along which the system of equations is considerably simplified. The method is very useful when there are only two independent variables.

Let the general system of partial differential equations be

$$\underset{\sim}{A}\, \underset{\sim t}{w} + \underset{\sim}{B}\, \underset{\sim x}{w} = 0 \qquad\qquad (A1.1\text{-}1)$$

where the coefficient matrices $\underset{\sim}{A}$ and $\underset{\sim}{B}$ depend on x, t and $\underset{\sim}{w}$ but do not depend on the derivatives of $\underset{\sim}{w}$. There may exist a wave front $\Phi(x, t) = 0$ across which there may

*For a detailed study of the theory of partial differential equations see Jeffrey and Taniuti (1964).

occur discontinuities in the normal derivatives of the solu-

tion.   If we introduce new variables $\zeta(x,t)$ and $\phi(x,t)$

where ζ is the arc length along the curve $\phi(x,t) = 0$,

then Equation (Al.1-1) becomes
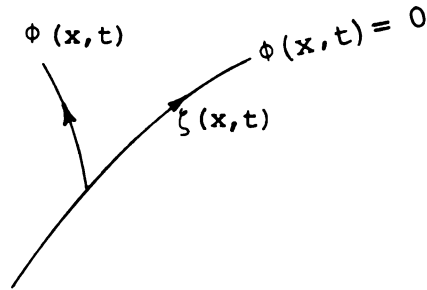
$$(A\phi_t + B\phi_x)\frac{\partial w}{\partial \phi} + (A\zeta_t + B\zeta_x)\frac{\partial w}{\partial \zeta} = 0 \quad . \tag{Al.1-2}$$

In order that the jump discontinuities, if any, across

these characteristic lines be permitted, set the coeffi-
determinant
cient∤of the normal derivatives across these lines equal

to zero, i.e.,

$$\left| A\phi_t + B\phi_x \right| = 0 \tag{Al.1-3a}$$

or, alternatively,

$$\left| cA - B \right| = 0 \tag{Al.1-3b}$$

where

$$c = \frac{-\phi_t}{\phi_x} = \frac{\zeta_t}{\zeta_x} = \frac{dx}{dt}.$$ (A1.1-3c)

This means (1) that the characteristic curves are curves across which the normal derivatives are not determined by the equations and the values of the functions on the curves, and it will also be shown (2) that the characteristic curves are curves along which the differential equations can be transformed into interior differential equations, containing only derivatives with respect to a parameter varying along the curves.

The first property permits discontinuities in the normal derivatives of an acceptable solution across a characteristic, while the second property furnishes a convenient procedure of solution.

We now seek to transform the system (A1.1-2) into a set of interior differential equations by premultiplying it by a vector $\underset{\sim}{\ell}^T$, which is to be determined. We obtain

$$\underset{\sim}{\ell}^T (\underset{\sim}{A}\phi_t + \underset{\sim}{B}\phi_x)\frac{\partial \underset{\sim}{w}}{\partial \phi} + \underset{\sim}{\ell}^T (\underset{\sim}{A}\zeta_t + \underset{\sim}{B}\zeta_x)\frac{\partial \underset{\sim}{w}}{\partial \zeta} = 0.$$ (A1.1-4)

If this system is not to contain derivatives $\partial \underset{\sim}{w}/\partial \phi$ then the coefficient matrix of $\partial \underset{\sim}{w}/\partial \phi$ should vanish. Then

$$\underset{\sim}{\ell}^T \ (\underset{\sim}{A}\phi_t + \underset{\sim}{B}\phi_x) = 0 \qquad\qquad (A1.1-5)$$

If we choose the elements of $\underset{\sim}{\ell}^T$ as the roots of the system of algebraic Equations (A1.1-5), then the surviving terms in the system of Equations (A1.1-4) will contain only derivatives with respect to ζ, and it will therefore be the system of interior differential equations that we are seeking.

The system (A1.1-5) of linear algebraic equations is homogeneous. The necessary and sufficient condition for the existence of a solution is that the determinant of coefficients vanishes, i.e.,

$$\left| \underset{\sim}{A} \ \phi_t + \underset{\sim}{B} \ \phi_x \right| = 0 \qquad\qquad (A1.1-6a)$$

or, alternatively,

$$\left| c \ \underset{\sim}{A} - \underset{\sim}{B} \right| = 0 \qquad\qquad (A1.1-6b)$$

where

$$c = \frac{-\phi_t}{\phi_x} = \frac{\zeta_t}{\zeta_x} = \frac{dx}{dt} \ . \qquad\qquad (A1.1-6c)$$

Equations (A1.1-6) are the same as Equations (A1.1-3),

which shows the truth of the earlier assertion that the

characteristic directions are the directions in which

the equations can be transformed into interior differen-

tial equations. The slopes $c = dx/dt$ of the character-

istics are the eigenvalues of the matrix $c\underset{\sim}{A}-\underset{\sim}{B}$, and the

$\underset{\sim}{\ell}$ required for the transformation is a left eigenvector

of the matrix, such that

$$\underset{\sim}{\ell}^T \ (c\underset{\sim}{A} - \underset{\sim}{B}) \ = 0. \tag{A1.1-7}$$

With this choice of c and $\underset{\sim}{\ell}^T$, the system of Equations

(A1.1-4) becomes

$$\underset{\sim}{\ell}^T \ (\underset{\sim}{A}\zeta_t + \underset{\sim}{B}\ \zeta_x)\frac{\partial \underset{\sim}{w}}{\partial \zeta} = 0 \tag{A1.1-8}$$

or, since $\underset{\sim}{B} = c\underset{\sim}{A}$, while $\zeta_x = \frac{1}{c}\ \zeta_t$, Equation (A1.1-8) be-
comes

$$2\ \underset{\sim}{\ell}^T \ \underset{\sim}{A}\ \frac{\partial \underset{\sim}{w}}{\partial \zeta}\ \zeta_t = 0 \tag{A1.1-9}$$

along the characteristic curve. Since Φ is constant along

the curve,

$$\frac{\partial \underset{\sim}{w}}{\partial \zeta}\ \zeta_t = \frac{d\underset{\sim}{w}}{dt}. \tag{A1.1-10}$$

From Equations (A1.1-9) and (A1.1-10), the interior differential equation becomes

$$\underset{\sim}{\ell}^T \underset{\sim}{A} \; d\underset{\sim}{w} = 0 \qquad\qquad (A1.1-11)$$

along the characteristic curve if $\underset{\sim}{\ell}$ is a left eigenvector of $c\underset{\sim}{A} - \underset{\sim}{B}$, associated with the eigenvalue c.

A1.2   SIMPLE WAVE SOLUTION

The set of Equations (A1.1-1) is a hyperbolic system of partial differential equations. A simple wave solution of this system is a particular solution of this system of equations, in which the vector $\underset{\sim}{w}$ is a constant vector along a characteristic line $\frac{dx}{dt}$ = c. c is the wave speed, which is function of the elements of $\underset{\sim}{w}$. Since $\underset{\sim}{w}$ is defined constant along c, thus the characteristic lines are straight in the simple wave region. $\underset{\sim}{w}$ is constant implies the following

$$\frac{\partial \underset{\sim}{w}}{\partial x} \frac{dx}{dt} + \underset{\sim}{w}_t = 0 \quad\text{or}\quad c\underset{\sim}{w}_x + \underset{\sim}{w}_t = 0. \qquad (A1.2-1)$$

Elimination of w_t from Equations (A1.1-1) and (A1.2-1), yields

$$(c\underset{\sim}{A} - \underset{\sim}{B})\underset{\sim}{w}_x = 0 \qquad\qquad (A1.2-2)$$

and elimination of w_x yields

$$(c\underset{\sim}{A} - \underset{\sim}{B})\underset{\sim}{w}_t = 0. \qquad\qquad (A1.2-3)$$

Equations (A1.2-2) and (A1.2-3) imply that

$$(c\underset{\sim}{A} - \underset{\sim}{B})d\underset{\sim}{w} = 0 \qquad\qquad (A1.2-4)$$

for the change $d\underset{\sim}{w}$ associated with any change dx, dt involving going from one straight characteristic of the simple wave to another one. [Equation (A1.2-4) is of course trivially satisfied for a change $dx = cdt$, where c is the wave speed of the straight characteristic, since then $d\underset{\sim}{w} = 0$.]

If $\underset{\sim}{\ell}$ is a left eigenvector of $(c\underset{\sim}{A} - \underset{\sim}{B})$ and $\underset{\sim}{A}$ and $\underset{\sim}{B}$ are symmetric, then

$$(c\underset{\sim}{A} - \underset{\sim}{B})\,\underset{\sim}{\ell} = 0 \,. \qquad\qquad (A1.2-5)$$

Equations (A1.2-4) and (A1.2-5) imply that, as we go from one straight characteristic of a simple wave to a neighboring one, $d\underset{\sim}{w}$ is proportional to $\underset{\sim}{\ell}$.

APPENDIX 2

LAGRANGIAN FORMULATION OF EQUATIONS OF

MOTION IN MATERIAL COORDINATES

The combined-stress plastic-potential flow theory
is formulated in terms of the rates of deformation (time
rates of the natural or logarithmic strain components)
and the Cauchy stress components, both referred to the
deformed configuration and using the spatial (Eulerian)
coordinates x_k of the deformed position of the particle
whose initial position coordinates are the material co-
ordinates X_K of the particle. Only in this appendix is
the notation of capital X_K for material coordinates and
lower-case x_k for spatial coordinates. Throughout the
body of the thesis lower-case x denotes the material co-
ordinate. Both sets of coordinates will be supposed
measured from the same set of rectangular Cartesian axes.
Then they are related as follows

$$x_1 = X_1 + U_1, \quad x_2 = X_2 + U_2, \quad x_3 = X_3 + U_3$$

where U_1, U_2, and U_3 are the displacement components, which are considered as functions of the X_K in the Lagrangian formulation. The combined-stress yield condition is also stated in terms of the Cauchy stresses.

For comparison with experimental measurements of wave propagation it is convenient to have the solutions in terms of material coordinates; for example, a strain gage is located by giving its initial position. It also turns out that the equations and simple wave solutions take an especially simple form when material coordinates are used. In the cases of uniaxial stress waves in a bar and of uniaxial strain in a half space the resulting simplified equations are not limited to small strains, since the combined-stress plasticity theory is not used. Even when $\epsilon_{11} = \partial U_1/\partial X_1$ is not small, the engineering stress-strain curve of the bar can be used to determine the dependence of the nominal stress T_{11}^o on ϵ_{11}. For combined-stress waves, however, the rates of deformation D_{ij} can be approximated as time rates of the small strain components only when the strains are small compared to unity (less than about 0.05). Then, for example

$$D_{11}[x_1(X_1), x_2(X_1), x_3(X_1)] \approx \frac{\partial \epsilon_{11}(X_1)}{\partial t} \qquad \text{(A2-1)}$$

when the displacements are functions only of the one material coordinate X_1 and the time, as is assumed in the problems treated in this study. This replacement of the D_{ij} in the constitutive equations by the corresponding rates of small strain is the only approximation limiting the half-space plane-wave analysis to small strains, since we shall see that the equations of motion are exact for the half-space case. Additional approximations are implied by the neglect of the variation of the displacement components through the thickness in the tube case.

The equations of motion in terms of material coordinates take an especially simple form when the nonsymmetric first Piola-Kirchoff stress tensor T^{o}_{Km} is used. This tensor gives the force vector on a deformed surface element per unit area of the undeformed element. Thus

$$N_K T^{o}_{Ki} dS_o = dP_i = n_j \sigma_{ji} dS, \qquad \text{(A2-2)}$$

where the first equality expresses the components dP_i in terms of the T^{o}_{Ki}, the undeformed area dS_o and its unit

165

normal components N_K, while the second equality is the usual equation in terms of the Cauchy stresses, the deformed area dS, and its unit normal components n_j; see, for example, Malvern (1969), or Eringen (1967). The two stress tensors are related by

$$\sigma_{ji} = \frac{\rho}{\rho_o} \frac{\partial x_j}{\partial X_J} T^o_{Ji} \qquad (A2-3)$$

where ρ and ρ_o are the current and initial density at the particle. Both sides of Equations (A2-2) and (A2-3) are to be understood as expressed in terms of the X_M and t, by using the equations

$$x_k = x_k(X_1, X_2, X_3, t) \qquad (A2-4)$$

defining the motion.

The equations of motion in terms of the material coordinates then take the following form (for negligible body forces)

$$\frac{\partial T^o_{Ji}}{\partial X_J} = \rho_o \frac{\partial v_i}{\partial t} \qquad (A2-5)$$

where the $v_i(X_1, X_2, X_3, t)$ are the particle velocity components $v_i = \partial U_i/\partial t$.

For the two cases considered in this study, the stresses are assumed independent of X_2 and X_3. Hence the equations of motion reduce to

$$\frac{\partial T_{1i}^{o}}{\partial X_1} = \rho_o \frac{\partial v_i}{\partial t} \qquad \text{(A2-6)}$$

The only stresses appearing in these equations of motion are T_{11}^{o}, T_{12}^{o}, T_{13}^{o}. (In the tube case we assume T_{13}^{o} to be zero and neglect the lateral inertia term $\rho_o \,\partial v_3/\partial t$). These are related to the Cauchy stresses σ_{11}, σ_{12}, σ_{13} as follows, by Equations (A2-3),

$$\left.\begin{aligned}
\sigma_{11} &= \frac{\rho}{\rho_o}\left[\frac{\partial x_1}{\partial X_1} T_{11}^{o} + \frac{\partial x_1}{\partial X_2} T_{21}^{o} + \frac{\partial x_1}{\partial X_3} T_{31}^{o}\right] \\[2ex]
\sigma_{12} &= \frac{\rho}{\rho_o}\left[\frac{\partial x_1}{\partial X_1} T_{12}^{o} + \frac{\partial x_1}{\partial X_2} T_{22}^{o} + \frac{\partial x_1}{\partial X_3} T_{32}^{o}\right] \\[2ex]
\sigma_{13} &= \frac{\rho}{\rho_o}\left[\frac{\partial x_1}{\partial X_1} T_{13}^{o} + \frac{\partial x_1}{\partial X_2} T_{23}^{o} + \frac{\partial x_1}{\partial X_3} T_{33}^{o}\right].
\end{aligned}\right\} \qquad \text{(A2-7)}$$

Since $x_1 = X_1 + U_1$, and U_1 is independent of X_2 and X_3, Equations (A2-7) reduce to

$$\sigma_{11} = \frac{\rho}{\rho_o} (1+\epsilon_{11}) \ T^o_{11}$$

$$\sigma_{12} = \frac{\rho}{\rho_o} (1+\epsilon_{11}) \ T^o_{12}$$

$$\sigma_{13} = \frac{\rho}{\rho_o} (1+\epsilon_{11}) \ T^o_{13}$$

$$\text{(A2-8)}$$

where

$$\epsilon_{11} = \frac{\partial U_1}{\partial X_1} .$$

The density ratio can be obtained from the continuity equation in material coordinates

$$\frac{\rho_o}{\rho} = \frac{dV}{dV_o} = J = \text{determinant } |x_{k,M}| \qquad \text{(A2-9a)}$$

where J is the Jacobian determinant of the transformation. [See Malvern (1969)].

$$\frac{\rho_o}{\rho} = \begin{bmatrix} 1 + \dfrac{\partial U_1}{\partial X_1} & \dfrac{\partial U_1}{\partial X_2} & \dfrac{\partial U_1}{\partial X_3} \\[2em] \dfrac{\partial U_2}{\partial X_1} & 1 + \dfrac{\partial U_2}{\partial X_2} & \dfrac{\partial U_2}{\partial X_3} \\[2em] \dfrac{\partial U_3}{\partial X_1} & \dfrac{\partial U_3}{\partial X_2} & 1 + \dfrac{\partial U_3}{\partial X_3} \end{bmatrix} \qquad \text{(A2-9b)}$$

For the case of plane waves in a half space all the displacements are independent of X_2 and X_3, so that this reduces to

$$\frac{\rho_o}{\rho} = 1 + \epsilon_{11} \, , \tag{A2-9c}$$

whence we have

$$\left.\begin{array}{l} \sigma_{11} = T^o_{11} \, , \\[2ex] \sigma_{12} = T^o_{12} \, , \\[2ex] \sigma_{13} = T^o_{13} \end{array}\right\} \tag{A2-10}$$

in this case without any assumption of small strains.

For the thin-walled tube case, however, if the X_3-direction is taken as the thickness direction (radial direction) at a point, while X_2 is tangential to the circumferential direction, we would not expect $\epsilon_{22} = \partial U_2/\partial X_2$ and $\epsilon_{33} = \partial U_3/\partial X_3$ to vanish because of the Poisson effect. If we assume that plane sections remain plane, we would have

$$\frac{\rho_o}{\rho} = (1+\epsilon_{11})\,(1+\epsilon_{22})\,(1+\epsilon_{33}) \tag{A2-11}$$

and

$$\left.\begin{array}{c} \sigma_{11} = \dfrac{T^{o}_{11}}{(1+\epsilon_{22})\,(1+\epsilon_{33})} \\[4mm] \sigma_{12} = \dfrac{T^{o}_{12}}{(1+\epsilon_{22})\,(1+\epsilon_{33})} \end{array}\right\} \qquad (A2\text{-}12)$$

Thus in the tube case, replacement of T^{o}_{11} by σ_{11} and T^{o}_{12} by σ_{12} requires restriction to small strains.

In either case the other stress components are not equal. For example, $T^{o}_{21} \neq \sigma_{21}$, but T^{o}_{21} does not enter the equations of motion.

BIBLIOGRAPHY

Barker, L.M., Lundergan, C.D., Herrmann, W., "Dynamic
      Response of Aluminum," J. App. Phys., Vol. 35,
      pp. 1203-1212, 1964.

Bell, J. F., "The Dynamic Plasticity of Metals at High
      Strain Rates: An Experimental Generalization,"
      Behavior of Materials Under Dynamic Loading,
      edited by N. J. Huffington, Jr., New York:
      ASME, pp. 19-41 (1965).

Bleich, H. H. and Nelson, I., "Plane Waves in an Elastic-
      Plastic Half Space Due to Combined Surface Pres-
      sure and Shear," J. App. Mech., Vol. 33, Trans.
      ASME Vol. 88, Series E, pp. 149-158, 1966.

Butcher, B. M. and Karnes, C. H., "Strain-Rate Effects
      in Metals," J. App. Phys., Vol. 37, pp. 402-411,
      1966.

Clifton, R. J., "An Analysis of Combined Longitudinal and
      Torsional Plastic Waves in a Thin-Walled Tube,"
      5th U.S. Natl. Congr. App. Mech., New York:
      A.S.M.E., 1966, pp. 465-480.

Craggs, J. W., "The Propagation of Infinitesimal Plane
      Waves in Elastic-Plastic Materials," J. Mech.
      Phys. Solids, Vol. 5, pp. 115-124, 1957.

Craggs, J. W., "Plastic Waves," in Progress in Solid
      Mechanics, edited by I. N. Sneddon and R. Hill,
      Amsterdam: North-Holland Publishing Co., New
      York: Interscience Publishers Inc., pp. 143-197,
      1961.

Cristescu, N., "On the Propagation of Elastic-Plastic Waves for Combined Stresses," _Prikl. Mat. Mekh._, Vol. 23, pp. 1605-1612, 1959.

Cristescu, N., _Dynamic Plasticity_, Amsterdam: North-Holland Publishing Co., New York: John Wiley and Sons, Inc. (Interscience Publishers Div.), 1967.

Donnell, L. H., "Longitudinal Wave Transmission and Impact," _ASME Trans._, _App. Mech. Div._, Vol. 52(1), pp. 153-167, 1930.

Drucker, D. C., "A More Fundamental Approach to Plastic Stress-Strain Relations," _Proc. 1st U.S. Natl. Congr. App. Mech._, New York: ASME, pp. 487-491, 1951.

Eringen, A. C., _Mechanics of Continua_, New York: John Wiley and Sons, Inc., pp. 108-110, 1967.

Hill, R., _The Mathematical Theory of Plasticity_, Oxford University Press, 1950.

Hodge, P. G., "A General Theory of Piecewise Linear Plasticity Based on Maximum Shear," _J. Mech. Phys. Solids_, Vol. 5, pp. 242-260, 1957.

Hodge, P. G., "Piecewise Linear Plasticity," _Proc. 9th Intnatl. Congr. App. Mech._, Brussels, pp. 65-72, 1957.

Hopkins, H. G., "Dynamic Nonelastic Deformations of Metals," _App. Mech. Surveys_, edited by H. N. Abramson and others, New York: A.S.M.E., pp. 847-867, 1966.

Jeffrey, A. and Taniuti T., _Nonlinear Wave Propagation_, New York: Academic Press, 1964.

Ke-chzhi, K., "On Work-Hardening of Plastic Solids," _Prikl. Mat. Mekh._, Vol. 22, pp. 758-762, 1958.

Lipkin, J. and Clifton, R. J., "An Experimental Study of Combined Longitudinal and Torsional Plastic Waves in a Thin-Walled Tube," 12th Intnatl. Cong. App. Mech., Stanford University, 1968.

Lubahn, J. D. and Felgar, R. P., Plasticity and Creep of Metals, New York: John Wiley and Sons, Inc., 1961.

Malvern, L. E., "The Propagation of Longitudinal Waves of Plastic Deformation in a Bar of Material Exhibiting a Strain Rate Effect," Ph.D. Dissertation, Brown University, Providence, R.I., 1949; published in J. App. Mech., Vol. 18, pp. 203-208, 1951 and Quarterly Appl. Math., Vol. 8, pp. 405-411, 1951.

Malvern, L. E., Introduction to the Mechanics of a Continuous Medium, Englewood Cliffs, N.J.: Prentice-Hall, Inc., pp. 222-224, 1969.

Naghdi, P. M., "Stress-Strain Relations in Plasticity and Thermoplasticity," Plasticity, edited by E. H. Lee and P. S. Symonds, Oxford: Pergamon Press, pp. 121-169, 1960.

Nan, N., "Elastic-Plastic Waves for Combined-Stresses," Technical Report No. 184, Stanford University, 1968.

Prager, W., "A New Method of Analyzing Stresses and Strains in Work-Hardening Plastic Solids," J. App. Mech., Vol. 23, pp. 493-496, 1956.

Rakhmatulin, K. A., "Propagation of a Wave of Unloading," Prikl. Mat. Mekh., Vol. 9, pp. 91-100, 1945; Translation A11-T2/15, Brown University, 1948.

Rakhmatulin, K. A., "On the Propagation of Elastic-Plastic Waves Owing to Combined Loading," Prikl. Mat. Mekh., Vol. 22, pp. 1079-1088, 1958.

Sokolovskii, V. V., "The Propagation of Elastic-Visco-Plastic Waves in Bars," Prikl. Mat. Mekh., Vol. 12, pp. 261-280, 1948; Translation A11-T6, Brown University, 1949.

* Department of Applied Mechanics

Taylor, G. I., "The Plastic Wave in a Wire Extended by an Impact Load," British Official Report RC 329, 1942.

Ting, T. C. T., "Interaction of Shock Waves Due to Combined Two Shear Loadings," Technical Report No. 180, Stanford University,* May 1968.

Ting, T. C. T. and Nan, N., "Plane Waves Due to Combined Compressive and Shear Stresses in a Half Space," Technical Report No. 185, Stanford University* 1968, to appear in J. App. Mech., Paper No. 69-APM-12.

Ting, T. C. T., "On the Initial Slope of Elastic-Plastic Boundaries in Combined Longitudinal and Torsional Wave Propagation," Technical Report No. 188, Stanford University,* Sept. 1968; to appear in J. App. Mech., Paper No. 69-APM-13.

Ting, T. C. T., "Elastic-Plastic Boundaries in Plane and Cylindrical Wave Propagation of Combined-Stresses," Technical Report No. 194, Stanford University* Dec. 1968.

Vitiello, D. L. and Clifton, R. J., "The Numerical Solution of a Problem in the Propagation of Plastic Waves of Combined Stress," Technical Report No. 4, Brown University,** 1967.

Von Kármán and Duwez, P., "The Propagation of Plastic Deformation in Solids," Proc. 6th Intnatl. Cong. App. Mech., Paris, 1946; Published in J. App. Phys., Vol. 21, pp. 987-994, 1950.

Williams, R. A. and Malvern, L. E., "Harmonic Dispersion Analysis of Incremental Waves in Uniaxially Prestressed Plastic and Viscoplastic Bars, Plates, and Unbounded Media," J. App. Mech., Vol. 36, Series E., pp. 59-64, 1969.

* Department of Applied Mechanics
** Division of Applied Mathematics